

Improvement of the strength of fiber-reinforced polymer by grafting cellulose nanofibers onto the reinforcements

by

Mouhamadou Moustapha SARR

Student ID Number: 1236005

A dissertation submitted to the
Engineering course, Department of Engineering,
Graduate School of Engineering,
Intelligent Mechanical Systems,
Kochi University of Technology,
Kochi, Japan

in partial fulfillment of the requirements for the degree of
Doctor of Engineering

Assessment Committee:

Supervisor: Tatsuro KOSAKA

Co-Supervisor: Kazuhiro KUSUKAWA

Co-Supervisor: Asami NAKAI, Gifu University

Committee Member: Toshiyuki KAWAHARAMURA

Committee Member: Yasunori MATSUMOTO

March 2022

(Intentionally left blank)

Abstract

Fiber-reinforced polymer composites (FRPs) are widely used in various fields of application including aerospace, automobile, marine, and structural applications due to their exceptional mechanical properties, good resistance of corrosion, and low density. However, damages, such as interfacial debonding, micro-cracks, and delamination, may occur in FRPs. In recent years, to improve the mechanical properties of composite materials, cellulose nanofibers (CNFs), with their outstanding mechanical properties, environmentally friendly, recyclability, low cost, and low density, have been added as a nano modifier in FRP composites. The performance of fiber-reinforced polymer composites is highly dependent on the fiber/matrix interface bonding. Thus, mixing CNFs with epoxy resin can improve both fiber/matrix interfacial strength and matrix toughness. However, this can also result in increasing the resin viscosity making it difficult to impregnate the reinforcing fibers. Furthermore, considering its hydrophilicity, CNF may still require additional surface treatment before its use in FRPs. Therefore, in this study, a new approach consisting of coating glass fibers (GF) with cellulose nanofibers (CNFs) was proposed to improve the interfacial strength and to avoid processing high viscosity resin or the formation of aggregations in the matrix.

The first part of the study focused on improving the interfacial strength of glass fiber-reinforced epoxy (GFRP) composites by incorporating CNFs. Therefore, CNFs were grafted onto single GF and continued by evaluation of the interfacial shear strength (IFSS) of glass fiber/epoxy (GF/EP) composites using microdroplet tests. The vacuum-assisted resin transfer molding (VaRTM) technique was used to incorporate CNFs into woven glass fiber and to manufacture the GFRP composite laminates. The flexural strength of the composites was determined by three-point bending tests. A Field-emission scanning electron microscope (FE-SEM) was used to characterize the morphology of the GF surface treated with CNFs, and eventually to determine the strengthening mechanisms. The CNF-treated GF showed a rougher surface than that of the untreated GF. A maximum increase of 78% in the IFSS was obtained at the optimum CNF concentration (10 ppm wt%). Meanwhile, the flexural strength of the CNF-modified (GF-CNF/EP) composites was improved. In contrast, it was found that the thicker CNF layer led to a decrease in the IFSS of GF-CNF/EP composites. The results suggested that grafting a low quantity of CNF onto glass fiber can significantly improve the interfacial strength of glass fiber/epoxy composites.

In the second part, the manufacturing process of the composites was improved to avoid the irregular surface of one side of the composites by replacing the peel ply with an aluminum plate. Thus, the flexural strength and flexural fatigue of the GF/EP and GF-CNF/EP composites were evaluated by three-point bending tests. The flexural modulus remained constant in all CNF concentrations except 0.5 wt% while the flexural strength increased slightly with increasing the CNF concentration. An improvement of 6% (from 429 MPa to 454 MPa) was observed in the GF-CNF/EP composite at 0.1wt% in comparison with the neat GF/EP composite. Although the results are lower than those obtained in the previous experiment, they are more accurate because the surface of the composites is more regular and smoother. On the other hand, the fatigue life increased five times higher than the GF/EP composite for the same CNF concentration (0.1 wt%). At 0.5 wt%, the flexural modulus and strength decreased due to the thickening of the CNF layer, and the formation of aggregates onto glass fiber resulting in hindering the impregnation of GF with EP resin. The fracture surface indicated that the presence of CNFs on the GF surface increased the interfacial bonding between GFs and EP resulting in improving the fatigue life. The mechanisms behind the improvement in flexural strength and flexural fatigue were considered as mechanical interlocking and matrix toughening.

Finally, cellulose nanofibers (CNFs) were used to improve the fracture toughness of glass fiber reinforced epoxy composites (GFRPs). Although grafting CNFs onto GFs by vacuum impregnation has shown to be a potential method to improve flexural strength and fatigue life of GFRP composite, it may be limited for improving interlaminar fracture toughness (IFT). Because with this method CNFs were more present on the outer part of GF laminate than that in the middle. Therefore, in this section different CNF suspensions (0.05, 0.075, and 0.1 wt%) were sprayed onto the surface of glass fiber laminates at the mid-plane. VaRTM process was used to manufacture the GFRP composite laminates. End notched flexure tests were conducted to evaluate the effect of CNFs on the interlaminar fracture toughness mode II (G_{IIC}) of the composite laminates. The results indicated an enhancement of G_{IIC} by 28% with the addition of 0.05 wt% of CNFs to GF/EP composites, whereas 0.1 wt% of CNFs led to a reduction of the IFT due to the incomplete impregnation of GF with epoxy resin. Shear hackles and large epoxy deformations were found to be the predominant mechanisms for improving the interfacial strength of GF-CNF/EP composites.

Acknowledgments

Thanks to Allah the Almighty for granting me health and mind for the accomplishment of this thesis.

Foremost, I would like to express sincerely my gratitude to my supervisor *Associate Professor Tatsuro Kosaka* who gave me the opportunity to study at his laboratory. Since I came from the field of metallic material, he taught me the basic knowledge of composite materials. His close guidance and advice were invaluable for me to accomplish my Ph.D. studies. He also helped me in revising my manuscripts and thesis. This thesis would not be possible without his support and guidance.

Special thanks go to the committee members for their constructive and insightful comments and suggestions to polish my dissertation. I also especially thank *Prof. Kazuhiro Kusukawa* for his encouragement and advice. Thanks to my co-supervisor *Prof. Asami Nakai* from Gifu University (Japan) for her support and advice. I would like to thank *Associate Prof. Akio Ohtani* (Kyoto Institute of Technology) who helped us to conduct microdroplet tests.

I express my gratitude to Kochi University of Technology for its financial support through its Special Scholarship Program. Thanks also go to IRC members, especially, *Yoko Morio, Saki san, Miki san, and Yoshida san* for their close assistance and support during my study at KUT.

Thanks go to *Prof. Gordan Bateson* for the revision of my papers. I'm very grateful to *Dr. Mouctar Kamara* for the revision of my papers. I sincerely thank him for his support in my academic and social life all over my stay in Japan from my master's until the achievement of my doctoral degree.

I would like also to express my gratitude to all of my lab members, especially, *Hiraku Inoue* for the experiments, *Fujioka Genko, Tei, Hideo, Onishi, Ishihara, Ide*, etc. Special gratitude and thanks to my fellow SSP doctoral students *Namal, Islam, Ayat, Sukma, Meiliefiana, Asma, and Rostislav* for being nice friends. Thanks to *Dr. Fean* for his comments and suggestions to polish my dissertation. They nicely made my social life at KUT like home.

I would not end without thanking my lovely wife *Daba Seck*, my children *Serigne Moustapha*, and *Pape Mor* for their patience, prayers, and support. I would also express my gratitude to my father *Moussa Sarr* and my guide *El hadji Malick Sy* for their constant prayers, support, and encouragement. My thanks go to my brothers, sisters, uncles, aunts, and all of my friends who encouraged and supported me during the time I need it the most.

Dedication

I dedicate this thesis to my beloved mother *Astou Diop* and my grandmother *Daba SARR*.

May Allah, The Almighty and Merciful, forgive them and welcome them to paradise.

Disclaimer

Publications:

Journal papers

1. Mouhamadou Moustapha Sarr, Hikaru Inoue, Tatsuro Kosaka, “*Study on the Improvement of Interfacial Strength between Glass Fiber and Matrix Resin by Grafting Cellulose Nanofibers*”, Composites Science and Technology, 211 (2021) 108853. doi.org/10.1016/j.compscitech.2021.108853
2. Mouhamadou Moustapha Sarr and Tatsuro Kosaka “*Effect of cellulose nanofibers on the interlaminar fracture toughness of glass fiber/epoxy composites*”, submitted to Composite Structures (Under review).

Conference papers

1. Mouhamadou Moustapha Sarr, Hikaru Inoue and Tatsuro Kosaka, “*Improvement of Flexural Strength and Fatigue Properties of Glass Fiber/Epoxy Composites by Grafting Cellulose Nanofibers onto the Reinforcing Fibers*”, Proceedings of the American Society for Composites-36th Technical Conference, (20-22, Sept. 2021), pp. 1665-1672. [10.12783/asc36/35866](https://doi.org/10.12783/asc36/35866)

Conferences:

1. Mouhamadou M. SARR, Hikaru INOUE and Tatsuro KOSAKA, “*Improvement of Flexural Strength and Fatigue Properties of Glass Fiber/Epoxy Composites by Grafting Cellulose Nanofibers onto the Reinforcing Fibers.*” American Society for Composites-36th Technical Conference, Virtual conference, 20-22 September, 2021.
2. Mouhamadou M. SARR, Hikaru INOUE, and Tatsuro KOSAKA, “*Quantitative Evaluation on the Interfacial Treatment of Glass Fiber/Epoxy resin by Grafting Cellulose Nanofibers*”, Future Generation Symposium on Composite Materials 2020, Online 7-8 December, 2020.
3. Mouhamadou M. SARR, Hikaru INOUE and Tatsuro KOSAKA, “*Improvement of the strength of glass fiber/epoxy interface by grafting cellulose nanofibers*”, Japan Symposium on Composite Materials, Okayama (Japan), September 5th-6th, 2019
4. Mouhamadou M. SARR, Hikaru INOUE, and Tatsuro KOSAKA, “*Study on the improvement of interfacial strength between glass fiber and matrix resin by grafting cellulose nanofibers*”, 16th Japan International SAMPE Symposium & Exhibition (JISSE-16), Tokyo (Japan), September 2nd-4th, 2019
5. Mouhamadou M. SARR, Hikaru INOUE, and Tatsuro KOSAKA, “*Effect of cellulose nanofibers (CNF) on the interfacial strength of glass fiber/epoxy composites*”, Future Generation Symposium on Composite Materials, Wakayama (Japan), August 26th-27th, 2019

Table of Contents

Abstract	i
Acknowledgments	iii
Dedication	iv
Disclaimer	v
Abbreviations & Symbols	ix
List of figures	xi
List of tables	xiii
Chapitre 1: General introduction	1
Chapitre 2: Research background	4
2.1 Glass fibers.....	4
2.1.1 Manufacturing process	4
2.1.2 Classification and properties	5
2.2 Performance of epoxy matrix in FRP composites.....	7
2.2.1 Properties of epoxy resins	7
2.2.2 Applications.....	7
2.3 Glass fiber-reinforced polymer	8
2.3.1 VaRTM process.....	9
2.3.2 Applications of GFRP composites	10
2.3.3 Failure in FRP composites:	10
2.3.4 Improvement of glass fiber/epoxy interfacial strength.....	11
2.3.5 Effect of cellulose nanofibers on the performance of composites.....	14
2.4 Motivation.....	17
2.5 Objective	17
Chapitre 3: Study on the improvement of interfacial strength between glass fiber and matrix resin by grafting cellulose nanofibers	19
3.1 Introduction.....	19

3.2	Experimental methods.....	21
3.2.1	Materials	21
3.2.2	CNFs and silane preparation	21
3.2.3	Unsize glass fiber preparation	22
3.3	Mechanical test methods	22
3.3.1	Microdroplet test	22
3.3.2	Manufacturing of GF-CNF/EP composites and three-point bending test	24
3.4	Surface characterization	26
3.5	Results and discussion	27
3.5.1	Surface of the CNFs-treated glass fiber.....	27
3.5.2	Interfacial shear strength	30
3.5.3	Flexural strength.....	37
3.6	Conclusions.....	40

Chapitre 4: Improvement of Flexural Strength and Fatigue Properties of Glass Fiber/Epoxy Composites by Grafting Cellulose Nanofibers onto the Reinforcing Fibers
42

4.1	Introduction.....	42
4.2	Experimental methods.....	43
4.2.1	Materials:.....	43
4.2.2	Manufacturing of the GF-CNFs/Epoxy resin composites	43
4.2.3	Flexural properties	44
4.2.4	Fatigue test.....	44
4.3	Results and discussion	45
4.3.1	Morphology of laminated woven GF after CNFs treatment	45
4.3.2	Flexural strength.....	47
4.3.3	Flexural fatigue.....	48
4.4	Conclusions.....	51

Chapitre 5: Effect of cellulose nanofibers on the interlaminar fracture toughness of glass fiber/epoxy composites	52
5.1 Introduction	52
5.2 Experimental methods.....	54
5.2.1 Materials	54
5.2.2 Preparation of woven GFs with CNFs.....	54
5.2.3 Manufacturing of GFRP composites	54
5.2.4 End notched flexure tests.....	55
5.2.5 Surface characterization	57
5.3 Results and discussion	57
5.3.1 Morphology of the CNFs-treated woven GF laminates	57
5.3.2 Interlaminar fracture toughness G_{IIC}	58
5.3.3 Fractography	61
5.4 Conclusion	64
Chapitre 6: General conclusions.....	65
References	67

Abbreviations & Symbols

Abbreviations

<i>GF:</i>	<i>Glass fiber</i>
<i>CF:</i>	<i>Carbon fiber</i>
<i>EP:</i>	<i>Epoxy</i>
<i>FRP:</i>	<i>Fiber-reinforced polymer</i>
<i>GFRP:</i>	<i>Glass fiber-reinforced polymer</i>
<i>CFRP:</i>	<i>Carbon fiber-reinforced polymer</i>
<i>CNF:</i>	<i>Cellulose nanofiber</i>
<i>MFC:</i>	<i>Microfibrillated cellulose</i>
<i>CNC:</i>	<i>Cellulose nanocrystal</i>
<i>GO:</i>	<i>Graphene oxide</i>
<i>IFSS:</i>	<i>Interfacial shear strength</i>
<i>ILSS:</i>	<i>Interlaminar shear strength</i>
<i>CNT:</i>	<i>Carbon nanotube</i>
<i>UP:</i>	<i>Unsaturated polyester</i>
<i>MWCNT:</i>	<i>Multiwall carbon nanotube</i>
<i>VaRTM:</i>	<i>Vacuum-assisted resin transfer molding</i>
<i>TEMPO:</i>	<i>2,2,6,6-Tetramethylpiperidine-1-oxyl</i>
<i>HDPE:</i>	<i>High-density polyethylene</i>
<i>PEI:</i>	<i>Polyethylenimine</i>
<i>PTFE:</i>	<i>Polytetrafluoroethylene</i>
<i>PSF:</i>	<i>Polysulfone</i>
<i>ENF:</i>	<i>End notched flexure</i>
<i>FE-SEM:</i>	<i>Field emission scanning electron microscope</i>

Symbols

- F : Maximum load required to peel off the resin droplet
- L_e : Fiber embedded length in resin droplet
- d_f : Fiber diameter
- τ : Applied interfacial shear strength
- τ_a : Average of IFSS given by the Weibull distribution
- τ_0 : Weibull scale parameter
- ρ : Weibull shape parameter
- Γ : Gamma function
- $P(\tau)$: Probability of failure
- P : Maximum bending load
- L : Span length
- D : Maximum deflection at the center of the specimen
- t : Thickness of the specimen
- B : Width of the specimen
- E_f : Flexural modulus
- σ_f : Flexural strength
- ε_f : Flexural strain
- P_C : Critical load
- P_{NL} : Load at the nonlinear point from load vs. displacement curve
- C : Compliance at the critical load
- C_0 : Compliance within the linear part of load vs. displacement curve
- a_0 : Crack initiation
- a : Crack propagation
- G_{IIc} : Critical energy release rate mode II
- G_{Ic} : Critical energy release rate mode I

List of figures

Fig. 2-1. Schematic illustration of the manufacturing process of glass fiber.....	4
Fig. 2-2. Classification and properties of different types of glass fiber.	5
Fig. 2-3. Commercial forms of glass fibers.....	6
Fig. 2-4. Schematic setup of the manufacturing process for FRP composite by VaRTM.	9
Fig. 2-5. Failure modes of FRP composites [22]	11
Fig. 2-6. Improvement of the interfacial shear strength of GFRP composites by adding CNTs on using different routes [36].	13
Fig. 2-7. Effect of carbon nanofibers on the matrix viscosity of GFRP composites [37].	14
Fig. 2-8. The manufacturing process of CNFs by chemical and mechanical treatment [47]...	15
Fig. 2-9. Effect of microfibrillated cellulose (MFC) and bacterial cellulose (BC) on the IFSS of CFRP composites [3].	16
Fig. 3-1. Prepared CNFs suspensions with different concentrations.	21
Fig. 3-2. Schematic representation of microdroplet specimen (a) and the principle of microdroplet test (b).....	23
Fig. 3-3. Schematic illustration of CNFs treatment of woven glass fabrics and manufacturing process of composites by VATRM technique.....	25
Fig. 3-4. Field emission electron microscope HITACHI-SU8020.....	26
Fig. 3-5. FE-SEM images of untreated and CNF-treated GF: (a) as-received, (b) unsized, (c) 0.001 wt%, (d) 0.005 wt%, (e) 0.01 wt%, (f) 0.05 wt%, (g) 0.1 wt%, and (h) 0.5 wt%.	27
Fig. 3-6. Morphology and size of CNF clusters for treated GF: (a) 0.001 wt%, (b) 0.005 wt%, (c) 0.01 wt%, (d) 0.05 wt%, (e) 0.1 wt%, and (f) 0.5 wt%.....	28
Fig. 3-7. Evaluation of CNFs-grafted onto glass fiber: GF area grafted by CNFs (a), CNFs thickness layer (b), cluster density (c), and average cluster length (d).	29
Fig. 3-8. Weibull probability plots of IFSS for: (a) as-received GF-CNFs/EP, (b) GF-CNFs/EP, and (c) S/GF-CNFs.....	31
Fig. 3-9. Evolution of the IFSS of (a): as-received GF-CNFs/EP, (b) GF-CNFs/EP (black), and S/GF-CNFs/EP (red), and (c) CNFs and Silane treated GF/EP as a function of the number of passes.....	33
Fig. 3-10. SEM images of fiber fracture surface after microdroplet test for: (a) As-GF/EP, (b) GF/EP, (c) S/GF/EP (d) As-GF-CNF _{0.1} /EP, (e) GF-CNF _{10ppm} /EP, (f) GF-CNF _{50ppm} /EP, (g) GF-CNF _{0.1} /EP, (h) GF-CNF _{0.5} /EP, (i) 2P/GF-CNF _{0.1} /EP and (j)3P/GF-CNF _{0.1} /EP	35

Fig. 3-11. Flexural stress-strain curves of GF-CNFs/EP composites (a), and flexural strength of neat GF/EP and GF-CNFs/EP composites (b).	38
Fig. 3-12. SEM images of CNFs-treated glass fabrics and fracture surface of GF-CNFs/EP composites.	39
Fig. 3-13. Illustration of crack growth of interfacial debonding between reinforcing fibers and epoxy.	40
Fig. 4-1. Modified VaRTM process for manufacturing composite laminates.	44
Fig. 4-2. Specimens size and directions for flexural strength and bending fatigue tests.	45
Fig. 4-3. Evolution of CNF grafted on woven GF laminate.	45
Fig. 4-4. Characterization by different observation areas of GF laminate vacuum impregnated with 0.1 wt% CNF.....	46
Fig. 4-5. Flexural strength vs flexural strain curves and effect of CNFs on the flexural strength of GF/EP and GF-CNFs/EP composites.	47
Fig. 4-6. Morphology of the fracture surface of the untreated GF/EP and GF-CNFs/EP composites.....	48
Fig. 4-7. S-N curves of GF/EP and GF-CNFs/EP composites.....	49
Fig. 4-8. Fracture surface (b) and crack propagation (a-c) of the GF/EP and GF-CNFs/EP composites after flexural fatigue tests.	50
Fig. 5-1. Illustration of CNF incorporating GF and manufacturing GFRP composites laminates.	55
Fig. 5-2. Three-point ENF test: specimen set-up	56
Fig. 5-3. Illustration of compliance and critical load determination	57
Fig. 5-4. Morphology of untreated woven GF laminate (a), and CNFs-treated woven GF laminates: 0.05 wt% (b-c), 0.075 wt% (d-e), 0.1 wt% (f-g).....	58
Fig. 5-5. load vs. displacement curves of GF/EP and GF-CNFs/EP composites obtained from ENF tests.	59
Fig. 5-6. Interlaminar fracture toughness G_{IIC} of GF/EP and GF-CNFs/EP composite laminates	60
Fig. 5-7. FE-SEM photographs of fractured surfaces after ENF test for: neat GF/epoxy composite (a-b), and GF-CNF/epoxy composites with: 0.05 wt% (c-d), 0.075 wt% (e-f), 0.1 wt% (g-h).....	62
Fig. 5-8. Illustration of crack propagation in the GFRP composite laminates.....	63
Fig. 5-9. Fracture morphology of fiber traces at higher magnification for untreated, 0.075 and 0.1 wt% of GF/EP composites.	64

List of tables

Table 2-1. Physical and mechanical properties of glass fiber [6].	6
Table 2-2. Physical and mechanical properties of matrix resins [11]	8
Table 3-1. Nomenclature of manufactured CNFs-treated single GF/epoxy composites for microdroplet tests.	23
Table 3-2. Interfacial strength and Weibull distribution for GF-CNFs treated with and without silane.....	32
Table 5-1. average of interlaminar fracture toughness after ENF tests.....	60

Chapitre 1: General introduction

A composite is a material made from two or more constituent materials with largely different properties. The composition of these constituents leads to a stronger and more durable material than any of the constituents. Fiber-reinforced polymer (FRP) composites consist of a polymer matrix reinforced with fibers. Glass fiber (GF), carbon fiber (CF), and aramid fiber (AF) are commonly used as reinforcements in FRP composites. Each of these fiber types has its specific properties and field of applications. The performance of FRP composites depends on the properties of each constituent and the interfacial bonding between fiber and matrix.

Because of their outstanding mechanical properties as well as lightweight, FRP composites have been used for engineering applications such as automobile, aerospace, marine, biomedical, and structural applications. However, the high performance of FRP composites requires an efficient load transfer from matrix to fibers. Further, the fiber/matrix interface for pristine FRP composite is relatively weak compared to modified composites. To overcome this problem, good interfacial adhesion between the reinforcing fibers and matrix is highly desired. Therefore, two principal methods have been used to strengthen the fiber/matrix interface: fiber surface modification and matrix modification. These two methods have led to significant enhancement in the mechanical performance of FRP composites. It has been reported that surface modification of fiber can be physical, chemical, or a combination of both [1]. The chemical modification of fiber surface is carried out with sizing agents, for example, silane coupling agents are the most common to be used in FRP composites. While physically one can be made with nanomaterials including carbon nanotube (CNT) and graphene oxide (GO).

Those modifications, however, have their respective advantages. For instance, GFs treated with silane coupling have resulted in improving mechanical strength, while physical modification by coating GO on GF can significantly enhance the thermomechanical properties of composites [2]. On the other hand, the addition of nanofibers or nanoparticles into the matrix increases energy absorption and crosslinking density resulting from the high surface areas. Energy absorption and failure mode are largely affected by interface adhesion whose increase allows efficient load transfer between the fiber and the matrix. Moreover, the matrix modification by cellulose nanofibers (CNFs) can improve the matrix toughness leading to delaying matrix cracking and reducing delamination and crack propagation [3]. Accordingly, the fracture toughness and fatigue life of FRP composites can be improved by matrix toughening. However, the matrix modification method is limited by the increased viscosity of

the matrix and the lack of homogeneous dispersion of nanomaterials in the fiber bundles. Due to these drawbacks, a new method consisting of modifying physically the GF surface with CNFs is proposed in this dissertation. This method is suggested to avoid processing high-viscosity epoxy matrix, as well as to improve the mechanical performance of glass fiber-reinforced polymer (GFRP) composites. In this way, the following chapters describe and explain the methodology used and the results achieved during the study.

Chapter 1 defines FRP composites and their constituents. It also presents briefly the modification methods that have been used to improve the mechanical performance of composite materials.

Chapter 2 describes glass fiber and epoxy matrix. In this chapter, the general background of the study is described in detail and the most relevant methods and results from the literature are given.

Chapter 3 presents the improvement of interfacial strength of glass fiber/epoxy interface by grafting CNF on the reinforcement. To avoid the disadvantages of using a high-viscosity resin, CNFs are grafted onto the surface of GFs by a vacuum-assisted resin transfer molding (VaRTM) process. Different CNF concentrations were used for the surface modification of GFs. After the grafting process, the interfacial shear stress (IFSS) of GF/epoxy was improved. The optimum concentration of CNFs to improve IFSS is determined, and the strengthening mechanisms are clarified and quantitatively evaluated. The effect of CNFs on the flexural strength of GFRP composites is also investigated.

Chapter 4 provides the investigation of the improvement of fatigue life of GFRP composite modified with CNFs. To avoid surface roughness on one side of the GFRP composites, the manufacturing process of composites is changed. Then, CNFs are grafted to GF using the same method as in the previous chapter, and their dispersion in the GF fabrics is investigated. The influence of CNFs on fatigue life is investigated by three-point bending tests under high cycle stress. The mechanisms of failures in the manufactured composites are also studied. Discussion on the potential of vacuum impregnating CNFs suspension to GF fabric to improve the fatigue performance of GFRP composites is given.

Chapter 5 provides another method of grafting CNFs onto GFs to improve the interlaminar fracture toughness mode II. Although CNFs vacuum impregnation can improve the flexural strength and fatigue life of GFRP composites, CNFs are not homogeneously distributed in the entire GF laminate (e.g. at the middle of the GF laminate) due to the filtrating effect. To avoid

this drawback, CNFs were applied onto the interlaminar interface of GF laminates by the spraying method. Then, the effect of CNFs on interlaminar fracture toughness mode II is investigated and the fracture mechanisms are discussed.

Chapter 6 summarizes the results achieved in the study as well as some recommendations for future research.

Chapitre 2: Research background

2.1 Glass fibers

Glass fiber (GF) also called fiberglass is a melt-spun silica-based inorganic material generally used in composite materials. GF has a fine diameter varying from 5 to 24 μm . They are readily manufactured from raw materials such as silicates, clay, boric acid, soda, limestone, fluorspar, etc. GFs were made and used for decoration for the first time by ancient Egyptians, while the commercial GFs were manufactured in 1937 by a joint venture between Corning Glass and Owens-Illinois [4]. Nowadays, due to their esthetic and shiny characteristics, glass fibers have been used in many applications like furniture, utensils, mirrors, and artworks [4].

2.1.1 Manufacturing process

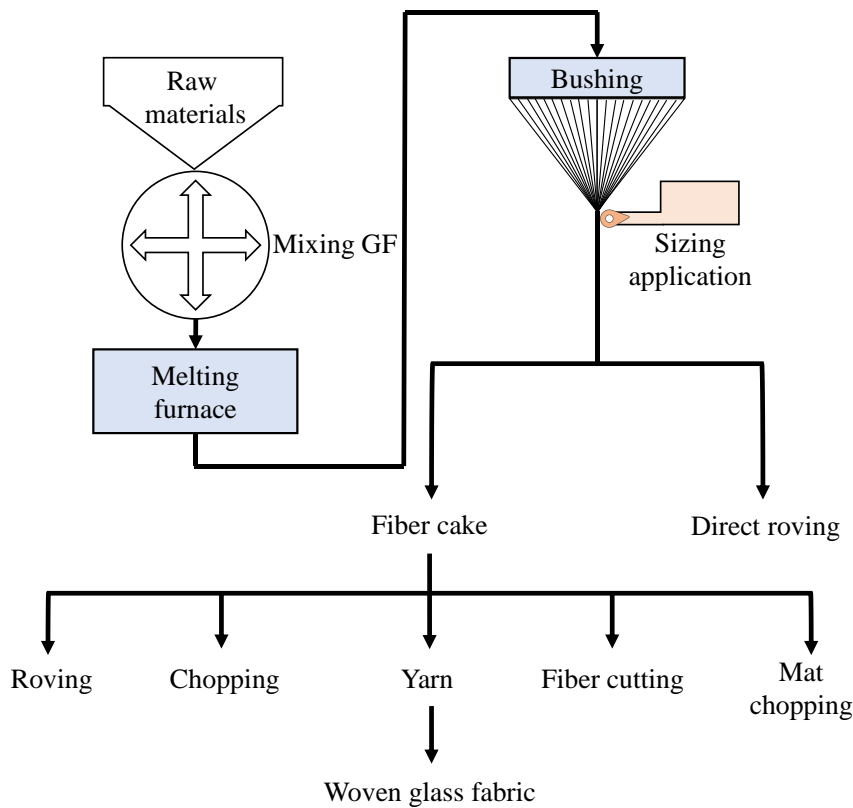


Fig. 2-1. Schematic illustration of the manufacturing process of glass fiber.

Commercially forming glass fiber involves a mixture of silica sand, limestone, boric acid, and other additional ingredients. The mixture is heated at a high temperature until the melting stage at about 1260°C . The molten glass then flows from the melting furnace through a fine-hole platinum bushing. Thereby, GFs are formed from the bushing holes and rapidly cooled down with water spray. GFs are sized (protective or functional coating) if required and then gathered. Then, various forms including yarns, fabrics (cloths), chopped strands, and mats have

been made for their industrial applications. The details of the manufacturing process have been described by Thomason [5]. A schematic description of the manufacturing process of GF is presented in Fig. 2-1.

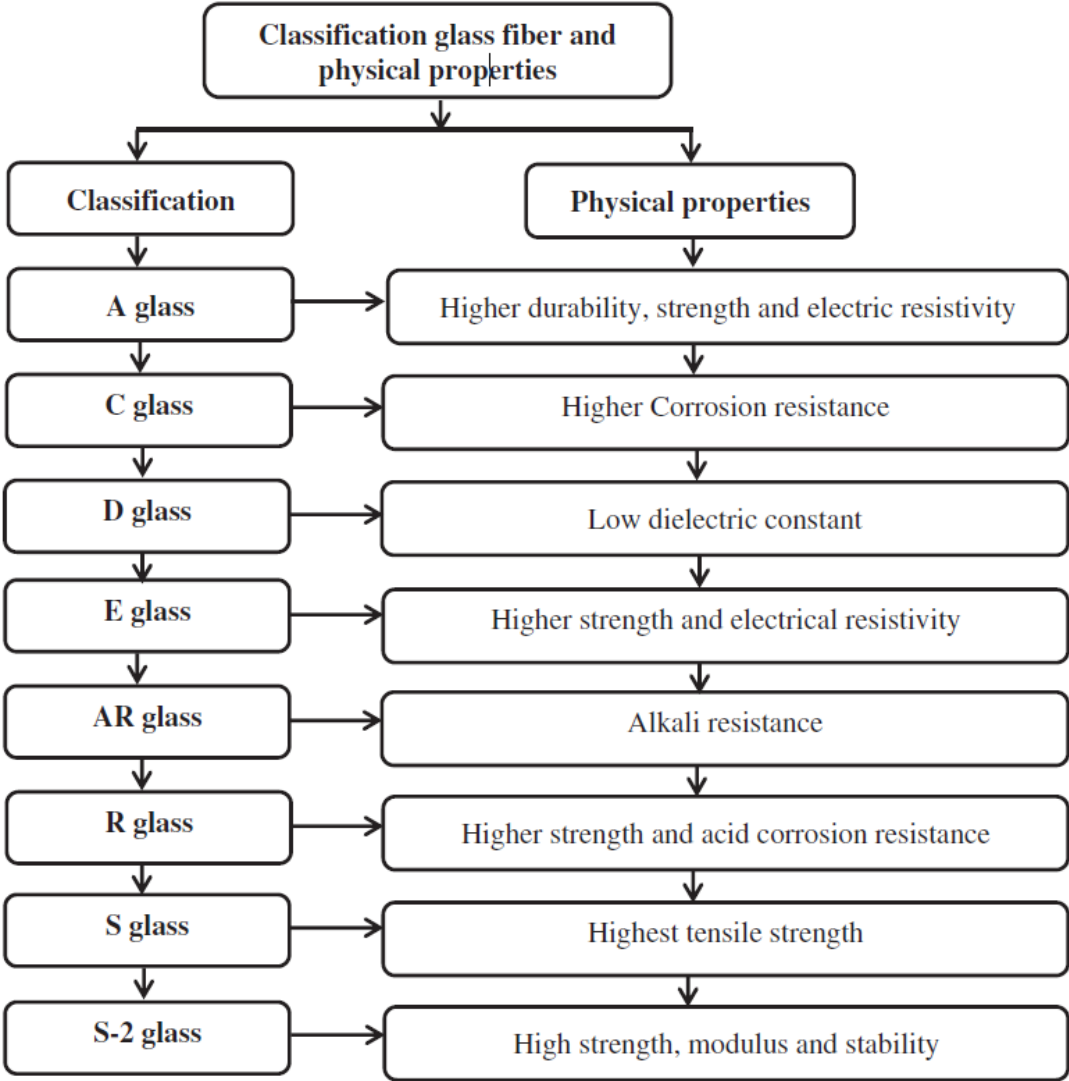


Fig. 2-2. Classification and properties of different types of glass fiber.

2.1.2 Classification and properties

Glass fibers are classified according to the combination and fraction of raw materials as well as the environment of their future applications (See Fig. 2-2). Therefore, it is very important to pay attention to the chemical combination because the properties of the final product highly depend on it. As mentioned before, GFs have excellent fire resistance due to their high melting point (over 1100°C). Glass fiber is a hard material that provides high tenacity. Moreover, GF offers an excellent combination of properties from high strength to fire resistance at a low cost. GFs also provide high flexibility in design because they can be molded into complex shapes. The versatility of GF makes it a unique industrial textile material. Table 2-1 gives a

summary of different GFs with their specific properties. Thereby, GFs are widely used in FRP composites, roofing applications, in building structures to prevent the crack of concrete, as well as in bridge construction [4]. Various commercial forms of GFs as reinforcement in composite materials are given in Fig. 2-3. Accordingly, FRP composites can be classified into fiber-reinforced polymer or particle-reinforced polymer depending on the type of reinforcement.

Table 2-1. Physical and mechanical properties of glass fiber [6].

Fiber type	Density (gm/cm ³)	Tensile Strength (MPa)	Young's Modulus (GPa)	Coefficient of thermal expansion (10 ⁻⁷ /°C)
A-glass	2.44	3310	68.9	73
C-glass	2.52	3310	68.9	63
D-glass	2.14	2415	51.7	2
E-glass	2.58	3445	72.3	54
AR-glass	2.7	3240	73.1	65
R-glass	2.54	4135	85.5	33
S-glass	2.46	4890	86.9	16

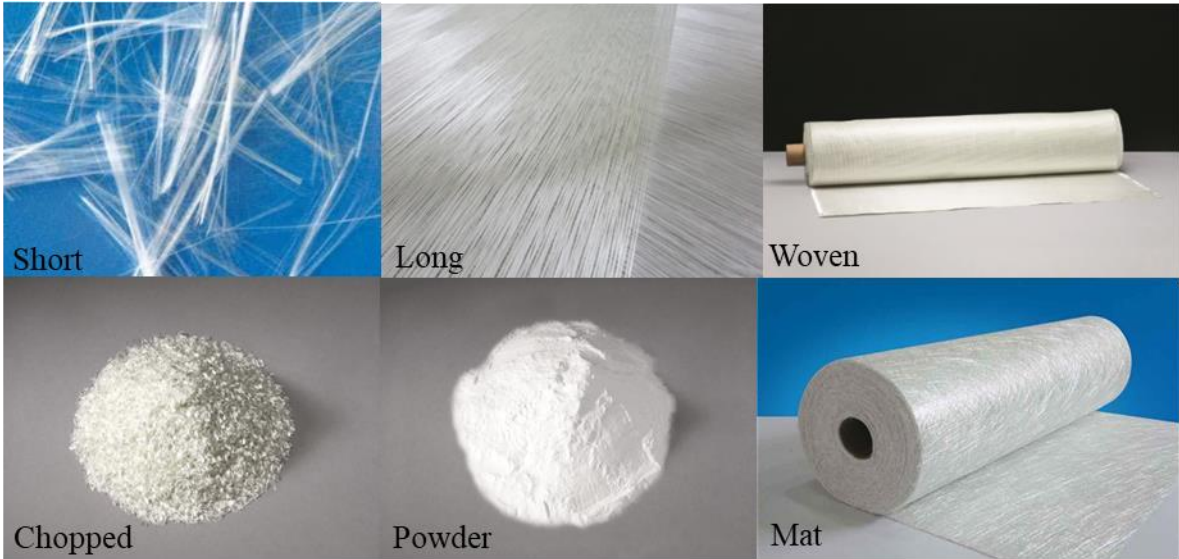


Fig. 2-3. Commercial forms of glass fibers.

The reinforcing fibers such as GFs offer high strength and stiffness but cannot be made into a shape or form when used alone. Therefore, they need to be impregnated with matrix resin for their engineering application. The reinforcement bears most of the applied load and has higher strength and stiffness than those of the matrix. The matrix is used primarily to bind the reinforcement together, transfer the transverse and shear stress between constituents. It also protects reinforcing fibers against external and environmental impacts. GFs account for more than 90% of all reinforcements in polymer matrices (thermoplastic and thermoset). These

polymeric matrices have very different properties and fields of application. Hence, there is a necessity to pay attention to the performance of matrix when designing composite materials.

2.2 Performance of epoxy matrix in FRP composites

2.2.1 Properties of epoxy resins

To design composite products, it is necessary to select carefully the reinforcement, the matrix, and the manufacturing process. The properties of epoxy matrix determine most of the damage types such as debonding, delamination, chemical resistance, high-temperature creep, and water absorption. Taking note of their high mechanical properties, chemical and heat resistance, thermoset resins including polyester, vinyl ester, epoxy, and polyurethane resins become more predominant than thermoplastics (nylon, polyether ether ketone, polyphenylene sulfide). Epoxy resins represent some of the utmost performance thermosetting resins used in FRP composites due to their excellent properties and affordable cost [7]. On the other hand, the performance of epoxy resins strongly depends on the curing and post-curing temperatures which range from 5 to 200 °C depending on the type of curing agent [8]. In most cases, curing epoxy resin at room temperature is not enough to fully cure the mixture (epoxy resin + hardener). Whilst, post-curing at high temperatures has been proved to be effective to improve mechanical properties of glass fiber-reinforced epoxy composites [9]. Therefore, post-curing at high temperatures is required to increase the chemical and thermal resistance, and electrical insulation of the final composite products.

2.2.2 Applications

Although epoxy resins are brittle and cannot be reused once cured, they offer excellent physical and mechanical properties in comparison with other polymer resins. As shown in Table 2-2, epoxy has higher mechanical performance and better thermal stability [10]. Besides that, due to their good thermal and chemical resistance, good adhesion to metals, and low shrinkage, epoxy resins have been extensively used in polymer matrix composites. They also have low viscosity and provide easy wetting of reinforcement resulting in excellent impregnation of the reinforcement, and a fast manufacturing process for composite materials. Therefore, the use of epoxy resins is widely expanded in various industrial applications including aerospace, automotive, chemical, and water tanks.

Table 2-2. Physical and mechanical properties of matrix resins [11]

Physical and Mechanical properties	Matrix resins		
	Epoxy	Polyester	Vinylester
Density (gm/cm ³)	1.2 – 1.4	1.1 – 1.4	1.15 – 1.35
Tensile Strength (MPa)	55 – 130	34.5 – 104	73 – 81
Young's Modulus (GPa)	2.75 – 4.10	2.1 – 3.45	3.0 – 3.5
Poisson's ratio	0.38 – 0.40	0.35 – 0.39	0.36 – 0.39
Coefficient of Thermal Expansion (10 ⁻⁶ /°C)	45 – 65	55 – 100	50 – 75

2.3 Glass fiber-reinforced polymer

Glass fiber-reinforced polymer (GFRP) composites are materials made of a polymer matrix reinforced with glass fibers. The mechanical performance of GFRP composites depends on the mechanical properties of the constituents, the thermal stability and the interfacial bonding between them allowing efficient stress transfer from matrix to fiber [12]. GFs are usually processed in plain weave or mat structures. These forms offer the possibility to control the fiber orientation and fiber volume fraction, which highly affect the mechanical properties of the final composite. Various techniques such as hand lay-up, autoclave, spray-up, injection molding, compress molding, pultrusion, vacuum bag molding, resin transfer molding (RMT) and VaRTM processes, have been used to manufacture GFRP composites [13]. These processes consist of impregnating the reinforcing fibers with the polymer matrix. However, each process has its specific applications relative to the complexity and size of the composite parts.

The selection of the manufacturing process has a remarkable effect on the mechanical performance, production cost and quality of the composite part. This can be guided by the following criteria: high property control, cost-effectiveness, high complexity of the composite product, high productivity, and quality of finishing surface. However, none of the manufacturing processes can offer simultaneously all the required characteristics [14]. For example, although it provides high-quality products, the autoclave process is limited to the possible size of the composites to be manufactured and the huge initial investment requirement for its installation. Similar to the autoclave, the pultrusion process also requires high investments and exhibits limited geometrical shape. It is generally processed at high pressure (up to 6900kPa) and high temperature (~185°C) [14, 15]. Besides, its productivity is low because it takes longer processing time and labor (laying-bagging-demolding). In addition, with the hand lay-up process, one side finished surface may require additional work and fiber volume

fraction is lower compared to that of VaRTM. In contrast to the autoclave process, VaRTM does not require high heat or high pressure. Therefore, the VaRTM process is widely used in various industries due to its flexibility for designing large FRP composites products.

2.3.1 VaRTM process

Vacuum-assisted resin transfer molding is a recent variation of RMT. The difference between RTM and VaRTM is that the upper mold is replaced with a plastic vacuum bag and resin is drawn into the laminate of GF fabrics using a vacuum pressure [14]. The following is VaRTM process in brief; A release agent molding is first applied on a stainless-steel plate. The laminate is then placed on the molding plate. Next, a flow media is laid between the laminate and vacuum bag to facilitate the infusion of the resin. To ensure no vacuum leakage, sealant tape is used at the entire boundary of the molding area. Infusion spiral is attached at the border of the mold (in this study: on the side of inlet and outlet ports). The molding area is then covered by the vacuum bag to make an airtight setup under vacuum pressure. A review by Tamakuwala et al. [16] has described this process in detail. Fig. 2-4 illustrates an experimental setup of manufacturing FRP composites by VaRTM process.

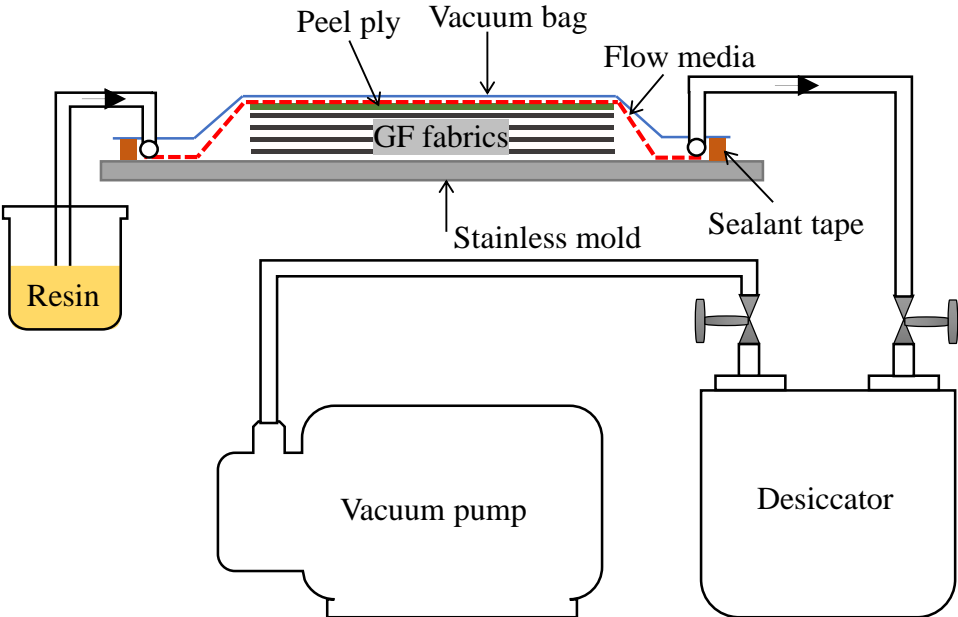


Fig. 2-4. Schematic setup of the manufacturing process for FRP composite by VaRTM.

VaRTM process allows no space for excess air in the manufactured composite [13]. The matrix resin is infused into the laminate under vacuum pressure which compacts the GF fabrics and reduces the formation of voids in the composite [17, 18]. In addition to the advantages aforementioned, VaRTM required less curing time and can be used for the open mold manufacturing process [16]. Hence, for any type of shape or size, VaRTM offers the possibility

to control the thickness as well as the fiber volume fraction (up to 70%) [16, 15]. Therefore, as a result of its cost-effectiveness, ease of manufacture and low-cost tooling, VaRTM is commonly used for manufacturing large FRP composites. It is developed for making composite parts used in marine, aerospace, wind power, and automobile industries [19].

2.3.2 Applications of GFRP composites

GFRP composites are widely used in many engineering applications due to their high corrosion resistance, high specific strength and stiffness, cost-effectiveness, and better damage resistance for impact loading [6]. They possess functional characteristics on a par with steel, specific gravity equal to one-quarter of steel, and higher stiffness than aluminum [20]. GFRP composites can be also used as fixtures in a variety of shapes and textures in building constructions due to the low thermal conductivity. Therefore, they are used in marine, automobile, aerospace, power generation, electronics, and bridge constructions. Some examples of GFRP composite parts: are pipelines, windmill blades, water tanks, roofing sheets, washing machine bodies, aircraft parts, automobile parts, and more.

2.3.3 Failure in FRP composites:

It is well known that at the microscopic level fiber reinforced polymer composites are naturally anisotropic and structurally heterogeneous due to the fiber orientations in a specific order offering the possibility to design the mechanical performance of the composites. However, different failure modes (shown in Fig. 2-5) such as debonding, matrix cracking, fiber breakage, fiber pullout, fiber bridging, and delamination may result from the aforementioned characteristics of FRP composites. These damages account for the main drawbacks of composite materials. Therefore, it is necessary to examine macroscopically or microscopically the failure modes to evaluate the mechanical properties of composite materials. To design FRP components it is important to investigate how the failure of composites occurs. The failure modes of composites have been well described by Fragoudakis [21]. They affect strongly the performance of composite materials and are responsible for the degradation of their mechanical properties. Therefore, different methods have been used by many researchers to overcome or limit the effect of failure modes in FRP composites. Thereby, two routes have been used: the matrix toughening by adding nanomaterials or strengthening the fiber/matrix interface by modifying the fiber surface. These methods are well explained in the following sections of this chapter.

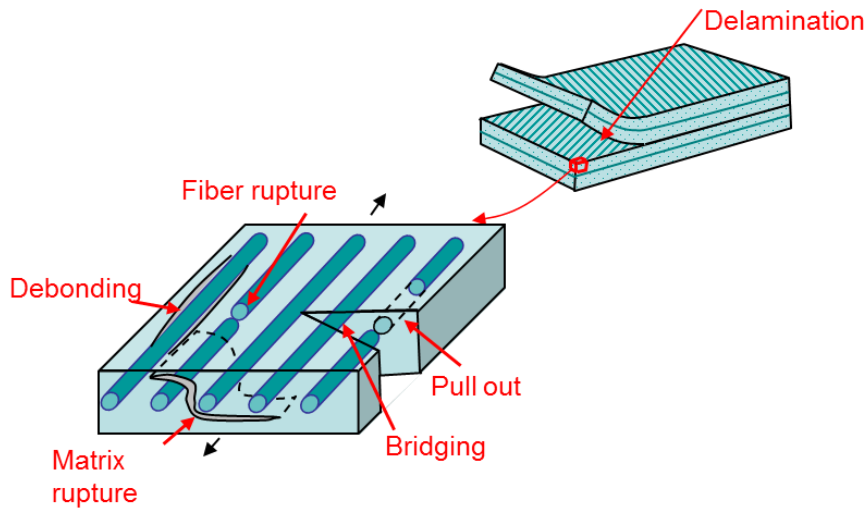


Fig. 2-5. Failure modes of FRP composites [22]

2.3.4 Improvement of glass fiber/epoxy interfacial strength

In FRP composite, many parameters such as fiber volume fraction, fiber orientation, matrix material, moisture, and temperature effectively influenced the energy dissipation of the material. Controlling the stress transfer between fiber and matrix is a required parameter to ensure good fiber/matrix adhesion, which results in better interfacial strength. Therefore, fiber surface modifications are generally used to improve the adhesion of the fiber/matrix interface. Several sizing agents have been applied to the fiber surface to increase its compatibility with the matrix. Silane coupling agents are one of the coupling agents that have been extensively used to protect GF and promote adhesion to the matrix [12, 23]. Since fiber and matrix are physically different, silane coupling agents can form a durable bonding structure between inorganic and organic materials. The presence of silanol groups on the glass fiber surface reacts with the hydroxy groups of fibers to form siloxane linkages making organofunctional groups which then react with the matrix functional groups. It is well known that the mechanical properties of composite materials can significantly improve resulting from the chemical and structural variances of the coupling agent interface layer [24].

To measure the interfacial adhesion between fiber and matrix, different experimental methods including, microdroplet debonding and single fiber fragmentation, micro-indentation, and fiber pull-out have been used. From these measurement techniques, the microdroplet debonding test is the most common method. The test consists of pulling out the fiber from a cured resin droplet, and the maximum load required for the debonding is recorded. The interfacial shear strength (IFSS) can be calculated with the following equation using the recording results:

$$\tau = \frac{F}{\pi \cdot d_f \cdot L_e} \quad (2.1)$$

Where, τ is the IFSS, F is the maximum load required for debonding the resin droplet, d_f is the fiber diameter, L_e is the embedded fiber length.

Gonzalez et al. [25] investigated the effect of surface treatment of natural fibers reinforced composites. Silane coupling agent and alkaline were adopted for fiber surface modification. As a result, the IFSS was improved by 122 % in the modified fiber/high-density polyethylene composite with respect to the unmodified one. This remarkable improvement was attributed to chemical treatment for rougher fiber surfaces resulting in better mechanical interlocking between the fiber and matrix. Additionally, Sahin et al [26] modified the surface of GF with a photoreactive silane as well as methacrylic functional organosilanes to improve the interfacial resistance between the GF and the acrylate-based photopolymer. Noteworthy enhancements of 128% and 84% were reported for the photoreactive silane-modified GF and methacryl silane-modified GF, respectively. Therefore, the chemical modification of fiber surface has proved its effectiveness in improving the interfacial strength in composite materials.

Iglesias et al. [24] studied the effect of three types of silane-treated glass fiber surface on mechanical properties of GF/epoxy composite. The results indicated a significant improvement in the stiffness of the silane-modified composites (with monomeric and linear molecule structure) by about six times higher than the unmodified composite. Whereas the crosslinked structure did not indicate any improvement due to the restriction of chemical bonds to the outer region of the silane coating layer. Arslan et al. [27] improved the mechanical properties of basalt/poly (butylene terephthalate) composites by modifying the basalt fiber surface with silane coupling. Similarly, Abdelmouleh et al. [28] obtained a significant improvement of 41% in flexural strength of silanes treated-cellulose fibers/unsaturated polyester (UP) composites resulting from a better interfacial bonding between fibers and UP matrix. It was also found that hydrogen bonding between glass fiber and silane coupling plays a vital role in improving the adhesion of the GF/matrix interface. Moreover, the interlaminar shear strength (ILSS) of glass fiber/UP composites has been enhanced by 20% with the addition of 0.4% of silane [29].

Besides the chemical modification method, physical modification by adding nanomaterials into FRP composites has been widely used to enhance further the mechanical properties of composite materials. Thus, nanomaterials are considered secondary reinforcements in the production of hybrid composite materials. Due to their specific mechanical performance, nanomaterials such as carbon nanotubes (CNTs) [30], cellulose nanofibers (CNFs) [3, 31],

silica-nanoparticles [32], graphene oxide (GO) [33], nanoclay [34], and cellulose nanocrystals (CNCs) [35] have been attractive materials for improving the mechanical properties of FRP composites. They are either added into the matrix as a modifier or directly incorporated at the fiber/matrix interface through the fiber surface. Therefore, many research studies have been focusing on adding nanomaterials into the matrix of composites. For instance, incorporating 2.5 wt% of nanoclay into the matrix of GFRP composites has resulted in improving the interfacial elastic modulus up to 43%. Interestingly, in Fig. 2-6 Godara et al. [36] have improved the IFSS of GFRP composite by incorporating CNTs with different routes: grafting CNTs onto GF (GF-CNT/EP), mixing CNTs with the matrix (GF/EP-CNT), and combining grafting and mixing methods (GF-CNT/EP-CNT). For CNT-modified composites, the IFSS was significantly improved in comparison with the pristine composite. By coating multiwall carbon nanotubes (MWCNTs) onto CFs and GFs surface, significant improvements in interfacial strength between the reinforcing fibers and the matrix were obtained [30]. Comparatively, it is indicated that the matrix modification method could be limited by the increase in matrix viscosity, which reduced the mechanical performance of composite materials [37]. The high viscosity of the matrix resulted in the incomplete impregnation of fibers with epoxy resin. Fig. 2-7 shows an example of the effect of matrix modification by nanomaterials on the viscosity. The grafting method has been then found to be the most effective method for improving interfacial strength.

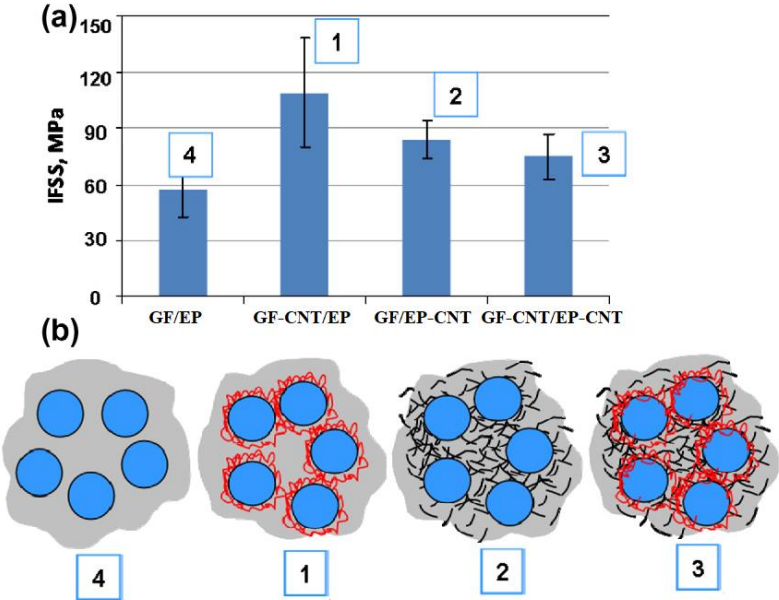


Fig. 2-6. Improvement of the interfacial shear strength of GFRP composites by adding CNTs on using different routes [36].

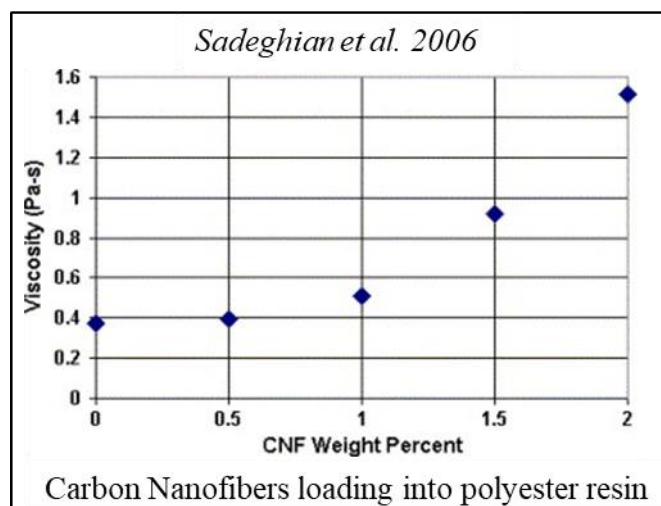


Fig. 2-7. Effect of carbon nanofibers on the matrix viscosity of GFRP composites [37].

2.3.5 Effect of cellulose nanofibers on the performance of composites.

Nanocelluloses have been extensively used in polymer-based nanocomposites as alternative and sustainable materials. Celluloses nanomaterials are derived from different sources, such as wood plants, algae, bacteria, and tunicates. Hence, two kinds of cellulose nanomaterials have been developed: cellulose nanofibers (CNFs) and cellulose nanocrystals (CNCs). CNFs are obtained by chemical treatment and mechanical disintegration. The manufacturing process of CNFs is presented in Fig. 2-8. Cellulose is well known as a biodegradable and recyclable “green” material. It is also the most abundant nanomaterial available on the earth with more than seven tons produced annually [38]. CNFs have five times the strength of steel, low thermal expansion on par with glass fiber, and high specific strength and stiffness. Moreover, cellulose fibers are more flexible than glass fibers during their processing, which results in excellent mechanical properties [39, 40]. In addition, CNF has low cost and high damping performance. Based on their excellent properties previously highlighted, CNFs have been used in various applications such as packaging, automobile, medical, buildings, and electronics [41]. However, CNF may suffer from its hydrophilicity, which makes CNF incompatible with hydrophobic polymers resulting in the formation of aggregations [42, 43]. To solve this problem, many chemical surface modifications have been adopted [44, 45, 46]. For instance, Sato et al. [45] have used 10 wt% CNFs as reinforcement for HDPE polymer. They also applied a surface modification of CNFs using alkenyl succinic anhydride. The tensile strength of the CNFs/HDPE composite increased by about 17% compared to the neat HDPE. After surface modification, the tensile strength was improved by 100%.

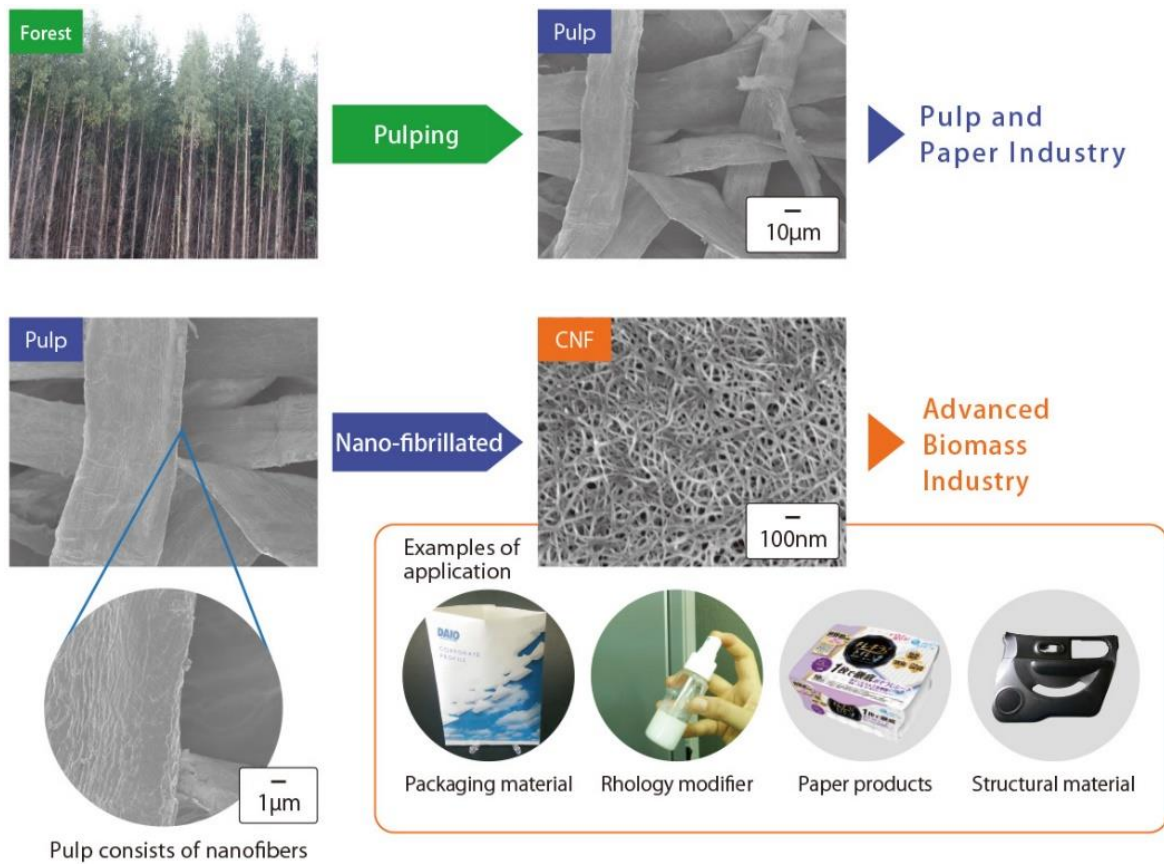


Fig. 2-8. The manufacturing process of CNFs by chemical and mechanical treatment [47].

Recently, CNFs have attracted the attention of many researchers to improve the mechanical properties of FRP composites. However, it is necessary to optimize the CNF content whose high concentrations can lead to the formation of aggregates bringing about the degradation of the properties of composites. Kumar et al. [35] improved the flexural strength (by 50%), tensile strength (by 24%), and storage modulus (by 56%) of GFRP composite by adding 2 wt% of CNCs into the matrix. Incorporating 1 wt% of CNFs into epoxy matrix has highly improved the mechanical performance of the composites [48]. In addition, coating TEMPO-mediated CNCs (t-CNC) onto GF exhibited significant improvement in flexural properties of the CNC-modified GFRP composites [49]. Meanwhile, the study of Shao et al. [3] indicated an improvement of 77% in the IFSS of microfibrillated cellulose (MFC)-modified CF/EP composites with respect to the neat CF/EP composite. Fig. 2-9 shows the influence of cellulose fibers on the IFSS of CFRP composites.

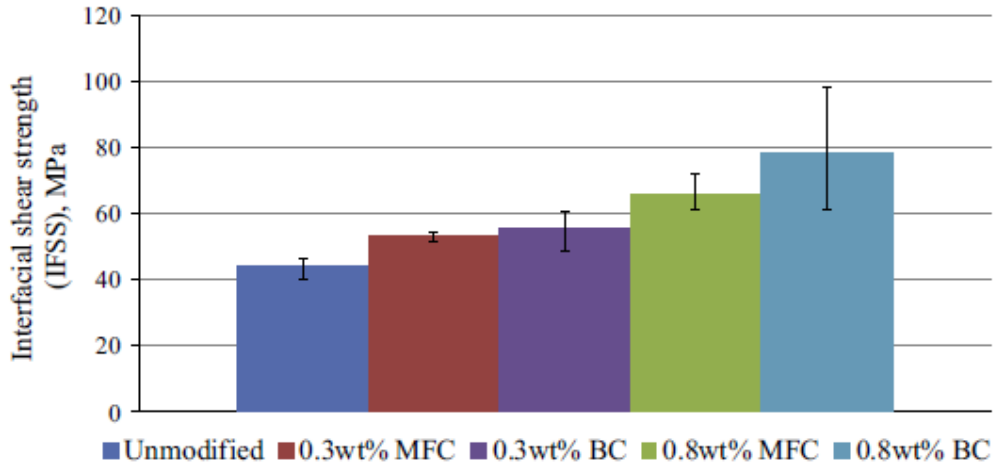


Fig. 2-9. Effect of microfibrillated cellulose (MFC) and bacterial cellulose (BC) on the IFSS of CFRP composites [3].

In structural applications, GFRP composites are becoming a desirable material due to their specific characteristics including high corrosion resistance and low cost in comparison with CFRP composites. However, the relatively low fatigue life limits their applications. Therefore, many researchers have been focusing on improving the fatigue life of GFRP composites by adding nanomaterials. For instance, MWCNTs have been added to the matrix of GFRP composites to improve the fatigue performance by more than 10 times compared to the pristine composite [50]. Manjunatha et al. [51] have added silica nanoparticles to GFRP composites. The results exhibited an improvement of the fatigue life by up to four times due to the presence of nanoparticles in the matrix. In addition, the fatigue life of CFRP composites was significantly improved up to 30 times by adding 0.3 wt% of cellulose fibers [3]. According to these studies, the incorporation of nanomaterials into the matrix contributed to inhibiting matrix cracking, and reducing crack propagation and delamination

On the other hand, the interlaminar fracture toughness (IFT) is a critical characteristic in the FRP composite laminates. Thus, different methods including incorporation of nanomaterials have been used recently for improving the IFT of composite laminates. For example, CNFs exhibited significantly enhancement in the interlaminar fracture toughness of CFRP composites [52]. Chen et al. [33] have improved the performance of glass fiber/epoxy composite by grafting GO onto the reinforcing fibers. The interlaminar shear strength (ILSS) of the composites increased by 41% resulting from the strong GF-GO/epoxy interface. Additionally, Quan et al. [10] demonstrated that incorporating 1 wt% of multiwall carbon nanotubes (MWCNT) into the matrix of CFRP composites improved the IFT mode II (G_{IIC}) significantly by 170% while the IFT mode I (G_{IC}) exhibited moderate enhancement. Similarly, Saboori et al. [53] reported an

increase of 27% in G_{IC} with 0.5 wt% of MWCNT-modified epoxy nanocomposites, which then decreased slightly with 1 wt% of MWCNT content. The low improvement of IFT in G_{IC} compared to that in G_{IIC} could be attributed to the difference in the toughening mechanisms.

2.4 Motivation

The wide range of properties offered by FRP composites and the ability to tailor these properties depending on the end use of the materials make composites attractive materials in various industrial applications. Since demands for high-strength materials with lightweight are increasing in the market, FRP composites are becoming a potential candidate for engineering applications. Therefore, as mentioned before the fiber/matrix interface plays an important role in the performance of composite materials [54]. The stronger the interfacial bond is between the fibers and the matrix, the better the stress transfer is from the matrix to the fibers. However, it has been shown that the onset and the growth of damage in FRP composites can be delayed by adding nanomaterials. Of these, natural fibers including cellulose nanofibers (CNFs), have been actively used in composite materials, because they have a low environmental impact in comparison with other nanomaterials (e.g. CNTs and GO). Carbon nanotubes and graphene oxide, although they exhibit excellent mechanical properties for improving the performance of FRP composites, their industrial use could be limited due to their negative effect on the human body. Therefore, the use of CNFs in composite materials can contribute to the realization of a low-carbon society. Up to date, matrix modification by CNFs and chemical modification of the surface of CNFs are the most common methods used to improve the mechanical properties of FRP composites. The challenge for this research is to improve the performance of FRP composites by incorporating CNFs without chemical modification of the surface. Thus, the achievement of the following objective may contribute to enhancing and manufacturing polymer composites with low-cost and sustainable nanomaterials.

2.5 Objective

The objective of this research work is to investigate the effect of CNF grafting on the reinforcement of GFRP composites on their mechanical properties. A new approach by vacuum impregnating GFs with CNFs is developed to improve the strength of GFRP composite with a low quantity of CNF. This approach might avoid processing high viscosity resin. To achieve this goal, the following tasks were addressed:

- Physical surface modification of glass fibers and quantitative evaluation of the strengthening mechanisms of the glass fiber/matrix interface;

- Improvement of the interfacial strength between GF and epoxy resin;
- Grafting CNFs onto GFs using vacuum impregnation method to improve the flexural properties and fatigue life of GFRP composites.
- Investigation of CNFs effect on the interlaminar fracture toughness mode II.

Chapitre 3: Study on the improvement of interfacial strength between glass fiber and matrix resin by grafting cellulose nanofibers

3.1 Introduction

Due to their exceptional mechanical properties, high corrosion resistance, and low density, fiber-reinforced polymer composites (FRPs) are widely used in various industries, including aerospace, automobile, marine, and structural applications. However, FRPs can suffer from damages, such as interfacial debonding, micro-cracks, and delamination, and these defects may limit the mechanical and chemical properties of the FRPs.

In recent years, CNFs have been used as reinforcement in nanofibers-reinforced polymer nanocomposites in which they are randomly oriented in the matrix to form a quasi-isotropic material. Another advantage of CNFs as reinforcing nanofibers is that they can be processed with thermoplastic matrices, promoting their use in structural applications. However, CNFs have a compatibility issue with most polymeric matrices because their hydrophilic nature leads to a weakening of the CNFs/matrix interface [55]. To overcome this drawback different methods of surface treatment, such as silane coupling agent [56], alkali treatment [57], and acetylation [58], have been developed to functionalize the surface of cellulose fibers.

Silane coupling agents are known as intermediary bonding inorganic materials to organic materials thanks to their specific functional groups. Cellulose nanocrystals (CNCs) treated with silane coupling can significantly improve their dispersity and compatibility in the polymer matrix [59, 56]. The reactivity of silanol groups (Si-OH) with glass, silica, and alumina is easy with a large number of hydroxyl groups (-OH) on the surface of inorganic materials. In addition, silane-treated microfibrillated celluloses (MFC) are effective in improving the mechanical properties of MFC/Epoxy composites [60]. Lu et al. [57] studied surface modification of bamboo cellulose fiber (BCF) using sodium hydroxide and silane coupling agents. Their results indicated that silane-treated BCF exhibited better mechanical properties than those of sodium-treated BFC and that this improvement resulted from the chemical bond between cellulose fibers and epoxy molecules.

To improve the interfacial strength of FRPs, different nanomaterials have been used in academic research. Tian et al. [61] and Shao et al. [62] improved the mechanical properties of CF/EP composites by modifying the epoxy matrix with silica-nanoparticle and CNFs, respectively. Shao et al. reported stronger interfacial adhesion in the modified fiber/matrix composites (at 0.8 wt.% CNFs) than in the unmodified composite, resulting in a significant

enhancement in the IFSS of 77 %. Furthermore, previous studies [36, 63] have established that using carbon nanotubes (CNT) coated on the surface of fibers is more effective in improving IFSS than adding them into the matrix. Godara et al. [36] applied CNT to glass fiber/epoxy composites in three different methods: (1) CNT mixed into the matrix, (2) grafted onto fibers, and (3) combines methods (1) and (2) simultaneously. Through all of these methods, grafting CNT onto glass fiber (GF) was revealed to be the most effective way to improve the IFSS by at least 44% higher than those obtained from methods (1) and (3). Similarly, Lui et al. [64] coated graphene oxide (GO) onto carbon fiber and manufactured CF-GO/PEEK composites. They achieved an improvement of ~50% and ~29% in IFSS and flexural strength, respectively. CNT and GO have been attractive for improving the mechanical performance of FRP composites, but the high cost and carcinogenicity limit their applications. The enhancement of these properties highly depends on the fiber/matrix interface for which the adhesion can be chemically or physically improved by fiber surface treatment or desizing the reinforcing fibers, respectively. Specifically, chemical bonding, Van der Waals bonding, mechanical interlocking, and wettability are the predominant mechanisms behind the improvement of interfacial adhesion between fiber and matrix [65, 66, 67].

Very recently, the addition of cellulose microcrystals (CMCs) in the matrix of GF/EP composite has shown a significant improvement in the interlaminar shear strength and flexural properties by 65% and 76%, respectively [68]. However, when CMCs were loaded into the matrix by more than 1 wt%, the mechanical properties have decreased due to the heterogeneous dispersion of CMC and aggregations. Although mixing cellulose nanomaterials with epoxy resin can improve both fiber/matrix interfacial strength and the matrix toughness, it may increase the resin viscosity and makes the matrix difficult to impregnate into fibers [61, 52]. In addition, at a certain amount of loading nanomaterials into FRPs, the mechanical properties may degrade due to aggregations [36, 50, 68]. The dispersion and aggregation of nanomaterials in the matrix strongly affect the mechanical properties of composite materials [69]. To avoid processing high viscosity resin and formation of aggregations in the matrix, CNCs have been added to chopped GF roving by dipping coating to improve flexural and interfacial strength of GF/EP composites [66].

To the best of the authors' knowledge, no study has reported enhancing the performance of FRP composites by grafting CNFs onto reinforcing fibers. Therefore, in this study, CNFs were grafted onto glass fibers to improve the interfacial strength of the CNFs-grafted glass-fiber-reinforced epoxy (GF-CNFs/EP) composites. The objective of this research is, firstly, to clarify

the improvement of the interfacial adhesion between glass fiber and epoxy resin by grafting CNFs; secondly, to investigate the effect of grafting CNFs on flexural strength of GF-CNFs/EP composites. For the first objective, microdroplet tests were conducted to evaluate quantitatively the interfacial strength between CNF-grafted GF and epoxy resin. For the second objective, a new approach using VaRTM for grafting CNFs onto GF fabrics, and then for manufacturing the GF-CNFs/EP composites was proposed. This method can avoid the disadvantage in the manufacturing process, which decreases the flexibility of glass fabrics by grafting CNFs. The flexural strength of composites was determined by three-point bending tests. The strengthening mechanisms and effect of silane treatment on the IFSS of GF-CNFs/EP composites were also discussed.

3.2 Experimental methods

3.2.1 Materials

Plain woven glass fabric (from Nittobo Techno Co., KS2750) with a single fiber diameter of 10 μm (as-received glass fiber) and a density of 104 g/m^2 was used. Epoxy-phenol novolac resin (Araldite LY5052) and cycloaliphatic polyamine (Aradur 5052) were supplied by Huntsman Advanced Materials LLC and then used as the main agent and hardener, respectively. CNFs slurry (2 wt%) was supplied by Kochi Prefectural Paper Technology Center, and silane coupling agent 3-glycidoxypropyltrimethoxy silane (KBM-403) was provided by Shin-Etsu Chemical Co., Ltd. The CNF width is between 10 to 50 nm [31].

3.2.2 CNFs and silane preparation

CNFs were diluted with purified water and then stirred by ultrasonication for 1 hour to make 0.5 wt% of CNFs suspension. From this concentration, seven other CNFs suspensions (0.0001, 0.0005, 0.001, 0.005, 0.01 wt%, 0.05 wt%, 0.1 wt%) were made by adding water and then stirring for 30 minutes.

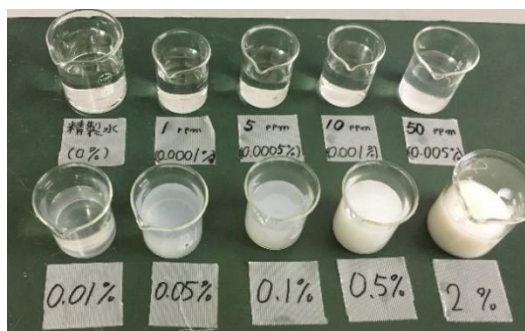


Fig. 3-1. Prepared CNFs suspensions with different concentrations.

Fig. 3-1 shows CNFs suspensions with different concentrations used in this study. As for silane preparation, 1.0 g of silane coupling agent was mixed with 99 g of aqueous acetic acid (1.0 wt%). The mixture was stirred for 30 minutes using a mixer with a rotational speed of 450 rpm; thus, 1.0 wt% of silane was prepared. The matrix was mixed with a mass ratio of 100:38 (epoxy resin/hardener). The mixture was stirred for about 5 minutes and then degassed for 20 minutes using a vacuum desiccator to remove voids.

3.2.3 *Unsize glass fiber preparation*

Woven glass fabrics were cut to the desired dimensions and heat-treated at 350°C for 1 hour to remove the sizing agent. Afterward, they were cooled down in the furnace at room temperature and successively washed with three different liquids (first, with acetone, then with isopropanol, and lastly, with purified water) using an ultrasonic cleaner for 10 minutes in each bath. Finally, after the rinsing stage, glass fabric sheets were dried using a heating gun. As a result, the average diameter of a single unsize fibre (GF) was estimated to be about 9.3 µm. Note that untreated as-received glass fiber was labeled As-GF (*Fig. 3-6a*).

3.3 Mechanical test methods

3.3.1 *Microdroplet test*

Microdroplet tests were conducted to evaluate the micromechanical properties (IFSS) of the untreated GF/EP and GF-CNFs/EP composites. The specimen for the microdroplet test is schematically shown in Fig. 3-2a. A single glass fiber was pulled out from the glass woven fabric, aligned (without flapping), and glued to a metal jig. The specimens were prepared as follows:

- The specimen was immersed in CNFs suspension for 5 seconds, and then dried at 60°C for 1 hour;
- When necessary (GF-CNFs treated with silane), the CNFs-treated GF was immersed in silane coupling agent for 5 minutes and dried at 60°C for 1 hour;
- To apply the resin droplets, CNF-treated glass fiber was dipped directly into epoxy resin and then cured at 80°C for 6 hours.

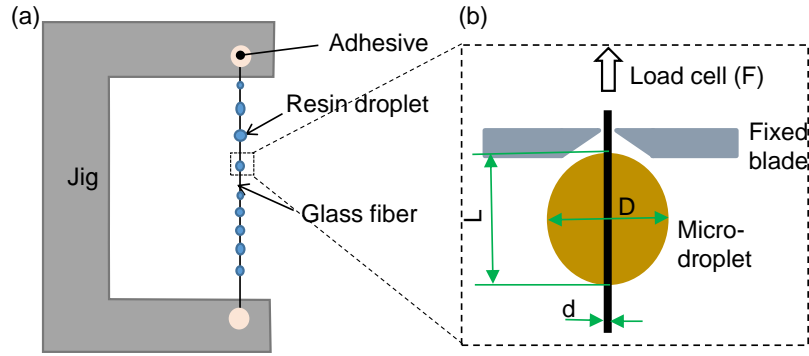


Fig. 3-2. Schematic representation of microdroplet specimen (a) and the principle of microdroplet test (b)

Table 3-1 shows CNFs treatment conditions and the nomenclature of CNFs-treated glass fiber-reinforced epoxy resin (GF-CNFs/EP) composites.

Table 3-1. Nomenclature of manufactured CNFs-treated single GF/epoxy composites for microdroplet tests.

Composites	CNFs (wt)	Silane	Composites	CNFs (wt)	Silane (1 wt %)	No. Pass
GF (untreated)	0 %	×	S/GF	0 %	○	1
GF-CNF _{1ppm}	0.0001 %	×	S/GF-CNF _{1ppm}	0.0001 %	○	1
GF-CNF _{5ppm}	0.0005 %	×	S/GF-CNF _{5ppm}	0.0005 %	○	1
GF-CNF _{10ppm}	0.001 %	×	S/GF-CNF _{10ppm}	0.001 %	○	1
GF-CNF _{50ppm}	0.005 %	×	S/GF-CNF _{50ppm}	0.005 %	○	1
GF-CNF _{0.01}	0.01 %	×	S/GF-CNF _{0.01}	0.01 %	○	1
GF-CNF _{0.05}	0.05 %	×	S/GF-CNF _{0.05}	0.05 %	○	1
GF-CNF _{0.1}	0.1 %	×	S/GF-CNF _{0.1}	0.1 %	○	1
GF-CNF _{0.5}	0.5 %	×	S/GF-CNF _{0.5}	0.5 %	○	1
2P/GF-CNF _{0.1}	0.1 %	×	2P-S/GF-CNF _{0.1}	0.1 %	○	2
3P/GF-CNF _{0.1}	0.1 %	×	3P-S/GF-CNF _{0.1}	0.1 %	○	3
As-GF	0 %	×	As-GF-CNF _{0.01}		×	1
As-GF-CNF _{10ppm}	0.001 %	×	As-GF-CNF _{0.1}		×	1

×: without silane; ○: with silane

Fig. 3-2b shows the principle of the microdroplet test. The fiber was set to pass freely between the fixed blades while they inhibited the resin droplet from passing through the gap between them. The test was conducted on the droplets with about 50 μ m of diameter (D) using interfacial property evaluation equipment (from Satoh Machinery Works Co., Ltd, Japan) connected to a 500 m.N load cell (LTS-50GA, Kyowa). The IFSS τ was estimated using Eq.

(2-1). To measure the embedded length, photographs were taken before and after peeling off each droplet using an optical microscope. The specimen was fixed to an extensometer, which moved longitudinally following the fiber direction with a speed of 0.3 mm/min. The data obtained from the microdroplet test may vary due to the significant variation in the interfacial shear strength. Therefore, a two-parameter Weibull distribution was used to evaluate the variation of the interfacial failure between the fiber and the matrix. To estimate the IFSS of the GF-CNFs/EP composites, the probability of the distribution expressed by Eq (3.1) [70] was used:

$$P(\tau) = 1 - \exp\left[-\left(\frac{\tau}{\tau_0}\right)^\rho\right] \quad (3.1)$$

where $P(\tau)$ is the probability of failure, ρ is the Weibull shape parameter, τ_0 is the Weibull scale parameter and τ is the applied interfacial shear strength. The average IFSS given by the Weibull distribution τ_a is evaluated using the expectation of the probability distribution function expressed as Eq. (3.2):

$$\tau_a = \tau_0 \cdot \Gamma\left(1 + \frac{1}{\rho}\right) \quad (3.2)$$

3.3.2 Manufacturing of GF-CNF/EP composites and three-point bending test

Fig. 3-3 schematically describes the CNF treatment and manufacturing procedure of GF-CNF/EP composites. Forty layers of unsized woven glass fabrics were laid up and then impregnated with CNF suspension using the vacuum-assisted resin transfer molding (VaRTM) technique. The grafting process of CNFs onto woven glass fabrics was completed by drying the GF laminate in an oven at 60°C for 3 hours. In comparison with the dip-coating method [66], vacuum impregnation was used to avoid the removal of the grafted CNFs onto fiber surfaces during the manufacturing process. Moreover, after grafting nanocellulose onto the reinforcing fibers, the stiffness of GF laminate increases making it difficult to be deformed or compressed during the VaRTM process for the resin infusion. This drawback can be avoided by vacuum impregnating the laminates with CNFs. The epoxy resin was impregnated into the CNFs-treated glass fabrics, and after that, the CNFs-treated glass fiber/epoxy resin (GF-CNFs/EP) composite laminates were cured at room temperature for at least 20 hours, followed by a post-curing at 80°C for 2 hours in a multi-oven. Four GF-CNFs/EP composites with different CNFs concentrations (Untreated, 0.001, 0.01, and 0.1 wt%) were manufactured from the procedure described above. Three specimens were cut (90 x 15 x 4 mm) from each composite and used for three-point bending tests.

Three-point bending tests were conducted to evaluate the flexural strength (macromechanical properties) of the GF-CNFs/EP composites. The test was conducted according to the ASTM D790 standard using a servo-hydraulic material testing machine (Shimadzu) with a crosshead speed of 2.5 mm/min and a span of 60 mm. The flexural properties were calculated using the following equations (3.3) and (3.4):

$$\sigma_f = \frac{3PL}{2Bt^2} \quad (3.3)$$

$$\varepsilon_f = \frac{6Dt}{L^2} \quad (3.4)$$

where σ_f denotes the flexural strength, ε_f is the flexural strain, P is the applied load at the moment of fracture, L is the span length, B is the width of the specimen, t is the thickness of the specimen, and D is the maximum deflection at the center of the specimen.

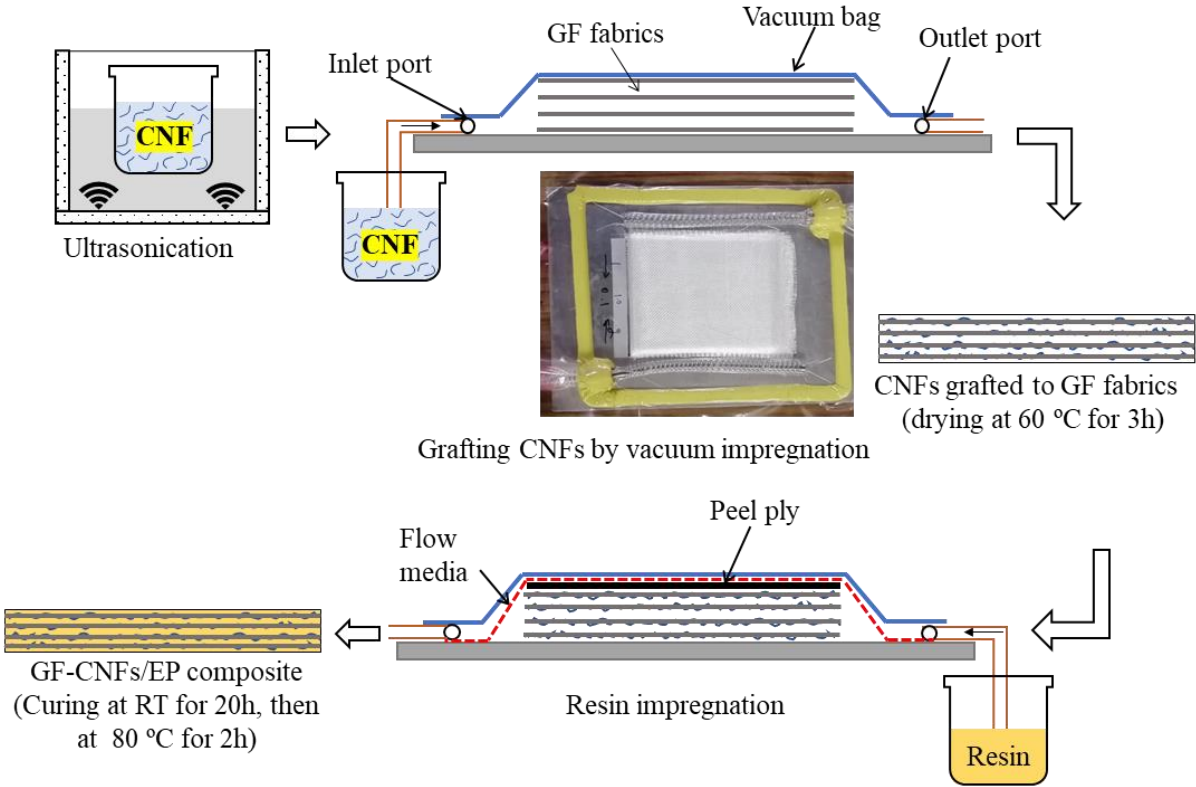


Fig. 3-3. Schematic illustration of CNFs treatment of woven glass fabrics and manufacturing process of composites by VATRM technique.

3.4 Surface characterization



Fig. 3-4. Field emission electron microscope HITACHI-SU8020

Before the formation of the resin droplets, CNF-treated glass fibers were observed using a field emission scanning electron microscope (FE-SEM/Hitachi-SU8020) to evaluate quantitatively the effect of CNFs on the reinforcement. Since CNF is at the nanoscale level, an FE-SEM machine was adopted to observe and characterize the surface morphology of the grafted GFs. FE-SEM provides surface, compositional and topographical information with a very ultra-high resolution. This machine offers a wide range of magnification from 20x to 800.000x with an acceleration voltage varying from 0.1 to 30 kV. In comparison with conventional SEM, FE-SEM produces less distortion in images with a very high resolution up to nanometers. Low accelerating voltages are recommended for non-conductive or for beam-sensitive specimens, which can be used without the sputtering process [71]. The FE-SEM machine was operated at 1.5 kV accelerating voltage and a probe current of 10 μ A. The photographs were analyzed using image processing software (GIMP and Image J) to estimate the quantity of CNFs grafted onto GF. As for the broken surface after the microdroplet test and three-point bending test, scanning electron microscope (SEM-JEOL JCM-5000) observations

were conducted to characterize the GF-CNFs/EP droplet interface and the morphology of the GF-CNFs/Epoxy composites.

3.5 Results and discussion

3.5.1 Surface of the CNFs-treated glass fiber

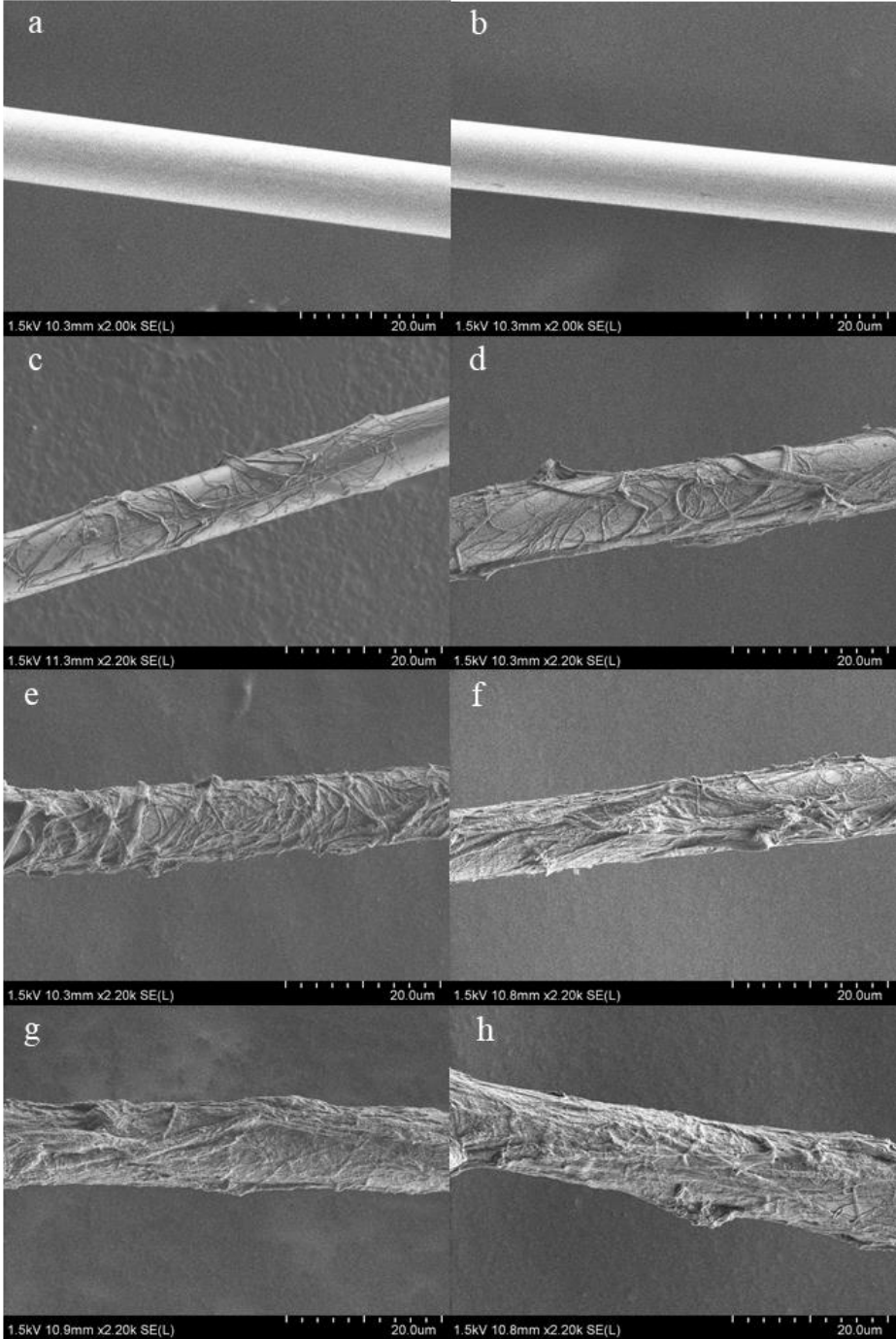


Fig. 3-5. FE-SEM images of untreated and CNF-treated GF: (a) as-received, (b) unsized, (c) 0.001 wt%, (d) 0.005 wt%, (e) 0.01 wt%, (f) 0.05 wt%, (g) 0.1 wt%, and (h) 0.5 wt%.

The morphology of glass fiber is characterized by evaluating the SEM images of untreated and CNFs-treated glass fiber (see Fig. 3-5b-c-d-e-f-g-h). A smooth surface can be observed for the untreated glass fiber (as-received and unsized) in Fig. 3-5a-b, whereas the surface of GF treated with CNFs (GF-CNFs) exhibit a rougher surface compared to untreated GF. Moreover, with increasing CNFs concentration, the thickness of the grafted layer onto glass fiber increases. It is found that under all conditions (from 0.0001 to 0.5 wt%), the glass fiber surface is not completely covered by CNFs, which means that CNFs are partially grafted. However, CNFs are more uniformly distributed with a low concentration (0.001 wt %) than those with higher concentrations (0.5 wt%). The single bracket in Fig. 3-6d shows a large length of CNFs clusters formed after the grafting process. It can be observed that certain parts of the fiber surface are fully grafted from 0.05 wt%, while CNFs clusters start to form from 0.005 wt%. The same phenomenon is found in the study of Xiao et al. [72] when CNTs were coated onto glass fiber.

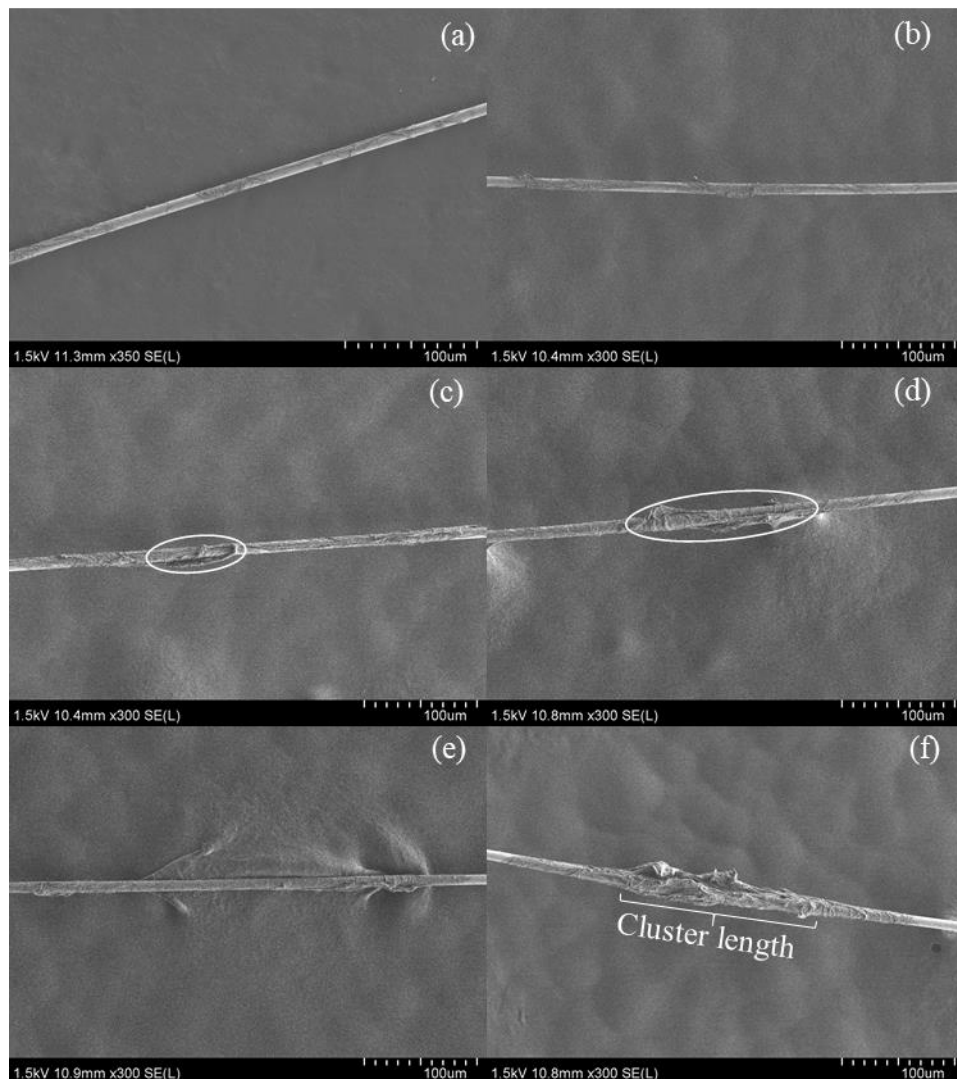


Fig. 3-6. Morphology and size of CNF clusters for treated GF: (a) 0.001 wt%, (b) 0.005 wt%, (c) 0.01 wt%, (d) 0.05 wt%, (e) 0.1 wt%, and (f) 0.5 wt%.

Fig. 3-7a shows the evolution of fiber surface grafted with CNFs. At 0.05 wt%, the surface of glass fiber is grafted by 71.7%, while at 0.5 wt%, nearly the same area (72.4%) is covered, meaning that the grafted area is saturated. However, it is important to note that the fiber surfaces covered by the CNFs clusters were not considered to measure the area of glass fiber grafted with CNFs and the thickness of the CNFs layer. As shown in Fig. 3-7b, the grafting thickness layer appears to increase with the CNFs content in the suspension, which may improve the stress transfer at the GF/epoxy interface [66]. It can be seen that the thickness of CNFs observed at lower concentrations (i.e., up to 0.01 wt%) slightly increases. However, the thickness increases significantly by 50 %, 100 %, and more than 200 % at 0.05, 0.1, and 0.5 wt%, respectively, compared to that of 0.01 wt%.

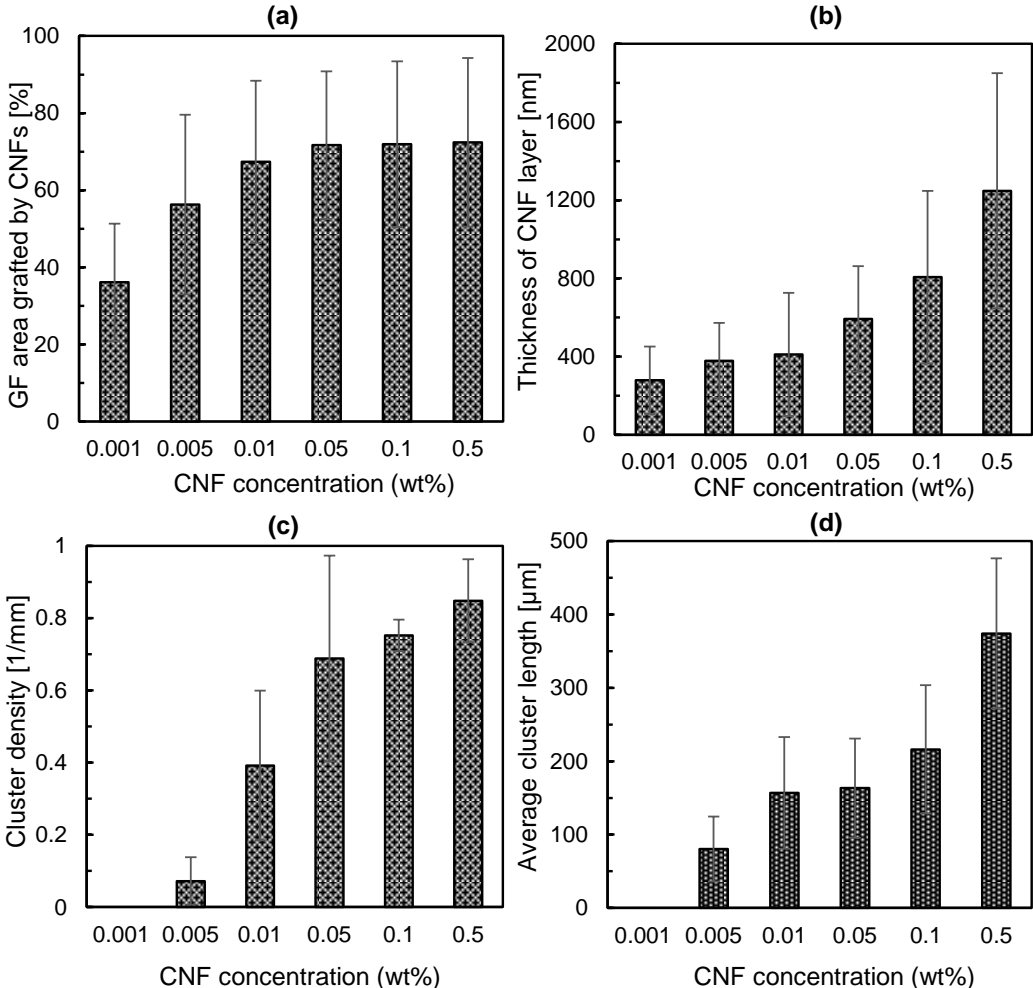


Fig. 3-7. Evaluation of CNFs-grafted onto glass fiber: GF area grafted by CNFs (a), CNFs thickness layer (b), cluster density (c), and average cluster length (d).

The cluster density in Fig. 3-7c was calculated from five specimens (CNFs-grafted glass fibers) with 25 mm in length. The number of CNFs clusters increases rapidly from 0.005 to 0.05 wt% with a difference of 0.616 in density, whereas a slight increase is observed beyond

0.05 wt% with a difference of 0.096 in density. The cluster density between 0.005 and 0.05 wt% varies from 0.072 to 0.688 and then varies from 0.688 to 0.848 between 0.05 and 0.5 wt%. The cluster density between 0.005 and 0.05 wt% varies from 0.072 to 0.688 and then varies from 0.688 to 0.848 between 0.05 and 0.5 wt%. The formation of the clusters may be attributed to the hydrophilicity of CNFs for which, without surface modification, forms aggregates in polymer matrices [73, 68]. The thickness varies remarkably from 279 nm (at 0.001 wt%) to 1248 nm (at 0.5 wt%), which may be attributed to the hydroxyl group present in the chemical structure of CNFs [74] due to their three-dimensional network with hydrogen bonds. A significant increase of CNFs in thickness (from 400 to 800 μm) is obtained, which may be explained by the slight change (from 0.01 to 0.1 wt%) in the cluster length. As found by Parveen et al., the addition of cellulose microcrystals into epoxy matrix has been involved in the formation of aggregations resulting in a decrease in mechanical properties of glass fiber/epoxy resin composites [68]. These results suggest that it is necessary to control the formation of the CNFs cluster, which, at a relatively high concentration level, may hinder the mechanical properties of GF/EP composites.

3.5.2 *Interfacial shear strength*

The Weibull distribution is used to estimate the variation of material failure due to the random fracture of the microdroplets. Consequently, graphical analysis by plotting $\ln[\ln(1/1 - P)]$ against $\ln\tau$ is used in Fig. 3-8 to determine the Weibull shape (or modulus) ρ . The probability of fracture P is obtained by ranking the interfacial strength data from the weakest to the strongest. Table 3-2 summarizes the results obtained from the Weibull probability plots of the interfacial shear strength data of GF-CNFs treated with and without silane. The variability of the interfacial strength can be characterized by the Weibull shape parameter. The higher the value of ρ , the smaller the variation of the interfacial strength. It is indicated that a greater value of the shape parameter leads to a smaller standard deviation. For instance, the shape parameter ρ for GF-CNF_{0.1} is 12.4 while the standard deviation is 2.7. Through all conditions of treatment, silane treated GF-CNFs/EP exhibits a significant increase in the scale parameter (τ_0) compared to that of GF-CNFs/EP without silane treatment. However, the low values of ρ for 0.5 wt% (with and without silane treatment) and 50 ppm with silane (S/GF-CNF_{0.005}) may be attributed to the small number of data. To ensure more accurate statistical analysis, it is recommended to use at least 20 data. As for the untreated glass fiber (GF), the low Weibull shape is probably due to the high variation of the interfacial shear strength (8 to 33 MPa) calculated from Eq. (1).

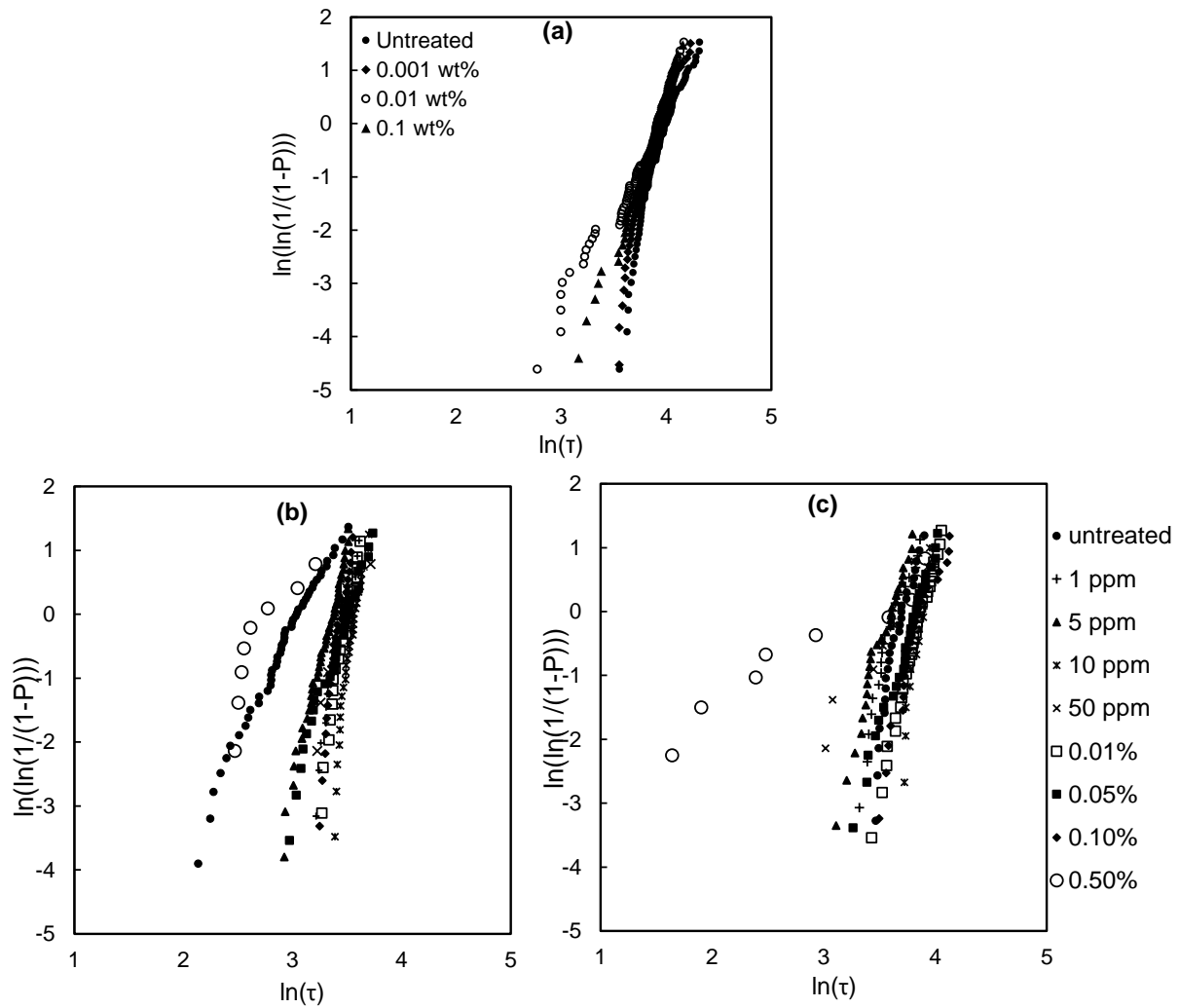


Fig. 3-8. Weibull probability plots of IFSS for: (a) as-received GF-CNFs/EP, (b) GF-CNFs/EP, and (c) S/GF-CNFs

Fig. 3-9a illustrates the influence of CNFs on the interfacial shear stress of as-received glass fiber treated with CNFs (As-GF-CNFs). The IFSS decreases (from 26 to 23 MPa) with the increase of CNFs concentration. Therefore, there is no improvement in the IFSS, which may be attributed to the incompatibility of CNFs with the sizing agent. This was revealed to be a factor of rapid formation of CNFs clusters on the surface of as-received GF, thus hindering the complete impregnation of the resin to the fiber. As can be seen in Fig. 3-10d, CNFs fragments without resin remained on the fiber surface. These results indicate lower interfacial adhesion between As-GF-CNFs and epoxy in comparison with the untreated as-received GF/EP (As-GF/EP).

However, the IFSS of the untreated As-GF/EP displays a better improvement compared to that of untreated GF/EP (Fig. 3-10b). This can be demonstrated by the morphology of their fracture

surface (Fig. 3-10a-b), where the surface of As-GF/EP (Fig. 3-10a) is rougher, indicating a better adhesion between the fiber and epoxy resin compared with GF/EP. The sizing agents are

Table 3-2. Interfacial strength and Weibull distribution for GF-CNFs treated with and without silane.

GF treated with CNFs	IFSS (MPa)	Std. Dev.	m	No. of measurements
GF/EP	19.4	6.0	3.6	49
GF-CNF _{1ppm} /EP	30.8	3.8	8.8	23
GF-CNF _{5ppm} /EP	27.1	4.1	7.2	44
GF-CNF _{10ppm} /EP	34.5	3.1	12.3	32
GF-CNF _{50ppm} /EP	30.6	5.1	5.8	8
GF-CNF _{0.01} /EP	31.9	3.4	9.9	22
GF-CNF _{0.05} /EP	30.8	6.0	5.5	34
GF-CNF _{0.1} /EP	30.2	2.7	12.4	27
GF-CNF _{0.5} /EP	15.8	4.8	3.0	8
S/GF/EP	39.1	5.1	8.4	26
S/GF-CNF _{1ppm} /EP	36.4	5.8	6.8	21
S/GF-CNF _{5ppm} /EP	34.2	6.0	6.1	28
S/GF-CNF _{10ppm} /EP	46.6	3.7	12.8	14
S/GF-CNF _{50ppm} /EP	34.2	9.0	3.2	8
S/GF-CNF _{0.01} /EP	45.5	6.8	7.4	34
S/GF-CNF _{0.05} /EP	43.5	8.6	5.4	30
S/GF-CNF _{0.1} /EP	45.9	8.1	6.2	25
S/GF-CNF _{0.5} /EP	28.8	18.4	1.1	9
2P/GF-CNF _{0.1} /EP	25.6	4.4	6.4	52
3P/GF-CNF _{0.1} /EP	23.4	7.9	3.1	45
2P/S/GF CNF _{0.1} /EP	9.7	2.7	4.1	40
3P/S/GF-CNF _{0.1} /EP	30.6	6.8	5.0	31
As-GF/EP	26	4.5	7	60
As-GF-CNF _{10ppm} /EP	24	3.9	7.5	52
As-GF-CNF _{0.01} /EP	23	5.8	4	60
As-GF-CNF _{0.1} /EP	23	4.1	6.1	51

generally applied to the surface of glass fibers to handle the fibers, hold individual filaments together, and improve the glass fibers/matrix interface adhesion. Besides, Zhao et al. [63] have found that removing the sizing agent may decrease the tensile strength of the fiber. However, the specific surface area increased, which may probably lead to stronger interfacial adhesion between fiber and matrix. Removing commercial sizing agents was found to be more effective by applying surface treatments on fibers [75, 76, 63]. Kim et al. [77] also burned out the organic sizing coated on glass fiber surfaces before applying silane treatments onto fibers, and their

results indicated a significant interfacial adhesion between glass fibers and matrix resin. This is because the hydroxyl groups of glass fiber can react with those of silane coupling agents resulting in hydrogen bonding. Therefore, as reported by previous studies [78, 64, 67], it is plausible that grafting nanomaterials onto the unsized fiber improves the adhesion between reinforcing fibers and nanofillers and is better than their application on the as-received fiber with the commercial coating.

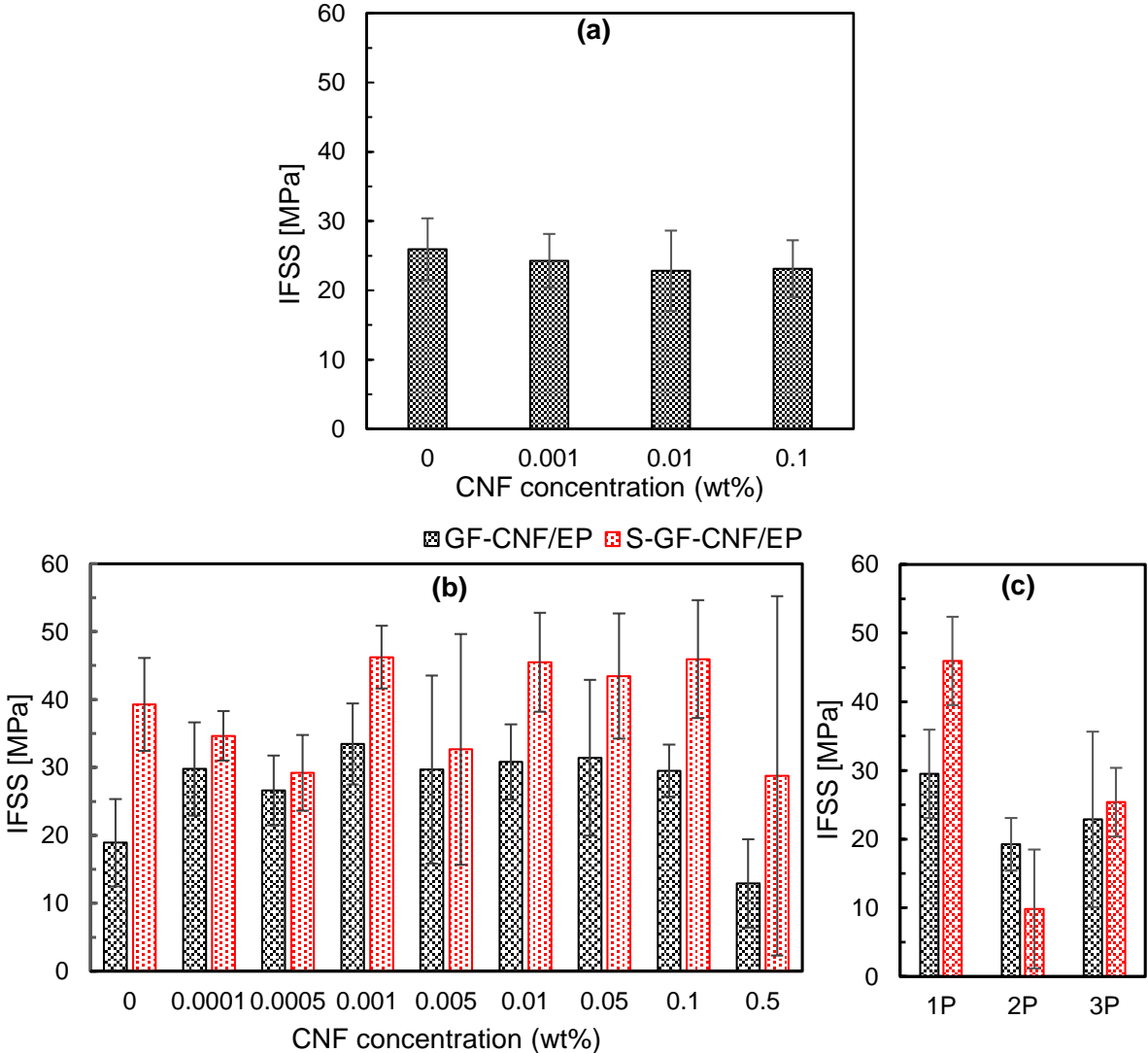


Fig. 3-9. Evolution of the IFSS of (a): as-received GF-CNFs/EP, (b) GF-CNFs/EP (black), and S/GF-CNFs/EP (red), and (c) CNFs and Silane treated GF/EP as a function of the number of passes.

Fig. 3-9b and c show the effect of CNFs and silane treatments on the IFSS of the unsized glass fiber as a function of CNFs concentration and the number of treatments (passes), respectively. The result indicates that the presence of CNFs at the GF/EP interface improves the interfacial strength significantly as its concentration increases (from 1 ppm to 0.1 wt%).

However, 0.001 wt% appears to be the optimum concentration because the IFSS increases by about 78% at this concentration compared to that of untreated GF/EP composites. This may be due to the thin CNFs/resin layer (279 nm) formed on the GF surface without any formation of clusters. For the CNF concentrations exceeding 0.001 wt%, the IFSS undergoes a reduction resulting from the onset of CNF clusters and the thickening of the CNF layer. At 0.5 wt%, an abrupt degradation of the interfacial strength can be noticed due to the thickening CNFs layer described in the previous section. The interfacial debonding is reduced by adding CNF (up to 0.1 wt%) to the reinforcing fibers. Similarly, adding CNFs (up to 0.8 wt%) in the matrix has resulted in the same strengthening mechanisms of the interfacial strength of CF/EP composites [62]. However, the quantity of CNFs used in our study is much lower than that used by Shao et al., and they both led to almost the same improvement in the IFSS.

According to the fracture surface morphology (Fig. 3-10h), the failure occurred at the CNFs/epoxy interface, which is revealed to be weaker than that of the GF/CNFs. Similar results were found by Asadi et al. [66], who coated CNCs onto glass fiber. They have found a maximum increase in the IFSS of 69% at 1 wt% of CNC followed by a decrease at 1.5, 2, 3, and 5 wt% of CNCs coating. Therefore, our results suggest that grafting CNFs on GF is more effective in improving the interfacial shear strength of GF/EP composites than CNC-coated fiber. This is supported by the findings of Xu et al. [79] where a comparative study of CNCs and CNFs has resulted in higher strength with the CNFs nanocomposites rather than with CNC nanocomposites.

The influence of silane coupling agent treatment on the interfacial strength of CNFs-treated glass fiber reinforced epoxy composites is plotted in the red bar in Fig. 3-9c-b. The IFSS of S/GF/EP increases significantly by ~102% in comparison with that of the neat GF/EP (i.e., without CNFs and silane treatment). In the S/GF-CNFs/EP systems where glass fibers are successively treated with cellulose nanofibers and silane coupling agent, the IFSS indicates a maximum increase of about 19% at 1 ppm, 0.01, and 0.1 wt% compared with that of S/GF/EP. It is well known that silane is commonly used to improve interfacial strength in the GF/polymer matrices due to the formation of covalent bonds between the silane-coated GF and epoxy matrix [68]. Besides improving interfacial strength, silane has been used to improve the tensile and flexural strength of glass fiber/epoxy composites by 37% and 78%, respectively [80]. In this study, we found that silane treatment to CNFs-grafted GF/EP composites had no significant effect on the IFSS compared to that of GF treated with silane only. Therefore, in comparison to

previous studies [60, 59, 56], it is suggested to modify the surface of CNFs with silane coupling agents before their application to the GF surface.

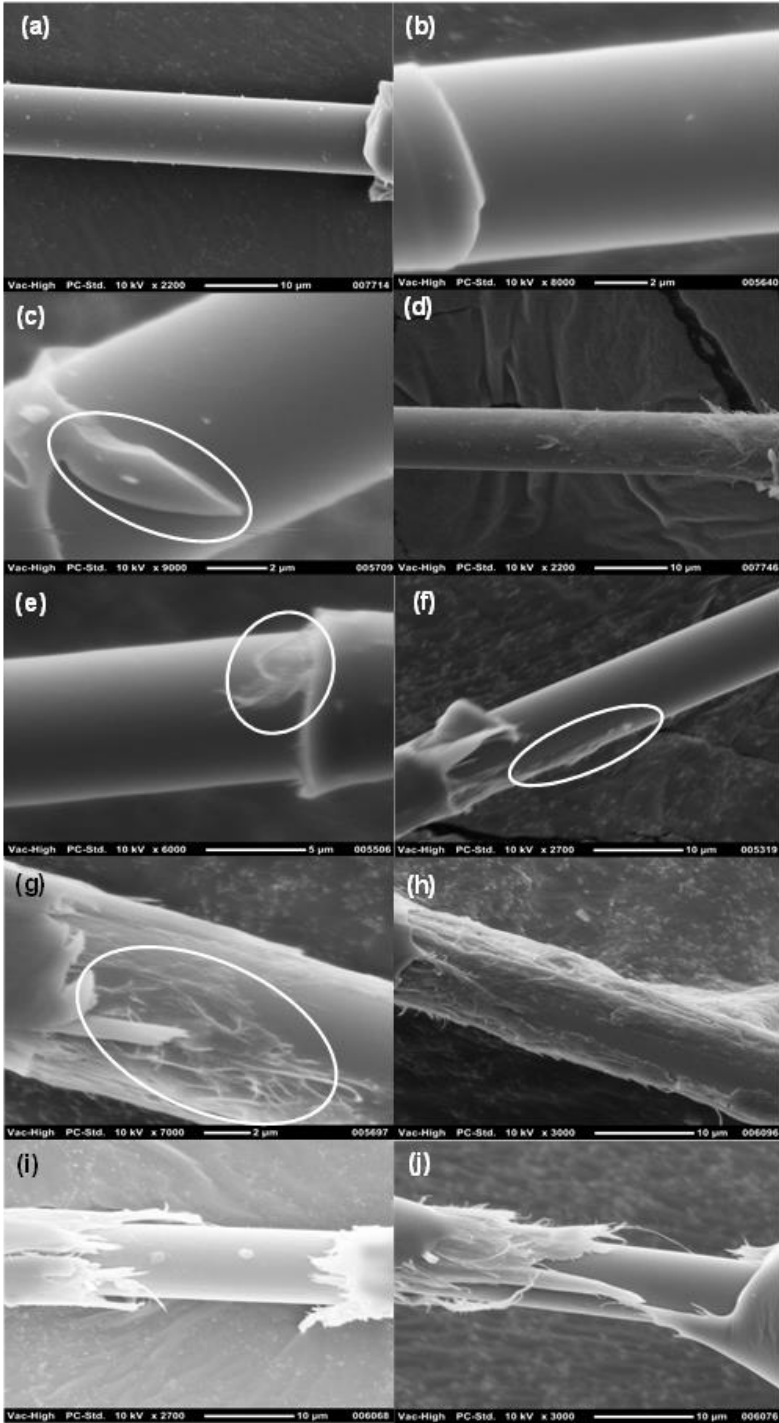


Fig. 3-10. SEM images of fiber fracture surface after microdroplet test for: (a) As-GF/EP, (b) GF/EP, (c) S/GF/EP (d) As-GF-CNF_{0.1}/EP, (e) GF-CNF_{10ppm}/EP, (f) GF-CNF_{50ppm}/EP, (g) GF-CNF_{0.1}/EP, (h) GF-CNF_{0.5}/EP, (i) 2P/GF-CNF_{0.1}/EP and (j) 3P/GF-CNF_{0.1}/EP

On the other hand, the decay of IFSS at 1 ppm, 5 ppm, and 50 ppm can be attributed to the non-uniform dispersion of CNFs on glass fiber, which shows the same trend as GF-CNFs/EP

composites. Regarding the fact that the IFSS at 0.5 wt% is smaller than that of untreated glass fiber, this is caused by the thickening of the interfacial CNFs layer due to its accumulation on the fiber surface. Fig. 3-9c shows the effect of repeating the CNFs treatment on the IFSS of both composite systems (GF-CNF_{0.1}/Epoxy and S/GF-CNF_{0.1}/Epoxy). As a result, there is a degradation of the interfacial strength after two and three passes of treatment. The IFSS of the GF-CNF_{0.1} and S/GF-CNF_{0.1}/Epoxy composites decreases by ~ 28% and 78%, respectively. The reason for this degradation can be explained by the smooth fracture surface of the resin droplets in Fig. 3-10i-j resulting from the non-impregnation of the epoxy resin to the fiber.

Fig. 3-10 shows the morphology of the interfacial fracture surfaces of untreated glass fiber (Fig. 3-10a-b-c) and CNFs treated GF (Fig. 3-10d-e-f-g-h-i-j) and unsized GF/EP after peeling off the epoxy resin droplets. The fracture surface of the unmodified (0 wt%) composites appears smoother than that of CNFs treated GF/EP. However, the surface of As-GF/EP (Fig. 3-10a) is rougher than the other untreated GF/EP (Fig. 3-10b-c). The morphology indicates a rougher fracture surface with an increase in the CNFs concentration, which may be due to the mechanical interlocking of the matrix resin with CNFs. This could be attributed to the bridging effect of CNFs onto GF. It is found that the presence of nanomaterials at the fiber/matrix interface reveals to be effective in strongly bonding the constituents of composites, thereby delaying the crack propagation [81, 62]. The increase in the surface roughness of reinforcing fibers after grafting nanomaterial is beneficial for mechanical interlocking between fibers and matrix [67]. As we can see from the SEM images (Fig. 3-10g), CNFs-EP residues remain on glass fiber. The quantity and amount of residual resin on the interfacial fracture increase with increasing CNFs concentration. However, at 0.5 wt%, a CNFs layer without resin can be seen on the fracture surface, which is caused by the thickening CNFs layer on GF, thus hampering the resin from impregnating the GF. This leads to a weakening of the shear strength at the GF/resin interface due to poor adhesion between the fiber/matrix interface.

According to previous studies [63, 72, 82], five strengthening mechanisms have been proposed to explain the improvement of fiber/resin matrix interface: (1) Van der Waals binding due to the increase of fiber specific area, (2) mechanical interlocking of CNT and matrix, (3) surface wettability of fiber by the matrix, (4) chemical bonding between CNTs and bulk materials (fiber and matrix), and (5) strengthening of polymer matrix near fiber/matrix interface. Although these mechanisms were applied to CNTs, they may also be valid for CNFs used in modifying glass fiber/epoxy resin composites. It has been shown by Asadi et al. [66] that

coating cellulose nanocrystals (CNCs) on glass fiber has possibly resulted in mechanical interlocking due to the increase in GF roughness and chemical affinity between CNCs and GF.

3.5.3 Flexural strength

The effect of CNFs on the flexural strength of the neat GF/EP and treated GF-CNFs/EP composites are shown in Fig. 3-11. The flexural properties are improved with increasing CNF concentrations (up to 0.1 wt%). It appears that the flexural stress-strain curves (Fig. 3-11a) indicate an increase in flexural stress and flexural elongation after CNFs treatment. For instance, after 0.001 wt% of CNFs treatment, the elongation increased from 1.8% to 2.2% and after that decreased with increasing the CNFs concentration. The flexural strength of the GF/EP and that of GF-CNFs_{0.1}/EP composites were measured as 326 MPa and 393 MPa, respectively, which led to an enhancement of 20 %. Grafting nanomaterials onto the reinforcing fibers has been reported to improve the interfacial adhesion between fibers and matrix, which resulted in transforming the ductile laminated composites to brittle [83]. This can be attributed to the presence of CNFs at the GF/EP interface owing to an increase in the interfacial stiffness. The flexural properties of FRP composites are significantly affected by the interfacial adhesion between fibers and matrix [64]. Kurita et al. [31] achieved a significant improvement in the flexural strength (~125%) of GFRP laminate by inserting layers of CNFs (0.1wt%) dispersed in epoxy resin. However, the concentration of cellulose fibers loaded into the matrix is limited because, at a certain quantity of nanocellulose in the matrix (e.g. over 1wt%), agglomerates are formed, thereby decreasing the flexural and tensile properties of the matrix composites [68, 84]. Interestingly, a maximum of 0.1 wt% CNFs concentration was used in this study to improve the flexural properties. Therefore, it is expected that a better enhancement might be obtained using higher CNFs concentrations.

The mechanism behind the improvement of the flexural properties at 0.1 wt% can be attributed to the CNFs bridging between glass fibers resulting in strengthening or toughening the matrix resin. With this in mind, the IFSS at the same CNFs content increases by 58%, which is much higher in comparison with the increase in the flexural properties of the GF-CNFs_{0.1}/EP composites. Therefore, different mechanisms may be applied distinctly to enhance the flexural and interfacial strength of the GF-CNF_{0.1}/EP composites. The improvement in the IFSS is most likely due to the strong interfacial adhesion between fibers and matrix, whereas that of the flexural strength may result from the matrix toughening. Conversely, Asadi et al. [66] reported an enhancement in the flexural strength of GF-CNC/EP by ~ 42%, which was attributed to the

strong interfacial adhesion between GF and epoxy resin. It is considered that the resin toughness widely contributes to the static strength of GF-CNFs/EP composites.

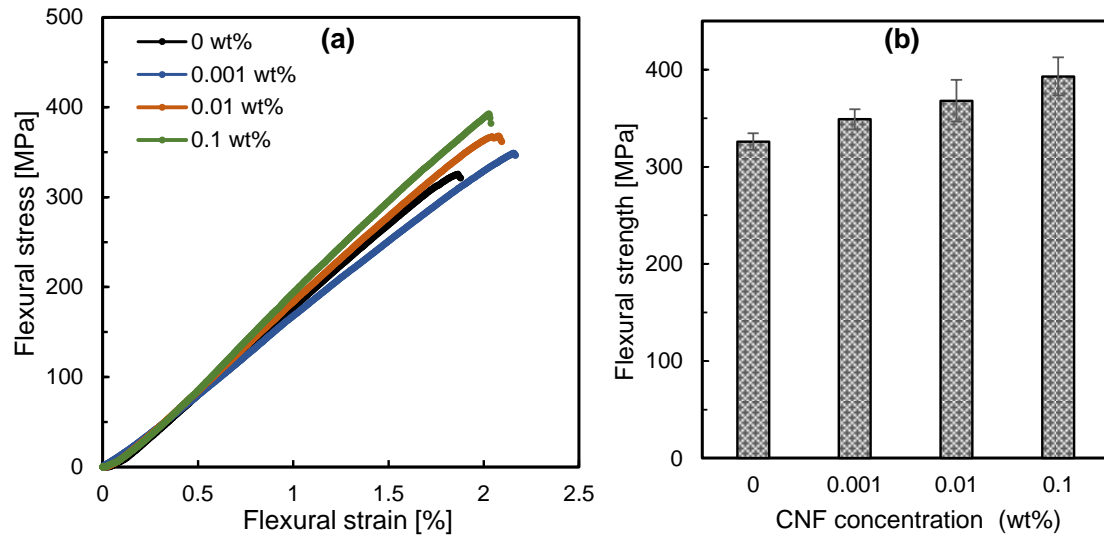


Fig. 3-11. Flexural stress-strain curves of GF-CNFs/EP composites (a), and flexural strength of neat GF/EP and GF-CNFs/EP composites (b).

On the other hand, the low improvement of the flexural strength in our study compared to the findings of Parveen et al. [68] is likely because CNFs are grafted solely on the upper part of the laminated glass fabrics. In other words, individual fibers (or fiber tows) are not completely treated, especially for those of glass fabrics in the mid of the laminate (see Fig. 3-12a-c-e). Therefore, based on previous studies [68, 31], to improve the flexural strength of glass fiber-reinforced polymer matrix, it is more appropriate to use cellulose nanofibers into the matrix instead of grafting it onto the fibers.

Fig. 3-12b-d-f shows the morphology of the fracture surface of GF-CNFs/EP composites. It can be observed that the fracture occurred at the GF-CNFs/EP interface for the neat and CNF-modified composites. However, the fracture surface becomes more brittle with increasing the CNF concentration indicating a better improvement in the adhesion between GF-CNFs woven fabrics and epoxy resin. As can be observed in Fig. 3-12b, the epoxy resin is largely peeled off from the fibers showing a smoother surface in the GF-CNF_{10ppm}/EP composite due to the low fiber/epoxy adhesion in comparison with that in the CNF_{0.1}/EP composite. However, the fracture surfaces of GF-CNF_{0.01}/EP and GF-CNF_{0.1}/EP composites appear to be rougher as the CNF concentration increases. Residual resins are observed, and they are more distributed when the CNFs content becomes higher. In addition, some resin fragments are still attached to the surface of the fibers after the interfacial fracture, and fiber breakage is shown in Fig. 3-12f, thus suggesting an improvement in the flexural strength. It can be considered that CNFs grafted onto

the reinforcing fibers inhibit the crack growth of interfacial debonding between fiber and matrix, which contributes to improving the flexural properties of GF-CNFs/EP composites. Other researchers [85, 64, 66], demonstrated that nanomaterials such as CNCs, GO, and CNTs coated on the reinforcement improved significantly the fiber/matrix adhesion. In addition, it has been found that CNTs coated onto unsized carbon fibers can “heal” the defects (grooves and voids) on the fiber surface resulting in strong adhesion of fiber/matrix interface [67]. As illustrated in Fig. 3-13, the GF/EP interface shows a linear debonding while GF-CNFs/EP interface exhibits an irregular debonding. This could be attributed to the hydrogen bonding between GF and CNFs and mechanical interlocking due to the increased surface roughness of GFs by CNFs.

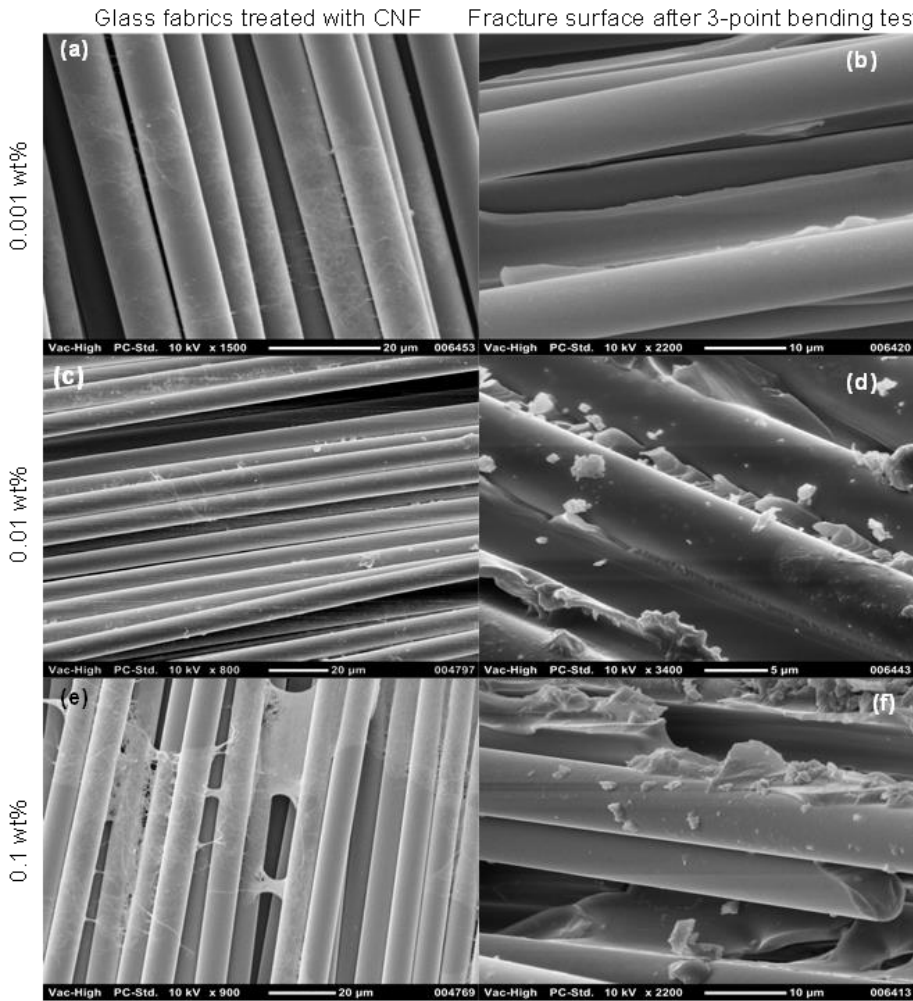


Fig. 3-12. SEM images of CNFs-treated glass fabrics and fracture surface of GF-CNFs/EP composites.

According to Xiao et al. [72], mechanical interlocking between fibers treated with nanomaterial and epoxy played an important role in the mechanical properties of FRP composites. Although grafting GF with low CNFs concentrations is effective in improving the flexural properties of GF-CNFs/EP composites, the damage mechanisms need to be clarified.

In the present study, fiber breakage and interfacial debonding between CNFs-treated GF and epoxy matrix were predominant based on the morphologies of the fracture surface. This result is in perfect agreement with that of previous studies [66, 72], where three fracture surface mechanisms were observed: matrix cracking, interfacial debonding, and fiber failure. However, the relative enhancement in flexural properties compared to that in interfacial shear strength is probably due to the incomplete impregnation of the resin into the grafted GF tows [66]. Besides, the formation of voids during the manufacturing process is a critical factor in the flexural properties of FRP composites. It is found that voids can be reduced by applying external pressure to the laminate before or after resin infusion to improve the flexural strength by more than 20% with respect to that of the laminates from conventional VaRTM (i.e. without external pressure) [17]. Although our results prove the effectiveness of adding CNFs to the GF, further studies are suggested for better improvement in flexural properties of GFRP composites by using the method aforementioned or by increasing the number of CNF treatments on laminated woven glass fabrics.

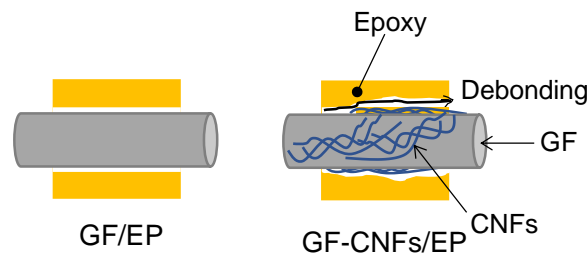


Fig. 3-13. Illustration of crack growth of interfacial debonding between reinforcing fibers and epoxy.

3.6 Conclusions

In this study, CNFs were successfully added to the surface of woven glass fabrics. The effect of CNFs-treated GF/Epoxy on interfacial shear strength and flexural strength was investigated, and the following conclusions are drawn:

- The CNFs layer on the glass fiber surface increased with the increase in CNFs concentration, which resulted in the formation of CNFs clusters from 50 ppm. However, suspensions with a low CNFs content have shown a more uniform CNFs dispersion onto glass fiber.
- Grafting CNFs at the glass fiber/epoxy interface improved the IFSS and flexural strength of GF-CNFs/EP composites by 78% and 20%, respectively, compared to the neat GF/EP composites. The strengthening mechanisms supporting these improvements have been

discussed, and they consisted primarily of interfacial debonding, mechanical interlocking, and resin toughness by CNFs bridging. However, at the highest CNFs concentration (0.5 wt%), the IFSS decreased abruptly by 57% and 37% for the GF-CNFs/EP and S/GF-CNFs/EP composites, respectively, resulting from the high thickness layer of CNFs grafted on the fiber surface.

Chapitre 4: Improvement of Flexural Strength and Fatigue Properties of Glass Fiber/Epoxy Composites by Grafting Cellulose Nanofibers onto the Reinforcing Fibers

4.1 Introduction

Fiber-reinforced polymer composites (FRPs) have been used as high-performance materials which can replace metals owing to their exceptional properties such as high tensile strength, high fatigue resistance, high corrosion resistance, and lightweight. Carbon fiber and glass fiber are commonly used as reinforcing fibers. FRPs are used in various industrial applications including automobile, aerospace, marine, and civil engineering. However, their mechanical properties are limited by debonding, delamination, matrix crack, and fiber breakage. To avoid these failures and improve the mechanical properties of FRPs, nanomaterials including carbon nanotubes, cellulose nanofibers, carbon nanofibers, and nanoparticles have been added to composites. The improvement of mechanical performance of FRPs can be obtained by increasing the interfacial strength between the reinforcing fibers and the matrix or by increasing the matrix toughness.

Previous studies have reported a significant improvement in the fiber/matrix adhesion and the matrix toughness by adding nanomaterials to FRPs [51, 3, 68]. Fiber surface modification and matrix modification are the common techniques used to improve the adhesion between fibers and matrix with nanofibers [68]. For instance, in our previous study CNFs were coated with glass fiber and, then a significant enhancement in interfacial adhesion has been achieved [86]. Moreover, interfacial modification of glass fiber/epoxy with cellulose nanocrystals (CNCs) led to an important improvement in interfacial, flexural, and tensile strength by 69%, 43%, and 10%, respectively [66]. On the other hand, incorporation of CNFs into carbon fiber/epoxy composites improved the interfacial strength by 77% and the fatigue life up to 30 times [3]. In the study of Parveen et al. [68], 1 wt% of cellulose microcrystals (CMCs) have been homogeneously dispersed into the matrix of GF/Epoxy-CMCs composites. As a result, the tensile strength has been slightly improved (~14%) whereas the flexural and interlaminar strength exhibited a significant increase up to 65% and 76%, respectively.

The weak interface between the reinforcement and the matrix is due to their difference in chemical and physical properties. Therefore, many research works have been conducted to increase the interfacial bonding by adding nanomaterials into conventional composites, which resulted in delaying the debonding, delamination, and crack propagation in FRPs. However, the

no dispersion and formation aggregations of cellulose in the matrix reduced the mechanical properties of composite materials [68]. To the best of the authors' knowledge, no study has reported the effect of CNFs on the flexural fatigue of FRPs. CNFs have been grafted to glass fiber/epoxy composites to improve interfacial strength and flexural strength [86]. Therefore, this study aims to investigate the influence of CNFs on flexural fatigue properties under low cycle flexural stress. The micro-mechanisms of the fatigue damage will be discussed.

4.2 Experimental methods

4.2.1 Materials:

Plain glass cloth (KS2750) with a density of 104g/m² was supplied by Nittobo Techno Co. Epoxy resin (Araldite LY5052) and the hardener (Aradur 5052) were purchased from Huntsman Advanced Materials Ltd. CNF was supplied by Prefectural Paper Technology Center in a slurry form. The matrix (epoxy + hardener) was prepared with a ratio of 100:38 (epoxy 108.3g + hardener 41.7 g). The sizing agent was removed from plain glass cloths for better interfacial bonding between fibers and matrix. The preparation of the reinforcement and the matrix resin was described in detail in our previous study [86].

4.2.2 Manufacturing of the GF-CNFs/Epoxy resin composites

Three CNF concentrations (0.001, 0.01% and 0.1 wt%) were prepared from 2 wt% of CNF slurry. First, distilled water was added into 2 wt% of CNF to make 0.5 wt% from which the other concentrations (0.001, 0.01, and 0.1 wt %) were made. Forty sheets of glass cloth were laid up and impregnated with the prepared CNF suspension by vacuuming using vacuum-assisted resin transfer molding (VaRTM) equipment. The impregnated GF laminate was dried at 60°C for 3 hours, and then the matrix resin was impregnated using the VaRTM technique to manufacture the GFRP composites. VaRTM process was modified by replacing the peel ply with an aluminum plate for a smoother surface finished (see Fig. 4-1). After the infusion of the resin, the composite laminate was cured at room temperature for 20 hours followed by post-curing in an oven at 80°C for 2 hours. The thickness of the manufactured composites was 4 mm. The details of CNF preparation and composite manufacturing have been described in our previous study [86].

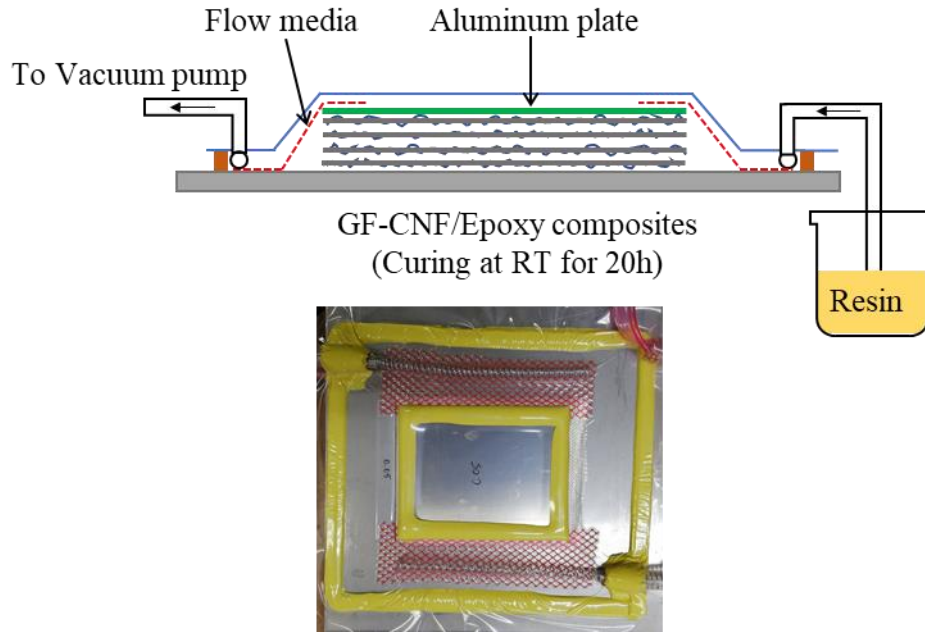


Fig. 4-1. Modified VaRTM process for manufacturing composite laminates.

4.2.3 Flexural properties

The flexural properties of untreated-GF/epoxy (GF/EP) and CNFs-treated GF/epoxy (GF-CNFs/EP) composites were determined by three-point bending test according to the ASTM D790 standard. The specimens were cut from the manufactured composite laminates in the dimensions of 90 mm in length and 15 in width. The specimens for the flexural test are schematically shown in Fig. 4-2. The tests were performed using a 10 kN computer-controlled servo-hydraulic test machine (Shimadzu) with a constant crosshead speed of 2 mm/min, and a span of 60 mm. The flexural strength and flexural modulus were calculated using equations 3.3 and 4.1, respectively.

$$E_f = \frac{PL^3}{4BDt^3} \quad (4.1)$$

4.2.4 Fatigue test

The flexural fatigue specimens were cut into the same dimensions as those of the bending test specimens (Fig. 4-2). The fatigue tests were performed under low cycle stress at a stress ratio of 0.1 with a maximum number of cycles of 10^6 . A frequency of 5 Hz was selected because the use of high frequency may cause internal heating in the specimen, which reduces the fatigue properties [87, 88]. The tests were carried out using 70% to 90% of the maximum flexural strength (429 MPa) for the neat GF/EP and GF-CNFs/EP composites. For more accuracy of the measurements, at least five specimens were tested for each condition.

The fracture surface of the GF/EP and GF-CNFs/EP composites was examined using a Field-emission scanning electron microscope (FE-SEM/Hitachi SU8020) operating at an accelerating voltage of 1.5 kV.

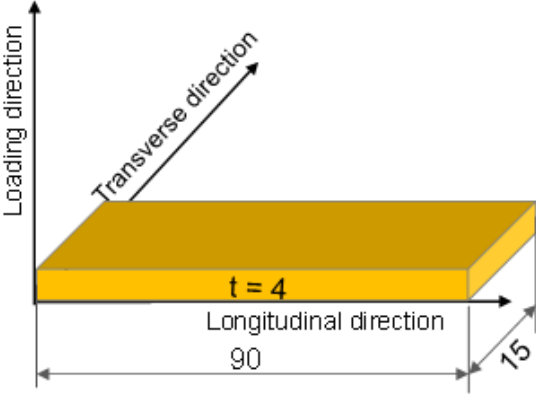


Fig. 4-2. Specimens size and directions for flexural strength and bending fatigue tests.

4.3 Results and discussion

4.3.1 Morphology of laminated woven GF after CNFs treatment

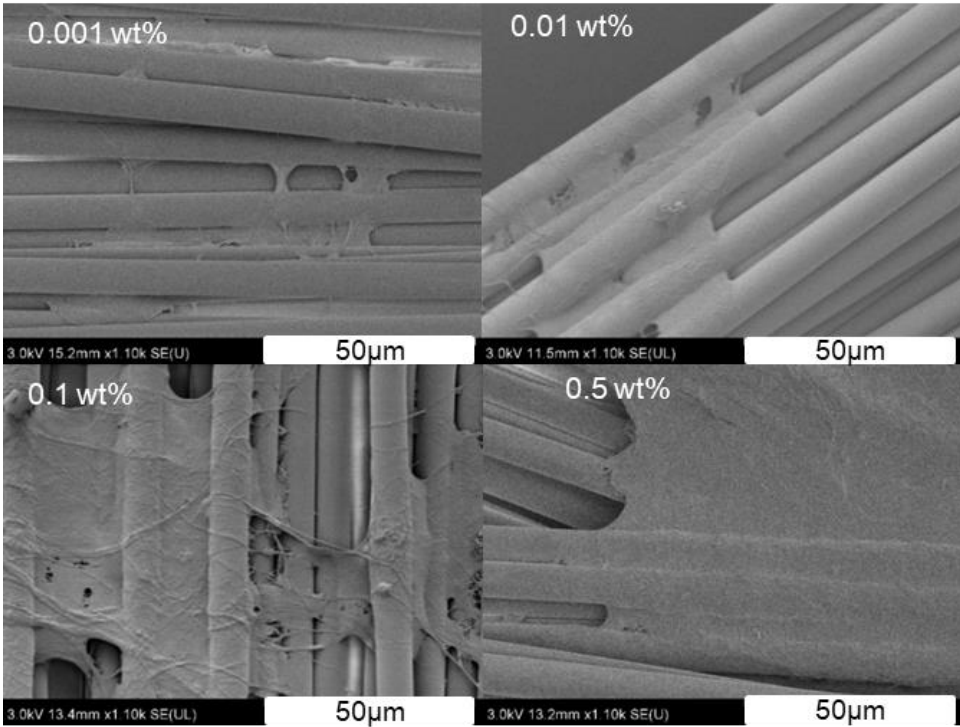


Fig. 4-3. Evolution of CNF grafted on woven GF laminate.

As found in Fig. 3-12, CNFs were successfully grafted on the GF surface after vacuum impregnation. It can be observed from Fig. 4-3 that a CNF layer is formed on glass fibers and then bridged between them. The layer increased with increasing the CNF concentration resulting in a thicker layer at the highest CNF concentration of 0.5 wt%. With this concentration,

GFs are completely covered by a denser CNF layer. Although the CNF layer in 0.1 wt% is thinner compared to that in 0.5 wt%, however, it exhibits a rougher surface indicating a higher specific surface area. Therefore, it is suggested that the CNF content plays a critical role to optimize the grafting process. On the other hand, Fig. 4-4 shows the FE-SEM images of GF laminate after vacuum impregnation and drying for 0.1 wt% with different observation areas. To further investigate the quantity of CNFs impregnated into GF laminate different areas were observed. As a result, it can be observed that CNFs are randomly distributed through the entire GF laminate. However, they are more present in the suction side of the GF laminate as well as in the upper and lower GF plies compared to the GF fabrics in the middle of the laminate.

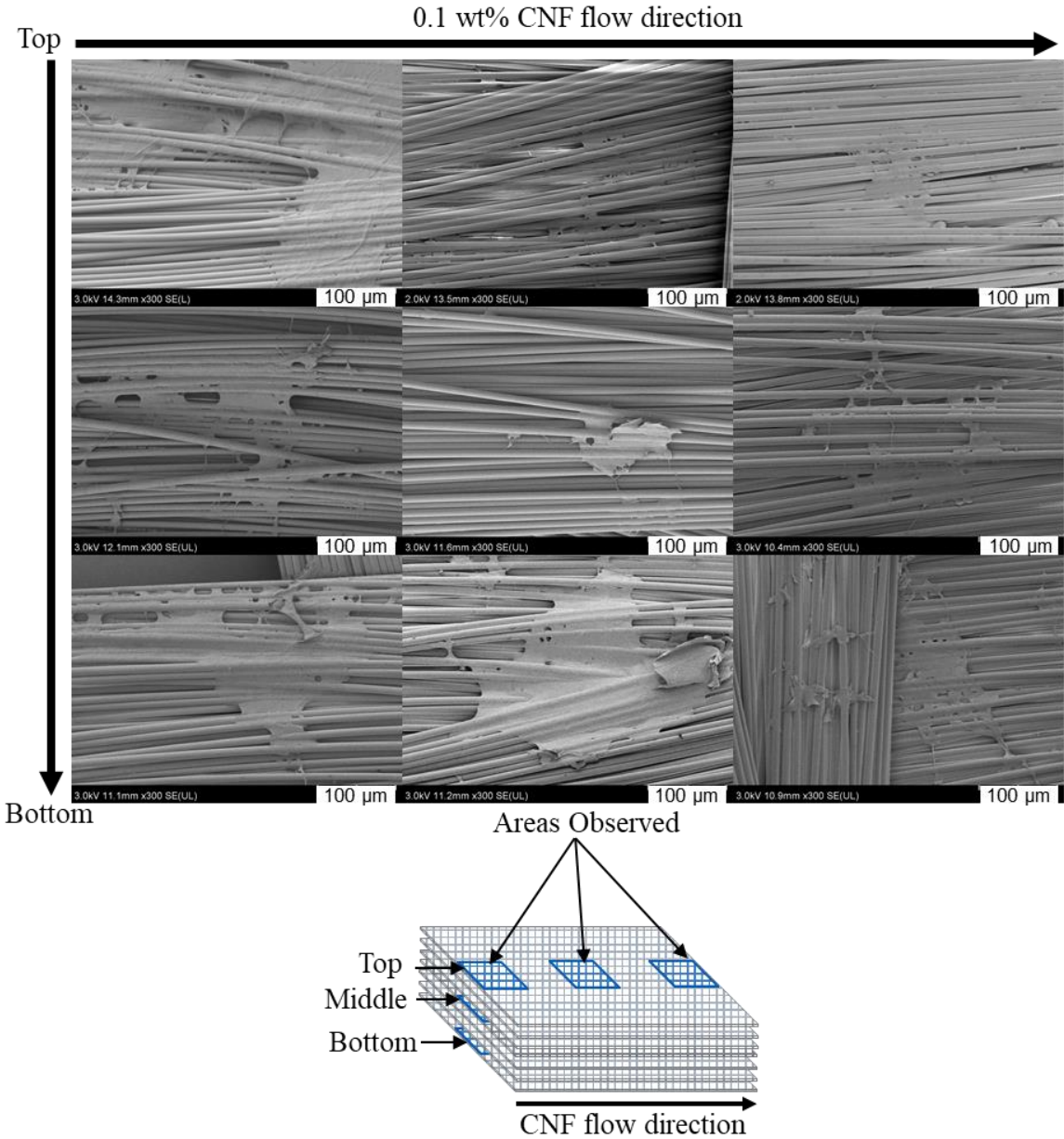


Fig. 4-4. Characterization by different observation areas of GF laminate vacuum impregnated with 0.1 wt% CNF

4.3.2 Flexural strength

Fig. 4-5 shows the flexural strength-strain curves of GF/EP and GF-CNFs/EP composites. Regardless of the incorporation of CNFs into GF/epoxy composites, the flexural modulus remains constant in all CNF concentrations except at 0.5 wt% while the flexural strength increases slightly with increasing the CNF concentration. An improvement of about 6% (from 429 MPa to 454 MPa) is observed for the CNF-modified GF/epoxy at 0.1wt% in comparison with the neat GF/epoxy composite. At 0.5 wt%, the flexural modulus and strength decrease due to the CNF clusters formed onto glass cloth resulting in hindering the impregnation of resin to fibers. Although CNF is effective to improve the mechanical properties of FRPs composites, there is a limit of concentration from which the properties are reduced [3, 31]. The effect of nanocellulose on mechanical properties has been investigated by Shao and co-workers. As a result, tensile modulus and strength have shown a slight increase while other properties such as tensile fatigue have been significantly improved.

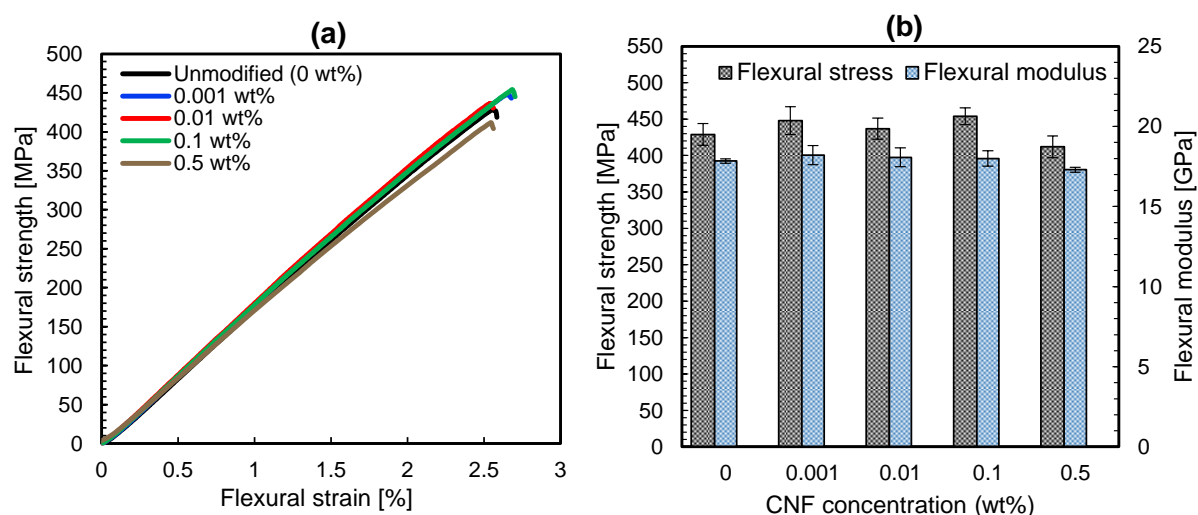


Fig. 4-5. Flexural strength vs flexural strain curves and effect of CNFs on the flexural strength of GF/EP and GF-CNFs/EP composites.

The fracture surface of the GF/EP and GF-CNFs/EP composites in the flexural testing were investigated and the surface morphology is given in Fig. 4-6. The main damage mechanism of the untreated GF/EP composite is interfacial debonding between fibers and epoxy matrix indicating a weak interfacial adhesion. As for the GF-CNFs/EP composites, the fracture surface is becoming rougher in comparison with the neat GF/EP composite. This can be attributed to the main damage mechanisms which are fiber breakage (in white circle), interfacial debonding, and matrix cracking. Similar mechanisms have been found in the literature [86, 66]. At 0.5 wt%,

CNF clusters are formed on the GF surface then inhibited the impregnation of resin to the reinforcing fibers resulting in decreasing the flexural properties of the composite.

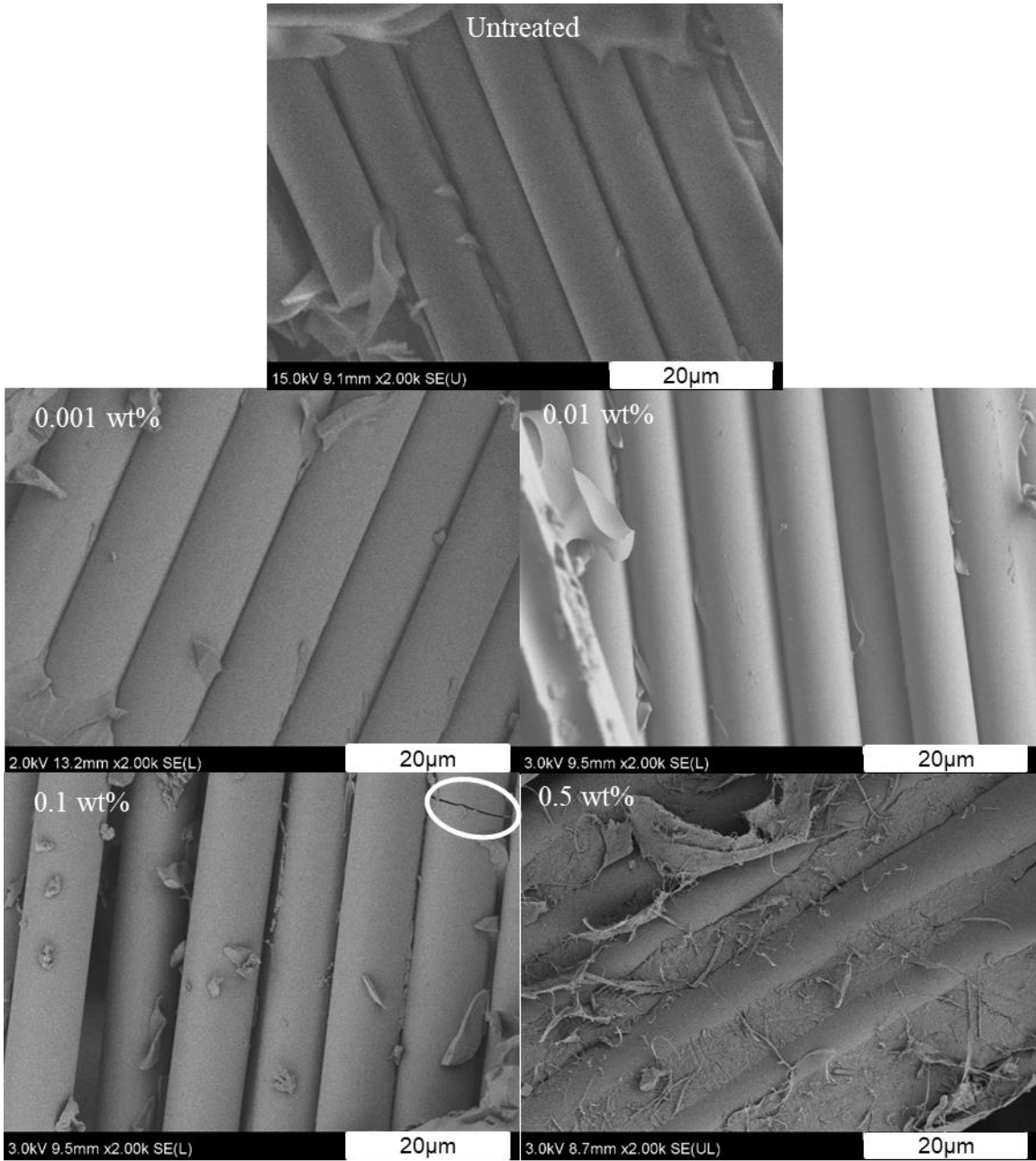


Fig. 4-6. Morphology of the fracture surface of the untreated GF/EP and GF-CNFs/EP composites

4.3.3 Flexural fatigue

The S-N curves of GF/EP and GF-CNFs/EP composites are depicted in Fig. 4-7. From this figure, it can be observed that the number of cycles increases with increasing the CNF concentration. The fatigue life of GF-CNFs/EP composites is significantly improved in comparison with the GF/EP composite. An improvement of the flexural fatigue up to 5 times

at a higher stress level is achieved by adding 0.1 wt% of CNFs to GF/EP composite. Similarly, fatigue properties of FRPs have been remarkably improved by incorporating 0.3 wt% of nanomaterials (CNF and MWCNT) [3]. The low number of cycles found in our study can be attributed to the high-stress level used during the fatigue tests. The effect of stress level has been investigated and the results indicated that to obtain a high number of cycles it is necessary to conduct fatigue tests with low-stress levels [89]. Moreover, the loss of stiffness became higher at higher stress levels, and it becomes low at lower stress levels. It is established that the addition of nanomaterials such as CNT and CNF into the matrix of FRP composites improves significantly the fatigue strength while the static tensile strength increases slightly [3, 50]. For instance, Shao et al. enhanced the fatigue performance of CFRP up to 30 times by adding 0.3 wt% of CNFs into the composites. Similarly, tensile fatigue has been improved by about three to four times by adding nanoparticles into the matrix of glass fiber/epoxy composites [51]. Interestingly, a small amount of nanomaterials added to FRP composites indicated a remarkable improvement in fatigue performance.

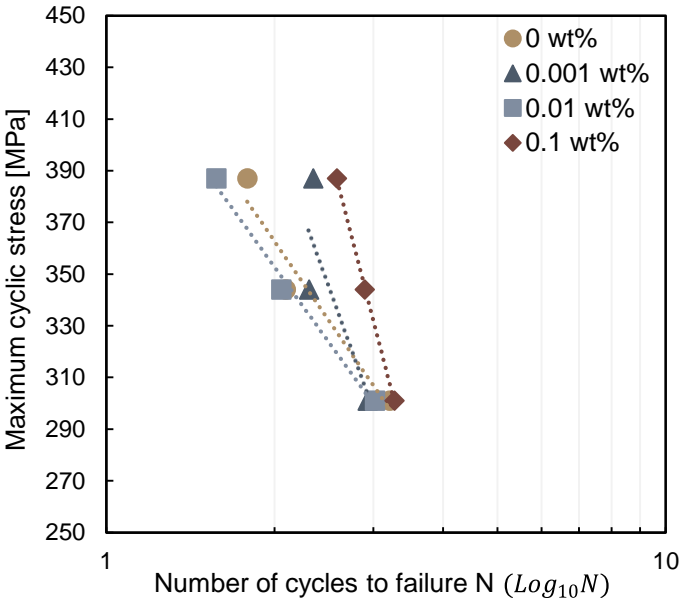


Fig. 4-7. S-N curves of GF/EP and GF-CNFs/EP composites.

Fig. 4-8b shows the morphology of the fracture surface of the GF/EP and GF-CNFs/EP composites. The fracture surface is smoother with the GF/EP and becomes rougher in the CNF-modified GF/epoxy composites. It can be seen that the failure mode in GF-CNFs/EP composites is different from that of the neat GF/EP (see Fig. 4-8a-c). In GF/EP composite, the crack concentrated at the midpoint of the specimen and then led to transversal fracture mode. However, the crack in GF-CNFs/EP composites dissipated and propagated along the specimen

length resulting in delaying the fracture of composites. This suggests that the presence of CNFs on the GF surface increases the interfacial bonding between fibers and matrix resulting in improving the fatigue life. Most of the damage in composite materials is independently or combinedly supported by fiber/matrix debonding, matrix cracking, fiber breakage, or delamination.

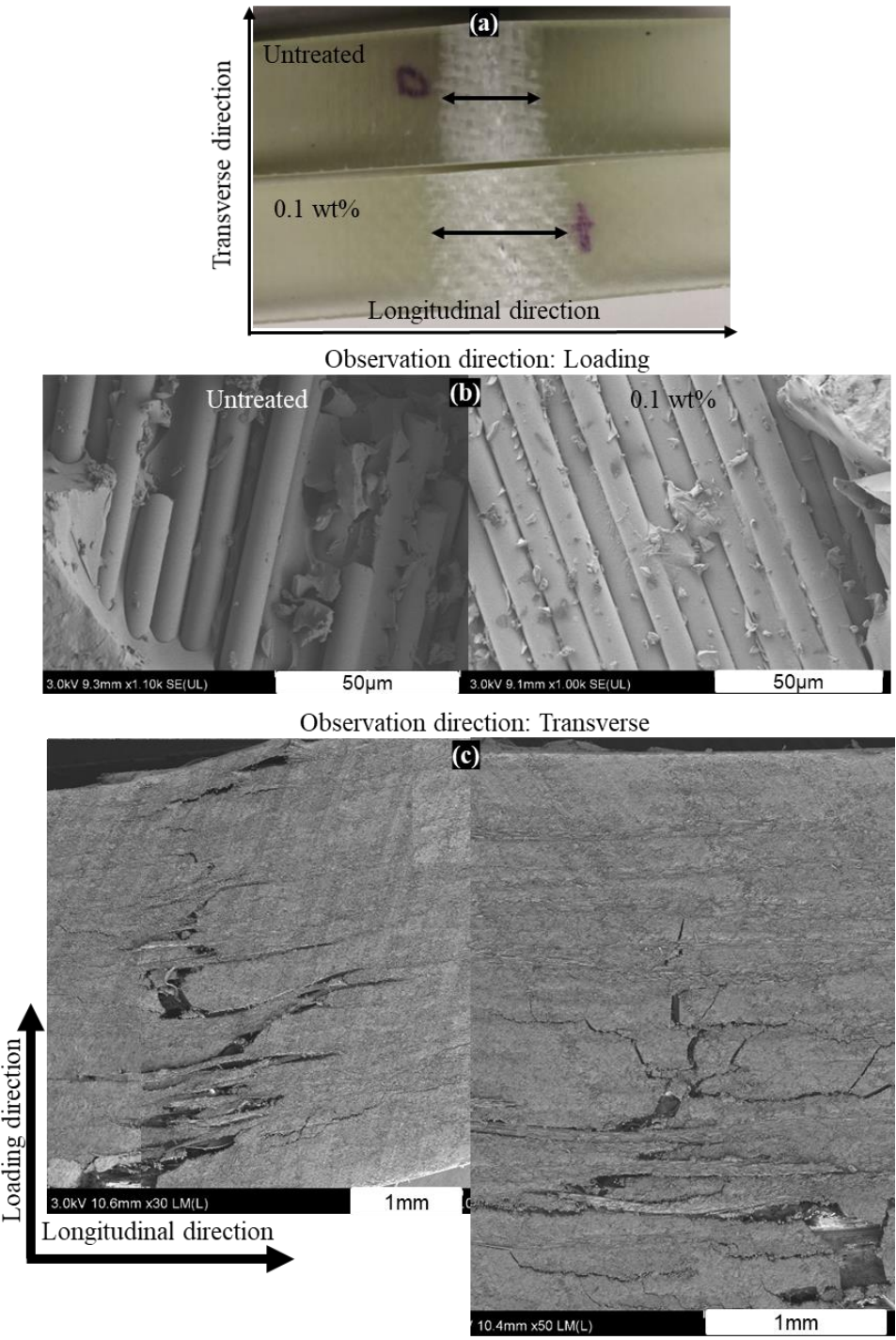


Fig. 4-8. Fracture surface (b) and crack propagation (a-c) of the GF/EP and GF-CNFs/EP composites after flexural fatigue tests.

4.4 Conclusions

In this study, different CNF concentrations have been impregnated into woven glass fabrics to improve the flexural and fatigue properties of GFRP composites. The flexural properties of GF-CNFs/EP composites as determined by three-point bending revealed a dose-dependent increase in flexural strength of up to 6% compared to the pristine GF/EP composite while the flexural modulus remained constant. Moreover, flexural fatigue has been significantly improved when increasing the concentration of CNFs in the composites. Overall, the incorporation of CNFs into GFRP composites seems to be a promising alternative to improve the fatigue life of composites. However, these results have to be interpreted with caution as a reverse trend has been reported in our study and elsewhere when exceeding a certain concentration, and needs further investigation.

Chapitre 5: Effect of cellulose nanofibers on the interlaminar fracture toughness of glass fiber/epoxy composites

5.1 Introduction

Glass fiber reinforced polymer (GFRP) composites are widely used as engineering materials in various industries (e.g., aerospace, automotive, marine) due to their combination of excellent mechanical, chemical, and physical properties. The need for efficient fuel consumption and lightweight structures in industrial applications has grown the use of fiber-reinforced polymers (FRP) composites. Thermoset polymers such as epoxy resins are commonly used in GFRP composites owing to their relatively high strength, good chemical resistance, low cost, excellent thermal stability, and good flexibility. However, they become brittle after being cured with crosslinked agents, making composites sensitive to damage, including crack initiation and propagation.

Cracks propagate under a repetitive constant load leading to delamination bringing about fracture of composite materials. Delamination or interlaminar failure occurs at the resin-rich interlayer between two reinforcing plies mainly undergoing tensile mode (mode I), shear mode (mode II), or tearing mode (mode III) loading conditions [90]. The resistance of composite materials to these failures is interlaminar fracture toughness (IFT) or critical energy release rate (G_C). The IFT mode II (G_{IIc}) is one of the most prevalent loading modes in composite laminates, especially for aerospace applications. This mode is also known as rotation mode, occurring under flexural loads. Hence, interlaminar fracture toughness is a critical parameter when designing fiber-reinforced polymer (FRP) composites because a low IFT leads to failure in the entire composite. Thus, it is necessary to improve the G_{IIc} of FRP composites through resin toughness at the resin-rich regions where delamination takes place. Various methods such as incorporating nanomaterials into the matrix [91, 92, 93], modifying the structure of the fiber preforms by Z-pinning [94], stitching [95], and interlaying composite laminates with interleaved nanofibers [96, 97] or thermoplastics [98] have been used to improve the interlaminar fracture toughness of composite laminates.

Many studies have focused on the interlaying method to avoid the drawbacks mentioned previously. Electrospun thermoplastic nanofibers used as an interlayer at the midplane of FRP composite laminates have significantly improved interlaminar fracture toughness [99]. Daelemans et al. [90] studied the toughening mechanism in carbon fiber/epoxy composite by interleaving polyamide (PA) nanofiber veils. They reported a maximum of 42% and 190%

improvements in both mode I (G_{IC}) and mode II (G_{IIC}), respectively. The noteworthy increase in mode II might be due to a good load transfer to nanofibers along fiber direction arising from crack propagation and shear stresses. Shin et al. [100] incorporated high concentrations of CNTs into epoxy using ultrasonication and three-roll milling to make CNTs/epoxy film-interleave, which were used to improve the fracture toughness of CFRP composites. This method increased the G_{IIC} of the composites up to $\sim 127\%$ with 3 wt% CNTs/epoxy film-interleaved. Moreover, Mirjalili et al. [101] investigated the effect of MWCNT as a toughening agent of CFRP composites by resin film infusion (RFI). They prepared two modified resin film systems: (1) with 0.3 wt% MWCNTs + resin/hardener, and (2) with 0.3 wt% MWCNTs + thermoplastic + resin/hardener. Significant improvements of 106% and 108% in G_{IC} and G_{IIC} , respectively, were observed with the composite manufactured with the (2) resin film system. Based on the literature review, the fracture toughness G_{IIC} is in general much higher than G_{IC} .

In recent years, other techniques, including coating CNFs on reinforcing fibers or applying CNF sheets using electro-activated deposition resin molding (ERM), have been developed [102]. Katagiri et al. [102] improved significantly mechanical properties of CFRP composites by applying CNF sheets on the surface of the composites. Uribe et al. [103] coated CNFs on the surface of CF by immersion and spraying methods. The results showed that spraying CNFs was the most effective method to improve the mechanical performance of CF/Epoxy composites. This method increased tensile strength and toughness up to 28% and 52%, respectively, higher than those from the immersion method. In our previous study [86], we developed a new approach of grafting CNFs on the surface of the reinforcing fibers by vacuum impregnation using the VaRTM technique. Subsequently, improvements of 78% and 20% were observed in the interfacial shear strength (IFSS) and flexural strength of GFRP composites, respectively. Nevertheless, the downside of this approach is the non-uniform dispersion of CNFs throughout the woven GF laminates due to the filtering effect of the reinforcing fibers. Zhu et al. [96] used waterborne epoxy with CNFs to manufacture CNF interleaves by freeze-drying. After that, CNFs interleaves were inserted between layers of CFRP laminates. The results revealed 22% and 25% improvements in G_{IC} and G_{IIC} , respectively, by adding a small quantity of CNFs. However, there are very limited studies on the effect of CNFs on interlaminar fracture toughness.

Based on the literature review, no studies have reported the effect of CNF grafting on reinforcing fibers on the interlaminar fracture toughness of FRP composite laminates. Therefore, in this study, a new simple method of modifying the structure of the interlaminar interface of

GF laminates was proposed to improve the interlaminar fracture toughness. CNF suspensions with different concentrations (0.05, 0.075, and 0.1 wt%) were applied to the interlaminar interfaces of woven GF laminates. The ability of CNFs to withstand crack propagation and delamination of GFRP composites was investigated. The critical energy release rate for IFT mode II (G_{IIC}) was evaluated by conducting three-point end notched flexure (ENF) tests. To clarify the toughening mechanisms, the morphology of fracture surfaces of GFRP composites after ENF tests was examined using a field-emission electron microscope (FE-SEM).

5.2 Experimental methods

5.2.1 Materials

In this study, woven glass fiber was supplied by Nittobo Techno Co. (Japan) with an areal density of 104 g/m². A low viscosity epoxy-phenol novolac resin (Araldite LY5052) and cycloaliphatic polyamine (Aradur 5052), used as curing agents, were purchased from Huntsman Advanced Materials (Switzerland). The mixing ratio recommended by the supplier was 100:38 by weight. CNF was received from Kochi Prefectural Paper Industry Technology Center (Japan) in the slurry form with 2 wt% of CNF content. The width of CNFs was estimated between 10 to 50 nm [24].

5.2.2 Preparation of woven GFs with CNFs

CNFs were mixed with purified water and ultrasonicated using an MCS-10 As-One to prepare three CNF suspensions with different weight fractions (0.05, 0.075, and 0.1wt%). Ultrasonication was used to disaggregate and disperse CNFs by hydrodynamic shear force. On the other hand, woven glass fibers were burnt out in a furnace at 350°C for 1 hour to remove the organic sizing agent. After cooling them down in the furnace, woven GFs were successively washed with acetone, isopropanol, and purified water. The washed woven GFs were then dried in an air oven at 60°C for 3 hours. The details of CNFs and woven GFs preparations are clearly described in our previous study [86].

5.2.3 Manufacturing of GFRP composites

Forty GF plies (135 x 105 mm²) were cut from unsized woven GFs, and then laid up in two laminates of twenty plies each. CNF suspensions were then sprayed three times onto the top surface of each 20-ply laminate using a manual spray-gun (Trusco, TSG-500G). After spraying CNFs, a 50 μm PTFE film with 40 mm width was placed at one end of the 20-ply laminate to form an initial crack. The laminates were stacked on each other and then dried in the air oven at 60°C for 5 hours. Before the drying process, an aluminum plate (125 x 100 x 5 mm³) was

placed on the 40-ply laminate and moderately pressed to ensure enough contact between the CNFs treated surface of each laminate. Hence, the VaRTM process was used to infuse epoxy resin (Epoxy 108.7g + curing agent 41.03 g) into the laminate. Before its use, epoxy resin (EP) was mixed and then degassed to remove air bubbles using a vacuum desiccator. The laminated composite was cured at room temperature (RT) for 20 hours, followed by post-curing at 80°C for 2 hours in the oven. The volume fraction of the untreated and CNF-treated GFRP composites was estimated at ~ 40%. Three specimens were cut from each composite laminate for ENF testing. Fig. 5-1 illustrates the different stages of the manufacturing process for GFRP composite laminates.

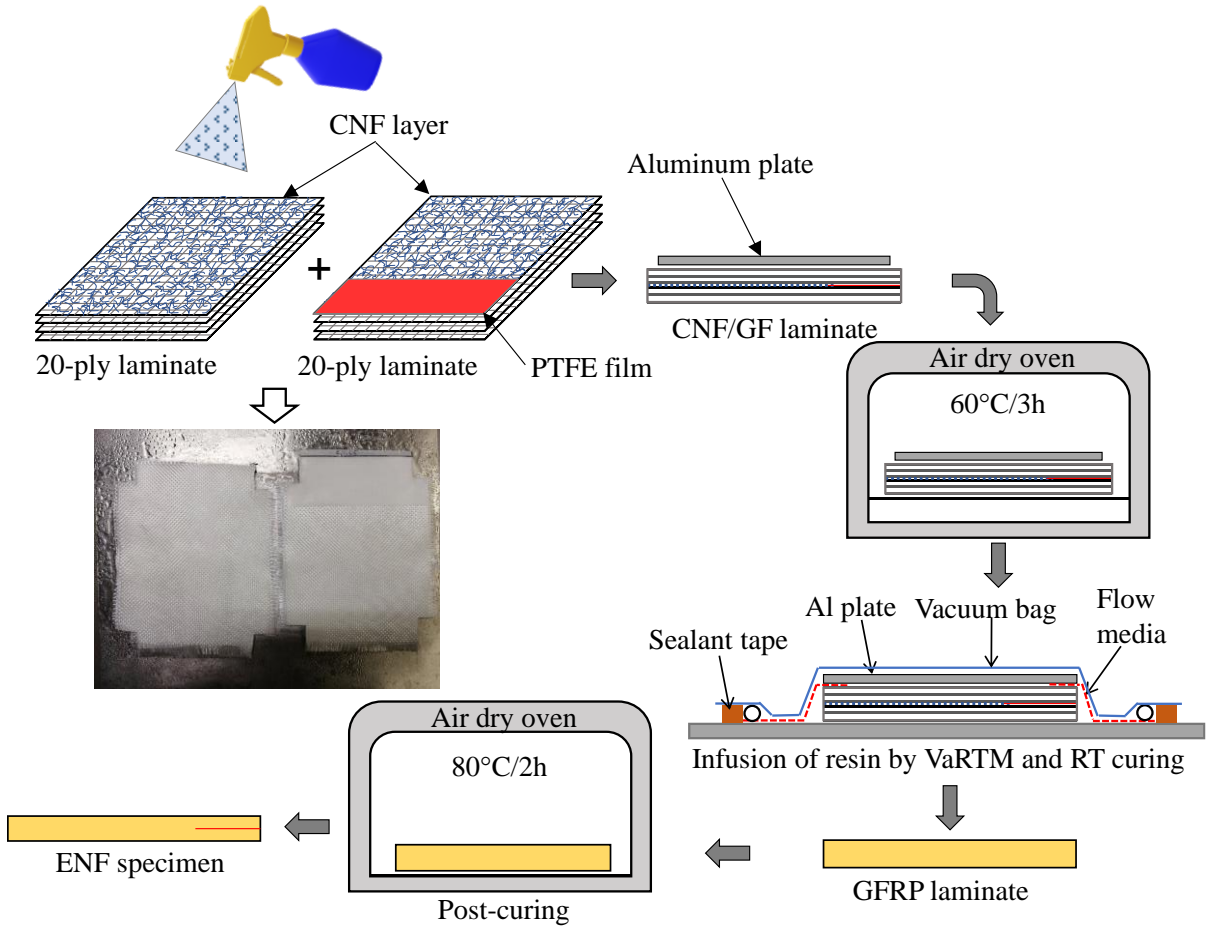


Fig. 5-1. Illustration of CNF incorporating GF and manufacturing GFRP composites laminates.

5.2.4 End notched flexure tests

ENF tests were performed using a 10 kN Shimadzu Autograph AGS-X (Japan) testing machine to evaluate the resistance of interlaminar fracture toughness G_{IIC} of the GFRP composites according to the JIS K7086 [104]. As shown in Fig. 5-2, the specimen (120 x 25 x

4 mm³) was positioned at a constant distance of 20 mm between the PTFE film tip and the center of the loading roller under a three-point bending mode. The first test failed because the specimen slipped under a relatively high bending load. Therefore, silicon rubber with 2 mm in thickness was placed on the underside of the specimen above the supporting rollers. The load (P) and displacement (δ) were controlled at a crosshead speed of 2 mm/min and recorded with a non-contact video type extensometer (TRAPEZIUM Lite X, Shimadzu, Japan). The interlaminar fracture toughness of GFRP composites was determined by calculating the critical energy release rate G_{IIC} using the following equations (1) and (2) [104]:

$$G_{IIC} = \frac{9P_c^2 a^2 C}{2B \left(3a^3 + 2 \left(\frac{L}{2} \right)^3 \right)} \quad (5.1)$$

$$a = \left[\frac{C}{C_0} a_0^3 + \frac{2}{3} \left(\frac{C}{C_0} - 1 \right) \left(\frac{L}{2} \right)^3 \right]^{\frac{1}{3}} \quad (5.2)$$

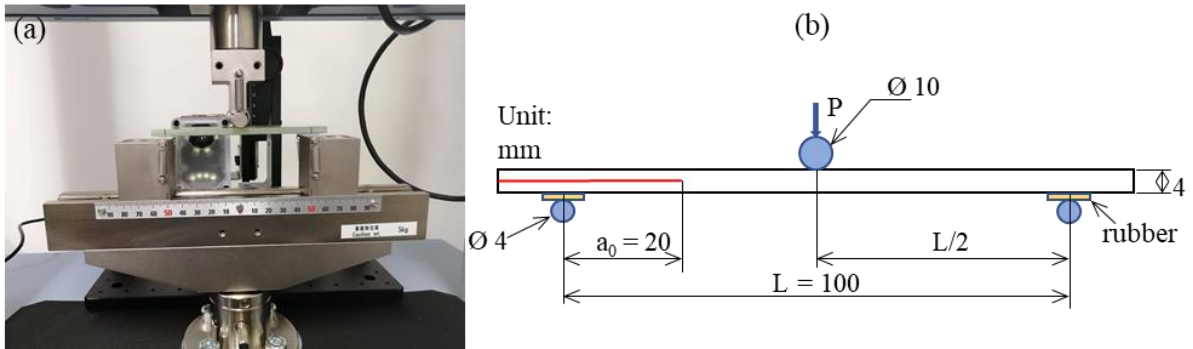


Fig. 5-2. Three-point ENF test: specimen set-up

where P_c indicates the critical load, which is determined from the load-displacement data. a and a_0 are the crack length at the critical load and initial crack length, respectively. C (δ_c/P_c) indicates the compliance at the critical load, and C_0 indicates the compliance within the linear elastic deformation before crack propagation (see Fig. 5-3). In this study, C_0 was determined using the data ranging from 300 to 500 N. L and B represent the span length and the width of the specimen, respectively. At least three specimens were tested for the neat GF/EP composite and the CNF-treated GF/EP composite laminates.

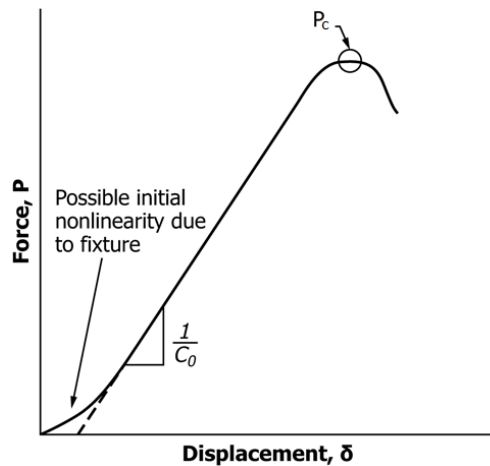


Fig. 5-3. Illustration of compliance and critical load determination

5.2.5 Surface characterization

The morphology of the CNFs treated woven GF laminates and the fracture surfaces of the GFRP composite laminates after the ENF test was examined to investigate the toughening mechanism using an FE-SEM (Hitachi SU8020, Japan). A low accelerating voltage of 1.5 kV was selected during the observation. to avoid the metal coating sputter which may change the morphology of the specimen.

5.3 Results and discussion

5.3.1 Morphology of the CNFs-treated woven GF laminates

Fig. 5-4 characterizes the morphology of woven GFs after spraying CNFs and drying the reinforced laminates. It can be observed that CNFs were randomly coated on the GF surface (Fig. 5-4b-d-f). Regardless of the CNF content, a web-like nanostructure is formed on the surface of GF laminates and bridged between fibers (Fig. 5-4c-e-g). The thickness of CNFs coated layer became larger with increasing its concentration. The surface of CNFs-treated GF is rougher than that of untreated GFs, increasing the specific surface area. This suggests the possibility of mechanical interlocking between GFs and epoxy matrix. In Fig. 5-4c-e, thinner CNF layers without aggregates can be observed, indicating a good dispersion of CNF and higher porosity, which may give rise to better resin impregnation. However, when 0.1 wt% of CNFs was sprayed, the CNF layer became thicker and denser. The density of the CNF layer may prevent the epoxy resin from impregnating the reinforcing fibers, which might lead to a low interfacial adhesion between GFs and epoxy. It was found that the densest CNF layer indicated lower porosity making resin impregnation difficult [105]. Moreover, CNF aggregations are formed, making heterogeneous dispersion over the GF surface.

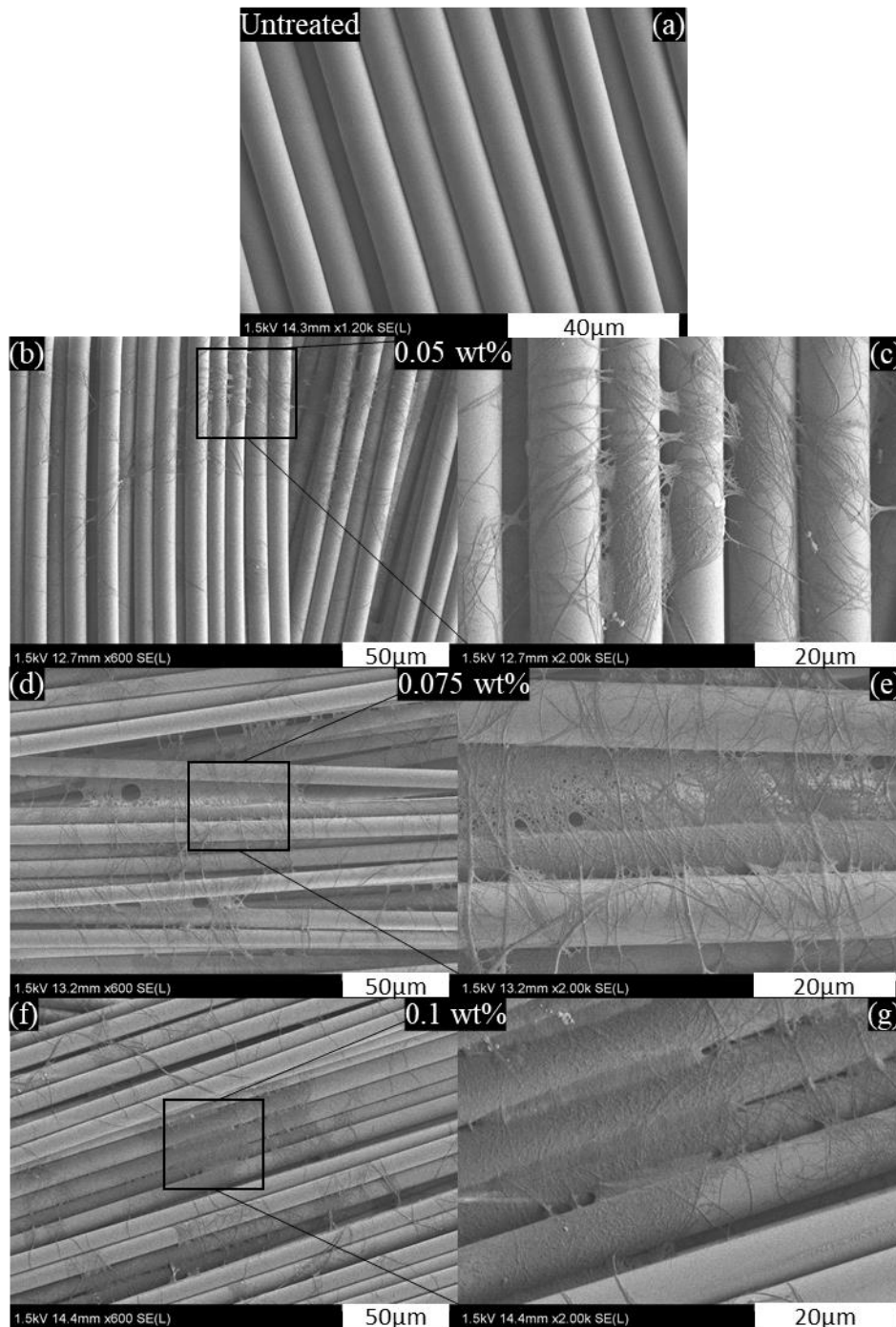


Fig. 5-4. Morphology of untreated woven GF laminate (a), and CNFs-treated woven GF laminates: 0.05 wt% (b-c), 0.075 wt% (d-e), 0.1 wt% (f-g).

5.3.2 Interlaminar fracture toughness G_{IIc}

The interlaminar fracture toughness of GFRP composite laminates was investigated under mode II loading. Fig. 5-5 shows load vs. displacement curves for neat GF/EP composite and CNFs-treated GF/EP composites. The load increased with the displacement showing a linear relationship and stable crack propagation. When the load reached the critical value, unstable

crack propagation occurred, and the load decreased. It is shown that the load for GF-CNFs/EP composites, except 0.1wt % CNFs, increased up to 926 N (from 881 N), resulting in better resistance to crack propagation and delamination. Almost the same slope can be observed from the curves because CNFs did not affect the thickness and density of GF-CNFs/EP composites. The initiation of crack growth ($G_{IIC\ initiation}$) is determined by appraising the fracture energy rate from the load at the nonlinear (P_{NL}) point from load-displacement curves. The crack propagation ($G_{IIC\ propagation}$) of GRFP composites is evaluated by calculating the critical energy release rate from the maximum load (P_c).

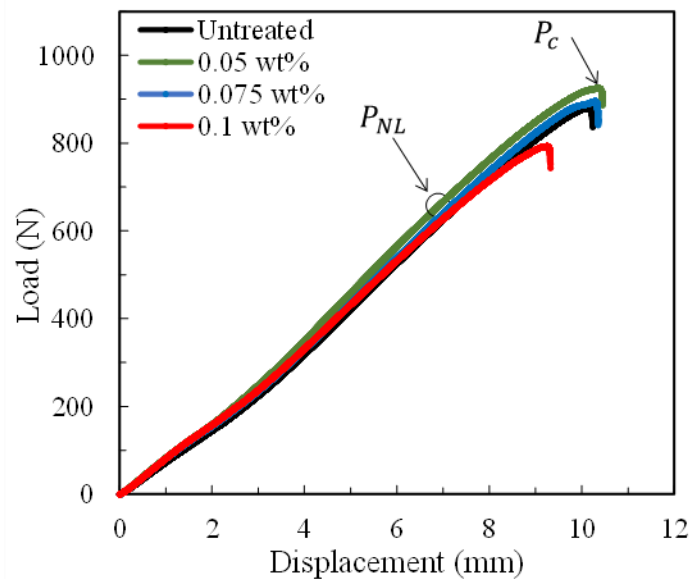


Fig. 5-5. load vs. displacement curves of GF/EP and GF-CNFs/EP composites obtained from ENF tests.

Energy release rates G_{IIC} for crack initiation and crack propagation were calculated using Eq (1) and (2). Fig. 5-6 shows the average interlaminar fracture toughness of GFRP composites. It can be easily seen that the G_{IIC} of GF-CNFs/EP composites (up to 0.075 wt%) is higher than that of the neat GF/EP composite. After spraying 0.05 and 0.075 wt% of CNFs, $G_{IIC\ initiation}$ increased slightly due to the low CNF content while $G_{IIC\ propagation}$ showed significant improvements. The $G_{IIC\ propagation}$ of the GF-CNF/EP composites with 0.05 and 0.075 wt% improved by 28% and 19%, respectively, in comparison with the GF/EP composite. The maximum improvement of $G_{IIC\ propagation}$ obtained from the composite with 0.05 wt% CNFs can be ascribed to the thin CNF nanostructures allowing a good impregnation of fibers with epoxy matrix.

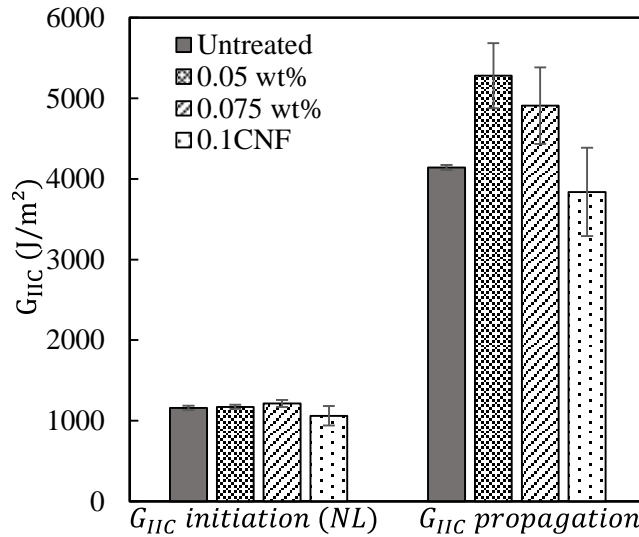


Fig. 5-6. Interlaminar fracture toughness G_{IIC} of GF/EP and GF-CNFs/EP composite laminates

In comparison, 0.075 wt% of CNFs exhibits a slight decrease in comparison with 0.05 wt%, which may result from the increase of CNF coating layers. However, these improvements in G_{IIC} can be attributed to the stronger interfacial bonding of GF-CNF/EP laminates compared to the neat GF/EP composite. The web-like CNF nanostructure observed in Fig. 4 might also contribute to toughening epoxy resin, indicating a better fracture toughness of the composites. On the other hand, a degradation of the interlaminar fracture toughness is exhibited at 0.1 wt% due to the thicker CNF coating layers, which may prevent epoxy resin from impregnating the reinforcing GF. With this CNF concentration, G_{IIC} propagation decreases from 4141 to 3838 N/m² indicating a weak GF-CNF/EP adhesion. Table 5-1 summarizes the average values of interlaminar fracture toughness of GFRP composites after ENF tests.

Table 5-1. average of interlaminar fracture toughness after ENF tests.

	P_c (N)	δc (mm)	a (mm)	B (mm)	L (mm)	G_{IIC} initiation (J/m ²)	G_{IIC} propagation (J/m ²)	Increase (%)
Untreated	881	10.1	29.0	25.22	50	1159	4141	-
0.05 wt%	926	10.3	29.1	25.02	50	1172	5282	28%
0.075 wt%	896	10.1	28.7	25.13	50	1213	4908	19%
0.1 CNF	783	9.2	28.5	25.04	50	1061	3838	-7%

The low energy release rate at crack initiation G_{IIC} initiation can also result from the high loading speed as reported in a study conducted by De Baere et al. [106], where two crosshead speeds (0.5 and 1 mm/min) were used. These results revealed that the specimen loaded with high speed resulted in lower crack initiation and higher crack propagation, compared to that

with low loading speed. The same trend was also found by Berger et al., who studied the effect of loading rate on the mode II interlaminar fracture toughness of CF/PEEK composites [107].

It is well known that the presence of CNFs on the GF surface increases the surface area, which induces mechanical interlocking between GF and EP. This can contribute to improving the interlaminar fracture toughness due to the irregular path of crack [96]. In the study by Wang et al. [97], CNFs-modified polyetherimide (PEI) nanofibrous interleaves were used to improve the interlaminar fracture toughness of CFRP composites. The mode II fracture toughness has been enhanced up to 20% with 6 wt% CNC. Moreover, the addition of MWCNT + n-butyl glycidyl ether into the epoxy matrix of GFRP resulted in increasing the interlaminar fracture toughness by about 23%. Interestingly, the result of this work exhibits higher improvement in G_{IIC} with a very low CNF concentration (e.g., 0.05 wt%) compared to the result obtained by Wang et al. The same comparison can also be made with the results of Zhu et al. [96] where a maximum improvement of 25% in G_{IIC} was reported with the same CNF concentration. On the other hand, the use of CNF with chopped flax fibers (FF) as interlayer resulted in a big improvement of up to 100% in G_{IIC} of CF/EP composites owing to the good compatibility between CNFs and FF [105]. Therefore, the compatibility of CNF with reinforcing fibers plays an essential role in its dispersity and resin impregnation.

5.3.3 Fractography

The fracture surfaces of the GF/EP and GF-CNF/EP composites are presented in Fig. 5-7 to better understand the toughening mechanisms of delamination. The SEM images reveal that the GF surfaces of GF-CNF/EP composites are rougher than those of neat GF/EP composite. Fiber breakage and smooth traces of fiber pull-out from interfacial debonding can be observed in Fig. 5-7a-b, corresponding to low interfacial adhesion between GF and EP. In Fig. 5-7c-e, residual epoxy and CNFs-EP (in red circles) fragments remain attached on the GFs surface, indicating a good fiber/epoxy interface bond. In addition, shear hackles between fibers (in black arrows) and large epoxy deformations (in white arrows) can be seen in Fig. 5-7c-e and d-f, respectively. However, epoxy deformations are more frequent in the 0.05 wt% composite than those in the 0.075 wt% composite laminate. Shear hackles are also more obvious in Fig. 5-7c, which can be ascribed to stronger interlaminar shear strength. The increased fracture surface of hackles creates more energy dissipation and hence improves interlaminar fracture toughness [91, 108]. The mechanisms aforementioned are attributed to shear stress due to the presence of CNFs at the mid-plane of GFRP composites indicating better resistance of interlaminar fracture toughness. It was found that adding CNFs onto the reinforcing fiber surfaces increases the

specific surface area, improving the interfacial bonding and mechanical friction between fibers and epoxy [105]. Furthermore, CNF bridging was revealed to be effective in dissipating the fracture energy of delamination in a specimen under shear loading and hindering crack propagation.

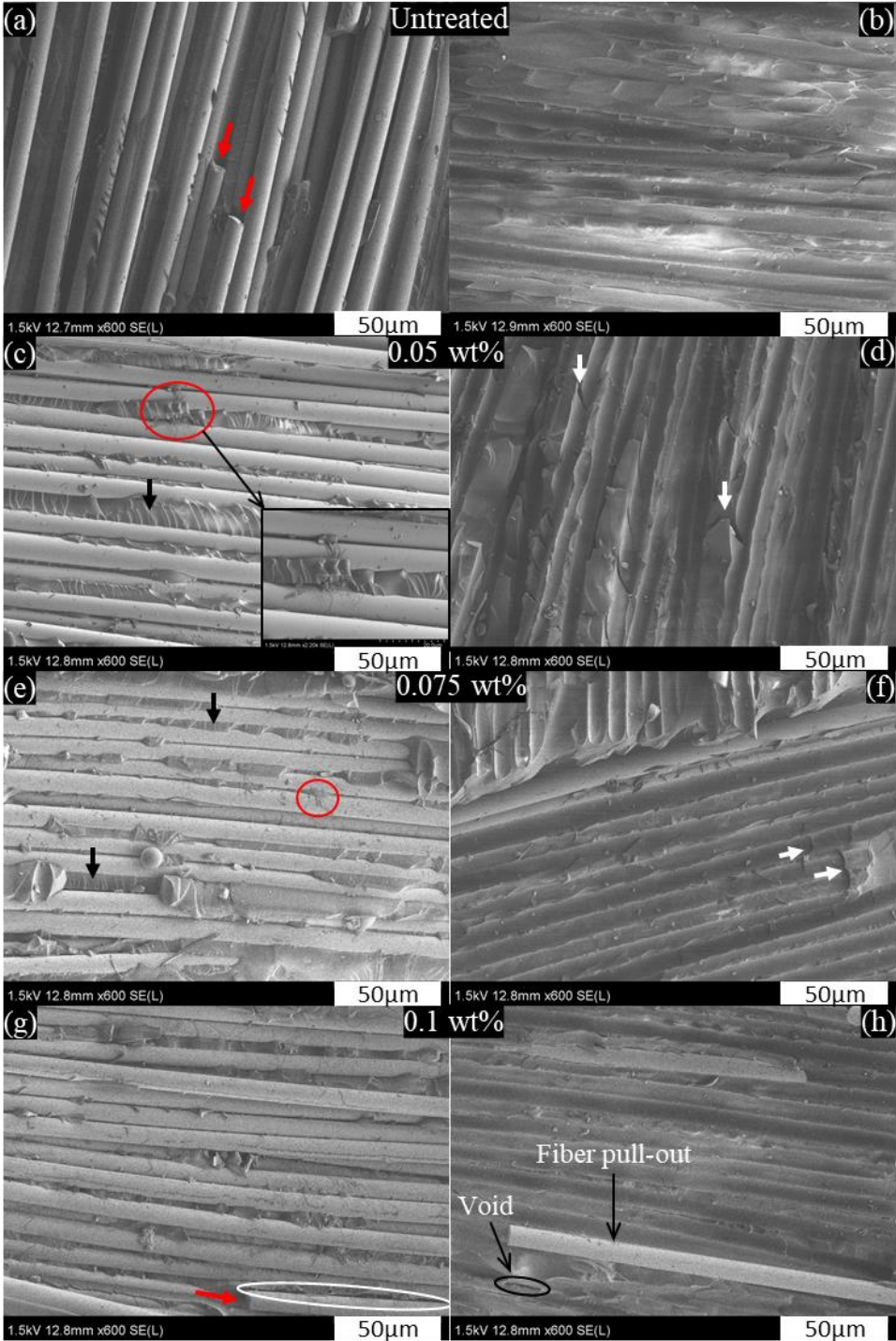


Fig. 5-7. FE-SEM photographs of fractured surfaces after ENF test for: neat GF/epoxy composite (a-b), and GF-CNF/epoxy composites with: 0.05 wt% (c-d), 0.075 wt% (e-f), 0.1 wt% (g-h).

In contrast, we can observe in Fig. 5-7g large fiber/epoxy debonding (in white circle) and fiber breakage (in red arrow), arising from low fiber/epoxy interfacial bond due to the thicker CNF coating layer. Fig. 5-7h indicates smoother fiber pull-out traces and large void (in black circle) compared to 0.05 wt% GF-CNF/EP composite (Fig. 5-7d). Despite the matrix deformation, reducing fiber/matrix interfacial strength decreases resistance crack propagation [109]. Epoxy matrix micro-cracking in composite contributed to a much lower G_{IIC} propagation. Therefore, these mechanisms could explain the reason for the low interlaminar fracture toughness in 0.1 wt% GF-CNF/EP composite. Moreover, Fig. 5-8 illustrates the crack propagation path at the interlaminar fracture toughness of the composite laminates. The path propagation of crack for the untreated composite laminate is regular resulting from a weak interlaminar adhesion interface. Meanwhile, at 0.05 wt% the crack propagation exhibited an irregular path, which may delay the crack propagation.

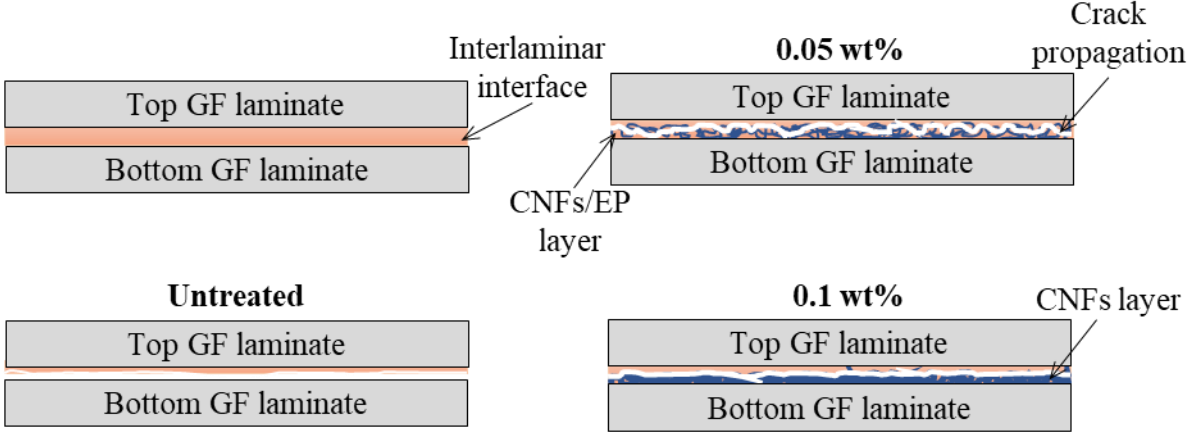


Fig. 5-8. Illustration of crack propagation in the GFRP composite laminates

The images of fracture surfaces with high magnification were taken to understand further the mechanism for improving the interlaminar fracture toughness. Fig. 5-9 shows the fracture morphology of fiber traces after ENF tests to elucidate the toughening mechanisms. It can be seen that the neat GF/EP composite shows smooth traces from fiber pull-out without epoxy deformations. In the specimen with 0.075 wt% CNFs, fiber traces are rougher (with epoxy deformations) than the neat GF/EP composite, indicating strong bonding between GF-CNF and EP. As for 0.1 wt% CNFs, flat fiber traces are observed resulting from resin unimpregnation regions caused by the bridging of thick and dense CNF layers between adjacent fibers. Hence, the interface between GF-CNF and EP is very weak, decreasing the composite's interlaminar fracture toughness.

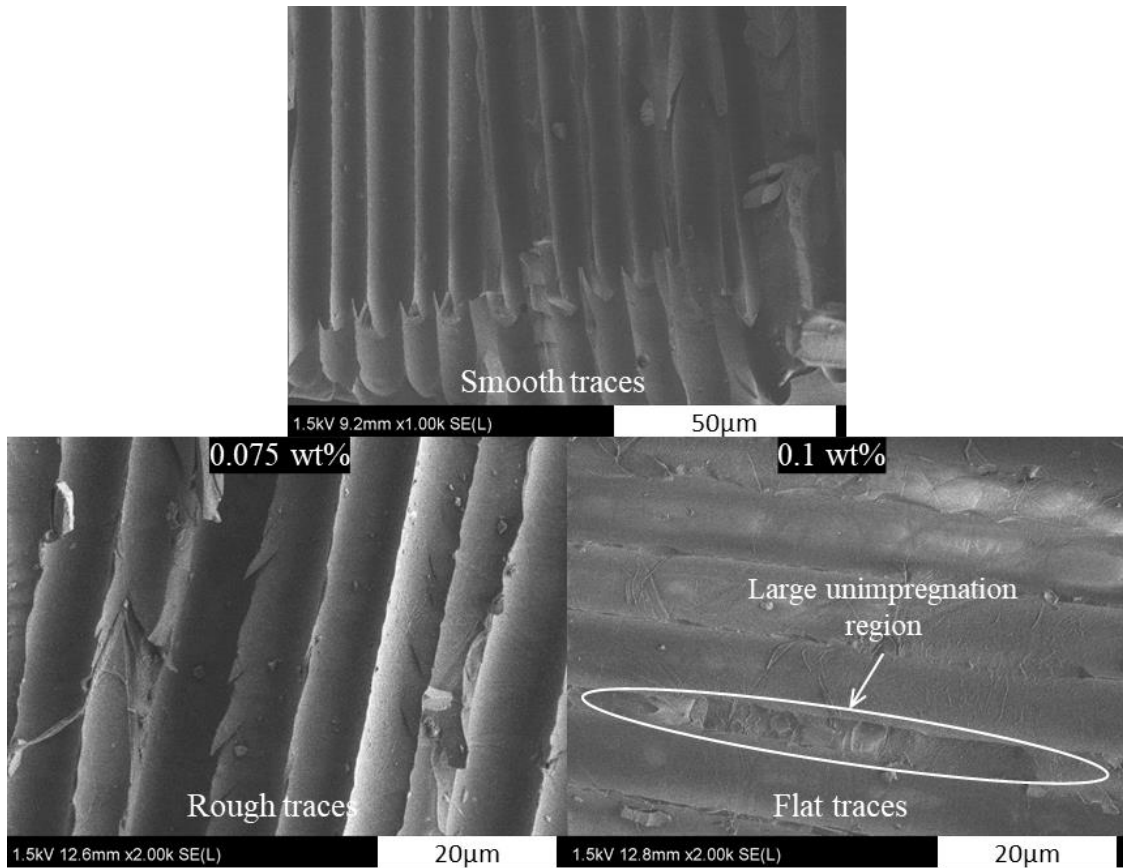


Fig. 5-9. Fracture morphology of fiber traces at higher magnification for untreated, 0.075 and 0.1 wt% of GF/EP composites.

5.4 Conclusion

This study proposed an alternative method of applying CNFs onto GFs to improve interlaminar fracture toughness mode II of GFRP composite laminates. The effect of CNFs on interlaminar fracture toughness G_{IIC} of the GF-CNFs/EP laminates was investigated. It was indicated that the presence of CNF at the interlaminar interface of GF/EP laminate can improve the G_{IIC} . The interlaminar fracture toughness of composite laminate at crack initiation $G_{IIC\text{ initiation}}$ was slightly increased, whereas $G_{IIC\text{ propagation}}$ exhibited significant improvement resulted from the stronger interfacial adhesion. The optimum concentration was revealed to be 0.05 wt% with an improvement of 28% in $G_{IIC\text{ propagation}}$. However, the highest CNF concentration (0.1 wt%) led to a degradation in G_{IIC} due to the thickening of the CNF coating layer, which prevented epoxy resin from impregnating GFs. The toughening mechanisms were also examined by FE-SEM analysis. Epoxy deformations, roughness of fiber traces and shear were the main reasons for improving the interlaminar fracture toughness mode II.

Chapitre 6: General conclusions

The objective of this study was to improve the interfacial strength of glass fiber-reinforced composites by grafting CNFs on the reinforcing fiber and then investigating its effect on the macromechanical properties. The dissertation presented an overview of alternative methods for improving the mechanical properties of GFRP composites. Firstly, CNFs were successfully grafted onto the GF surfaces by vacuum impregnation, and their effect on the interfacial strength and flexural strength of GFRP composites was investigated. Secondly, the method of manufacturing composites has been modified to make surfaces smoother and flatter. Hence, the flexural strength and fatigue life of the composites were evaluated. Finally, spray coating method was used to apply CNFs at the interlaminar interface of the GF laminates and the interlaminar fracture toughness mode II of the composite laminates was investigated.

The results indicated a significant improvement of 78% in the interfacial strength of the GF-CNFs/EP composites at low CNF concentration. Likewise, an enhancement of the macromechanical properties by flexural strength was obtained. It was found that the dispersity of CNFs through the GF laminate and the thickness of the CNF layer coated on the reinforcing fiber played a vital role in improving the performance of the composites. The formation of CNF clusters was observed from 0.005 wt%. The increase in number and thickness of CNF clusters when increasing CNF concentration resulted in decreasing the mechanical properties of GFRP composites. Moreover, the flexural properties of GF-CNFs/EP as determined by three-point bending revealed a moderate increase up to 6% compared to the pristine GF/epoxy composite while the flexural modulus remained constant. Flexural fatigue was significantly improved when increasing the concentration of CNFs up to 0.1 wt%. Overall, the incorporation of CNFs into GF laminate by vacuum impregnation revealed to be an alternative method to improve the fatigue life of FRP composites. On the other hand, it was found that the presence of thin layer and web-like structure of CNFs at the interlaminar interface of GF laminates resulted in significant improvement of interlaminar fracture toughness by 28%. However, the highest CNF concentration (0.1 wt%) led to a reduction in G_{IIC} due to the thickening of CNF layer. Epoxy matrix deformations, CNFs bridging, and shear hackles were found to be the main reason for the improvement in G_{IIC} .

Based on the results, the interfacial strength of FRP composites can be improved by grafting a low quantity of CNFs onto the reinforcing fibers. Vacuum impregnation of CNFs to woven glass fabrics revealed to be a promising method to incorporate nanomaterials into composite

materials. Thus, the VaRTM technique could be used in manufacturing FRP composites as a modifying method of fiber/matrix interface allowing to avoid processing high viscosity resin. In addition, due to the filtering effect of CNF during the grafting process by vacuum impregnation, further study is recommended for better improvement of the mechanical performance of FRP composites. Thus, it may be necessary to control the vacuum pressure by creating a space between the fibers to avoid the filtering effect.

References

- [1] A. Ahmad, R. Hamid and S. A. Osman, "Physical and Chemical Modifications of Plant Fibres for Reinforcement in Cementitious Composites," *Advances in Civil Engineering*, ID 5185806 (2019); 18 pages.
- [2] M. Jing, J. Che, S. Xu, Z. Lui and Q. Fu, "The effect of surface modification of glass fiber on the performance of poly(lactic acid) composites: Graphene oxide vs. silane coupling agents," *Applied Surface Science*, 435 (2018): 1046-1056.
- [3] Y. Shao, T. Yashiro, K. Okubo and T. Fujii, "Effect of cellulose nano fiber (CNF) on fatigue performance of carbon fiber fabric composites," *Composites: Part A*, 76 (2015) 244-254.
- [4] V. Mane and C. Markad, "An overview of glass fibers," www.textiletoday.com.bd, 2015.
- [5] J. L. Thomason, "Glass fibre sizing: A review," *Composites Part A*, 127 (2019) 105619.
- [6] T. P. Sathishkumar, S. Satheeshkumar and J. Naveen, "Glass fiber-reinforced polymer composites: a review," *Journal of Reinforced Plastics and Composites*, (2014) 33 (13): 1258–1275.
- [7] T.-D. Ngo, "Introduction to Composite Materials," in *Composite and Nanocomposite Materials - From Knowledge to Industrial Applications*, (2020) pp. 1-27.
- [8] S. Faragi, A. Hamedani, G. Alahyarizadeh, A. Minuchehr, M. Aghaie and B. Arab, "Mechanical properties of carbon nanotube- and graphene-reinforced Araldite LY/Aradur HY 5052 resin epoxy composites: a molecular dynamics study," *Journal of Molecular Modeling*, (2019) 25: 191.
- [9] G. B. N. V. S. Gupta, M. M. Hiremath, B. C. Ray and R. K. Prusty, "Improved mechanical responses of GFRP composites with epoxy-vinyl ester interpenetrating polymer network," *Polymer Testing*, 93 (2021) 107008.
- [10] I. S. Abbood, S. A. Odaa, K. F. Hasan and M. A. Jasim, "Properties evaluation of fiber reinforced polymers and their constituent materials used in structures – A review," *Materials Today: Proceedings*, 2021, 43 (2): pp. 1003-1008.
- [11] E. Gudonis, E. Timinskas, V. Gribniak, G. Kaklauskas, A. K. Arnautov and V. Tamulėnas, "FRP reinforcement for concrete structures: state-of-the-art review of application and design," *Engineering Structures and Technologies*, 2013 5 (4): pp. 147–158.

- [12] S. Erden, K. Sever, Y. Seki and M. Sarikanat, "Enhancement of the Mechanical Properties of Glass/polyester Composites via Matrix Modification Glass/polyester Composite Siloxane Matrix Modification," *Fibers and Polymers*, 11 (2010): 732-737.
- [13] D. K. Rajak, D. D. Pagar, P. L. Menezes and E. Linul, "Fiber-Reinforced Polymer Composites: Manufacturing, Properties, and Applications," *Polymers*, 11 (2019) 1667.
- [14] D. K. Rajak, P. H. Wagh and E. Linul, "Manufacturing Technologies of Carbon/Glass Fiber-Reinforced Polymer Composites and Their Properties: A Review," *Polymers*, 13 (2021) 3721.
- [15] F. Campbell, *Structural Composite Materials*, ASM International, 2010.
- [16] V. R. Tamakuwala, "Manufacturing of fiber reinforced polymer by using VARTM process: A review," *Materials Today: Proceedings*, 44 (2021) 987–993.
- [17] M. Amirkhosravi, M. Pishvar and M. C. Altan, "Fabricating high-quality VARTM laminates by magnetic consolidation: experiments and process model," *Composites Part A*, 114 (2018) 398-406.
- [18] W. D. Brouwer, E. C. F. C. Herpt and M. Labordus, "Vacuum injection moulding for large structural applications," *Composites Part A: Applied Science and Manufacturing*, 34 (2003) 551-558.
- [19] M. K. Kang, W. I. Lee and H. T. Hahn, "Analysis of vacuum bag resin transfer molding process," *Composites Part A: Applied Science and Manufacturing*, 32 (2001): 1553-1560.
- [20] K. A. Bhargava, *Engineering Materials Polymers, ceramics and composites*, Prentice/Hall of India, (2004): 224-242.
- [21] R. Fragoudakis, "Failure Concepts in Fiber Reinforced Plastics," in *Failure Analysis and Prevention*, IntechOpen, 2017.
- [22] L. Noels, "http://www.ltas-cm3.ulg.ac.be/FractureMechanics/?p=overview_P3," University of Liège, 2015.
- [23] J. K. Kim, M. Sham and J. Wu, "Nanoscale characterisation of interphase in silane treated glass fibre composites," *Composites Part A: Applied Science and Manufacturing*, 32 (2001): 607-618.
- [24] J. G. Iglesias, J. González-Benito, A. J. Aznar, J. Bravo and J. Baselga, "Effect of Glass Fiber Surface Treatments on Mechanical Strength of Epoxy Based Composite Materials," *Journal of Colloid and Interface Science*, 250 (2002): 251–260.
- [25] A. Valadez-Gonzalez, J. M. Cervantes-Uc, R. Olayo and P. J. Herrera-Franco, "Effect of fiber surface treatment on the fiber–matrix bond strength of natural fiber reinforced composites," *Composites: Part B*, 30 (1999) 309–320.

- [26] M. Sahin, S. Schlögl, G. Kalinka, K. B. Wang, I. Mühlbacher, W. Ziegler, W. Kern and H. Grützmacher, "Tailoring the interfaces in glass fiber-reinforced photopolymer composites," *Polymer*, 141 (2018): 221-231.
- [27] C. Arslan and M. Dogan, "The effects of silane coupling agents on the mechanical properties of basalt fiber reinforced poly(butylene terephthalate) composites," *Composites Part B*, 146 (2018): 145–154.
- [28] M. Abdelmouleh, S. Boufi, M. N. Belgacem, A. Dufresne and A. Gandini, "Modification of Cellulose Fibers with Functionalized Silanes: Effect of the Fiber Treatment on the Mechanical Performances of Cellulose–Thermoset Composites.," *Journal of Applied Polymer Science*, 98 (2005): 974–984 .
- [29] S. -J. Park and J. -S. Jin, "Effect of Silane Coupling Agent on Mechanical Interfacial Properties of Glass Fiber-Reinforced Unsaturated Polyester Composites," *Journal of Polymer Science: Part B: Polymer Physics*, 41 (2003): 55–62.
- [30] Z. Wang, B. Yang, G. Xian, Z. Tian, J. Weng, F. Zhang and S. D. X. Yuan, "An effective method to improve the interfacial shear strength in GF/CF reinforced epoxy composites characterized by fiber pull-out test," *Composites Communications*, 19 (2020): 168–172.
- [31] H. Kurita, Y. Xie, K. Katabira, R. Honda and F. Narita, "The insert effect of cellulose nanofiber layer on glass fiber-reinforced plastic laminates and their flexural properties," *Material Design & Processing Communication*., 2019; 1: e58..
- [32] J. Zhang, S. Deng, Y. Wang, L. Ye, L. Zhou and Z. Zhang, "Effect of nanoparticles on interfacial properties of carbon fibre–epoxy composites," *Composites: Part A*, 55 (2013): 35–44.
- [33] J. Chen, D. Zhao, X. Jin, C. Wang, D. Wang and H. Ge, "Modifying glass fibers with graphene oxide: Towards high-performance polymer composites," *Composites Science and Technology*, 97 (2014) 41-45.
- [34] M. Eesaee and A. Shojaei, "Effect of nanoclays on the mechanical properties and durability of novolac phenolic resin/woven glass fiber composite at various chemical environments," *Composites: Part A*, 63 (2014): 149–158.
- [35] S. Kumar, B. G. Falzon, J. Kun, E. Wilson, G. Graninger and S. Hawkins, "High performance multiscale glass fibre epoxy composites integrated with cellulose nanocrystals for advanced structural applications," *Composites Part A*, 131 (2020) 105801.
- [36] A. Godara, L. Gorbatikh, G. Kalinka, A. Warriar, O. Rochez, L. Mezzo, F. Luizi, A. van Vuure, S. Lomov and I. Verpoest, "Interfacial shear strength of a glass fiber/epoxy bonding in composites modified with carbon nanotubes," *Composites Science and Technology*, 70 (2010) 1346-1352.

- [37] R. Sadeghian, S. Gangireddy, B. Minaie and K. T. Hsiao, "Manufacturing carbon nanofibers toughened polyester/glass fiber composites using vacuum assisted resin transfer molding for enhancing the mode-I delamination resistance," *Composites Part A*, 37 (2006) 1787-1795.
- [38] X. Sun, Q. Wu, S. Lee, Y. Qing and Y. Wu, "Cellulose Nanofibers as a Modifier for Rheology, Curing and Mechanical Performance of Oil Well Cement," *Scientific Reports*, 2016.
- [39] S. K. De and V. M. Murty, "Short fiber-reinforced rubber composites," *Polymer Engineering reviews*, 4 (1984) 313–343.
- [40] W. Y. Hamad, "Cellulosic materials-fibers, networks and composites," *Kluwer Academic Publishers, Massachusetts*, 2002.
- [41] M. N. F. Norrahim, N. A. M. Kasim, V. F. Knight, N. A. Halim, N. A. A. Shah, S. A. M. Noor, S. H. Jamal, K. K. Ong, W. M. Z. Yunus, M. A. Farid, M. A. Jenol and I. R. Ahmad, "Performance evaluation of cellulose nanofiber reinforced polymer composites," *Funct. Compos. Struct.*, 3 (2021) 024001.
- [42] A. Chakrabarty and Y. Teramoto, "Recent Advances in Nanocellulose Composites with Polymers: A Guide for Choosing Partners and How to Incorporate Them," *Polymers*, 10 (2018) 517.
- [43] M. M. S. Lima and R. Borsali, "Rodlike Cellulose Microcrystals: Structure, Properties, and Applications," *Macromol. Rapid Commun.*, 25 (2004): 771–787 .
- [44] M. Jonoobi, J. Harun, A. P. Mathew, M. Z. B. Hussein and K. Oksman, "Preparation of cellulose nanofibers with hydrophobic surface characteristics," *Cellulose*, 2010; 17: 299–307.
- [45] A. Sato, D. Kabusaki, H. Okumura, T. Nakatani, F. Nakatsubo and H. Yano, "Surface modification of cellulose nanofibers with alkenyl succinic anhydride for high-density polyethylene reinforcement," *Composites: Part A*, 2016; 83: 72-79.
- [46] C. Miao and W. Y. Hamad, "Cellulose reinforced polymer composites and nanocomposites: a critical review," *Cellulose*, 20 (2013): 2221–2262 .
- [47] Daio-paper, " Cellulose NanoFiber (CNF)," <https://www.daio-paper.co.jp/en/development/cnf/>.
- [48] N. Saba, F. Mohammad, M. Pervaiz, M. Jawaid, O. Y. Alothman and M. Sain, "Mechanical, morphological and structural properties of cellulose nanofibers reinforced epoxy composites," *International Journal of Biological Macromolecules*, 97 (2017): 190-200.

- [49] S. Kumar, G. Graninger, S. C. Hawkins and B. G. Falzon, "A nanostructured cellulose-based interphase layer to enhance the mechanical performance of glass fibre-reinforced polymer composites," *Composites Part A*, 148 (2021) 106475.
- [50] M. Genedy, S. Daghash, E. Soliman and M. M. Reda Taha, "Improving Fatigue Performance of GFRP Composite Using Carbon Nanotubes," *Fibers*, 3 (2015) 13-29.
- [51] C. M. Manjunatha, A. C. Taylor, A. J. Kinloch and S. Sprenger, "The tensile fatigue behaviour of a silica nanoparticle-modified glass fibre reinforced epoxy composites," *Composites Science and Technology*, 70 (2010) 193-199.
- [52] M. H. Gabr, M. Abd Elrahman, K. Okubo and T. Fujii, "A study on mechanical properties of bacterial cellulose/epoxy reinforced by," *Composites: Part A*, 41 (2010) 1263-1271.
- [53] B. Saboori and M. R. Ayatollahi, "Experimental fracture study of MWCNT/epoxy nanocomposites under the combined out-of-plane shear and tensile loading," *Polymer Testing*, 2017; 59: 193-202.
- [54] D. Kalita and A. N. Netravali, "Interfaces in Green Composites: A Critical Review," *Rev. Adhesion Adhesives*, 3 (2015) 386-443.
- [55] W. Y. Hamad and C. Miao, "Cellulose reinforced polymer composites and nanocomposites: a critical review," *Cellulose*, 20 (2013): 2221–2262 .
- [56] H. Kargarzadeh, R. M. Sheltami, I. Ahmad, I. Abdullah and A. Dufresne, "Cellulose nanocrystal: A promising toughening agent for unsaturated polyester nanocomposite," *Polymer*, 56 (2015) 346-357.
- [57] T. Lu, M. Jiang, Z. Jiang, D. Hui, Z. Wang and Z. Zhou, "Effect of surface modification of bamboo cellulose fibers on mechanical properties of cellulose/epoxy composites," *Composites: Part B*, 51 (2013) 28-34.
- [58] A. Ashori, M. Babaei, M. Janoobi and Y. Hamzeh, "Solvent-free acetylation of cellulose nanofibers for improving compatibility and dispersion," *Carbohydrate Polymers*, 102 (2014) 369-375.
- [59] M. Roman and W. T. Winter, "Cellulose Nanocrystals for Thermoplastic Reinforcement: Effect of Filler Surface Chemistry on Composite Properties," *Cellulose Nanocomposites*, 938 (2006) 99-113.
- [60] J. Lu, P. Askeland and D. L. T., "Surface modification of microfibrillated cellulose for epoxy composite applications," *Polymer*, 46 (2008) 1285-1296.
- [61] Y. Tian, H. Zhang and Z. Zhang, "Influence of nanoparticles on the interfacial properties of fiber-reinforced epoxy composites," *Composites: Part A*, 98 (2017) 1-8.

- [62] Y. Shao, T. Yashiro, K. Okubo and T. Fujii, "Effect of cellulose nano fiber (CNF) on fatigue performance of carbon fiber fabric composites," *Composites: Part A*, 76 (2015) 244–254.
- [63] Z. Zhao, K. Teng, N. Li, X. Li, Z. Xu, L. Chen, J. Niu, H. Fu, L. Zhao and Y. Liu, "Mechanical, thermal and interfacial performances of carbon fiber reinforced composites flavored by carbon nanotube in matrix/interface," *Composite Structures*, 159 (2017) 761-772.
- [64] L. Liu, F. Yan, M. Li, M. Zhang, L. Xiao, L. Shang and Y. Ao, "Improving interfacial properties of hierarchical reinforcement carbon fibers modified by graphene oxide with different bonding types," *Composites Part A*, 107 (2018) 616-625.
- [65] F.-H. Zhang, R.-G. Wang, X.-D. He and L.-N. Ren, "Interfacial shearing strength and reinforcing mechanisms of an epoxy composite reinforced using a carbon nanotube/carbon fiber hybrid," *Journal of Materials Science*, 44 (2009) 3574–3577.
- [66] A. Asadi, M. Miller, R. J. Moon and K. Kalaitzidou, "Improving the interfacial and mechanical properties of short glass fiber/epoxy composites by coating the glass fibers with cellulose nanocrystals," *eXPRESS Polymer Letters*, 10 (2016) 587-597.
- [67] S. Xiong, Y. Zhao, Y. Wang, J. Song, X. Zhao and S. Li, "Enhanced interfacial properties of carbon fiber/epoxy composites by coating carbon nanotubes onto carbon fiber surface by one-step dipping method," *Applied Surface Science*, 546 (2021) 149135.
- [68] S. Parveen, S. Pichandi, P. Goswami and S. Rana, "Novel glass fibre reinforced hierarchical composites with improved interfacial, mechanical and dynamic mechanical properties developed using cellulose microcrystals," *Materials and Design*, 188 (2020) 108448.
- [69] D. Lui, A. M. Pourrahimi, R. T. Olsson, M. S. Hedenqvist and U. W. Gedde, "Influence of nanoparticle surface treatment on particle dispersion and interfacial adhesion in low-density polyethylene/aluminium oxide nanocomposites," *European Polymer Journal*, 66 (2015) 67-77.
- [70] W. Weibull, "A Statistical Distribution Function of Wide Applicability," *ASME Journal of Applied Mechanics*, 18 (1951) 293-297.
- [71] V. M. Dusevich, J. H. Purk and J. D. Eick, "Choosing the Right Accelerating Voltage for SEM (An Introduction for Beginners)," *Microscopytoday*, 2010.
- [72] C. Xiao, Y. Tan, X. Wang, L. Gao and L. Q. Z. Wang, "Study on interfacial and mechanical improvement of carbon fiber/epoxy composites by depositing multi-walled carbon nanotubes on fibers," *Chemical Physics Letters*, 703 (2018) 8–16.
- [73] K. Missoum, M. N. Belgacem and J. Bras, "Nanofibrillated Cellulose Surface Modification: A Review," *Materials*, 6 (2013) 1745-1766.

- [74] S. Sarkar and C. V. Liew, "Moistening Liquid-Dependent De-aggregation of Microcrystalline Cellulose and Its Impact on Pellet Formation by Extrusion–Spheronization," *American Association of Pharmaceutical Scientists*, 15 (2014) 753-761.
- [75] L. T. Drzal, M. J. Rich and P. F. Lloyd, "Adhesion of Graphite Fibers to Epoxy Matrices: I. The Role of Fiber Surface Treatment," *The Journal of Adhesion*, 16 (1982)1–30.
- [76] R. J. Sager, P. J. Klein, D. C. Lagoudas, J. Zhang, J. Liu, L. Dai and J. W. Baur, "Effect of carbon nanotubes on the interfacial shear strength of T650 carbon fiber in an epoxy matrix," *Composites Science and Technology*, 69 (2009) 898–904.
- [77] H.-H. Kim, S.-Y. Kim, D.-H. Kim, C.-Y. Oh and N.-J. Jo, "Effect of Silane Coupling Agent on the Flexural Property of Glass Fiber Reinforced Composite Film," *Journal of Materials Science and Chemical Engineering*, (2014) 2, 38-42.
- [78] P. I. Gonzalez-Chi, O. Rodríguez-Uicab, C. Martín-Barrera, J. Uribe-Calderon, G. Canché-Escamilla, M. Yazdani-Pedram, A. May-Pat and F. Avilés, "Influence of aramid fiber treatment and carbon nanotubes on the interfacial strength of polypropylene hierarchical composites," *Composites Part B*, 122 (2017) 16-22.
- [79] X. Xu, F. Liu, L. Jiang, J. Y. Zhu, D. Haagenon and D. P. Wiesenborn, "Cellulose Nanocrystals vs. Cellulose Nanofibrils: A Comparative Study on Their Microstructures and Effects as Polymer Reinforcing Agents," *ACS Applied Materials & Interfaces*, 5 (2013) 2999-3009.
- [80] K. Sever, M. Sarikanat, Y. Seki and I. H. Tavman, "Composites, Concentration Effect of γ -Glycidoxypropyltrimethoxysilane on the Mechanical Properties of Glass Fiber–Epoxy," *Polymer composites*, (2009) 1251-1257.
- [81] D. Rathore, R. Prusty and D. R. B. Kumar, "Mechanical performance of CNT-filled glass fiber/epoxy composite in in-situ elevated temperature environments emphasizing the role of CNT content," *Composites: Part A*, 84 (2016) 364-376.
- [82] M. Li, Y. Gu, Y. Liu, Y. Li and Z. Zhang, "Interfacial improvement of carbon fiber/epoxy composites using a simple process for depositing commercially functionalized carbon nanotubes on the fibers," *Carbon*, 54 (2013) 109-121.
- [83] A. Rahaman and K. K. Kar, "Carbon nanomaterials grown on E-glass fibers and their application in composite," *Composites Science and Technology*, 101 (2014) 1-10.
- [84] Y. Xie, H. Kurita, R. Ishigami and F. Narita, "Assessing the Flexural Properties of Epoxy Composites with Extremely Low Addition of Cellulose Nanofiber Content," *Applied Sciences*, 2020, 10, 1159.
- [85] A. Haghbin, G. Liaghat, A. Arabi, H. Hadavinia and M. Pol, "Investigations on electrophoretic deposition of carbon nanotubes on glass textures to improve polymeric composites interface," *Composites Science and Technology*, 155 (2018) 197-204.

- [86] M. M. Sarr, H. Inoue and T. Kosaka, "Study on the improvement of interfacial strength between glass fiber and matrix resin by grafting cellulose nanofibers," *Composites Science and Technology*, 211 (2021) 108853.
- [87] I. Palley and V. A. Kagan, "Plastics part design: low cycle fatigue strength of glass-fiber reinforced poly(ethylene terephthalate)," *Analytical Sciences, Honeywell International*.
- [88] A. Gaurav and K. K. Singh, "Fatigue behavior of FRP composites and CNT-Embedded FRP composites: A review," *POLYMER COMPOSITES*, (2016) 1-24.
- [89] W. Ferdous, A. Manalo, J. Peauril, C. Salih, R. Kakarla, P. Yu, P. Schubel and T. Heyer, "Testing and modelling the fatigue behaviour of GFRP composites – Effect of stress level, stress concentration and frequency," *Engineering Science and Technology an International Journal*, 2020.
- [90] L. Daelemans, S. V. Heijden, I. D. Baere, H. Rahier, W. V. Paepegem and K. D. Clerck, "Nanofibre bridging as a toughening mechanism in carbon/epoxy composite laminates interleaved with electrospun polyamide nanofibrous veils," *Composites Science and Technology*, 2015; 117: 244-256.
- [91] Y. Liu, C.-B. Qu, Q.-P. Feng, H.-M. Xiao and S.-Y. Fu, "Enhancement in Mode II Interlaminar Fracture Toughness at Cryogenic Temperature of Glass Fiber/Epoxy Composites through Matrix Modification by Carbon Nanotubes and n-Butyl Glycidyl Ether," *Journal of Nanomaterials*, (2015) 812061: 1-6.
- [92] A. T. Seyhan, M. Tanoglu and K. Schulte, "Mode I and mode II fracture toughness of E-glass non-crimp fabric/carbon nanotube (CNT) modified polymer based composites," *Engineering Fracture Mechanics*, 2008; 75 (18): 5151-5162.
- [93] A. J. Kinloch, K. Masania, A. C. Taylor, S. Sprenger and D. Egan, "The fracture of glass-fibre-reinforced epoxy composites using nanoparticle-modified matrices," *Journal of Materials Science*, 2008; 43: 1151-1154.
- [94] B. M'membe, M. Yasaei, S. R. Hallett and I. K. Partridge, "Effective use of metallic Z-pins for composites' through-thickness reinforcement," *Composites Science and Technology*, 2019, 175: 77–84.
- [95] D. Göktaş, W. R. Kennon and P. Potluri, "Improvement of Mode I Interlaminar Fracture Toughness of Stitched Glass/Epoxy Composites," *Applied Composite Materials*, 24 (2017) 351–375.
- [96] X. Zhu, Y. Li, T. Yu and Z. Zhang, "Enhancement of the interlaminar fracture toughness and damping properties of carbon fiber reinforced composites using cellulose nanofiber interleaves," *Composites Communications*, (2021); 28: 100940.
- [97] J. Wang, T. R. Pozegic, Z. Xu, R. Nigmatullin and R. L. Harniman, "Cellulose nanocrystal-polyetherimide hybrid nanofibrous interleaves for enhanced interlaminar

- fracture toughness of carbon fibre/epoxy composites," *Composites Science and Technology*, 182 (2019) 107744.
- [98] D. Quan, F. Bologna, G. I. A. Scarselli and N. Murphy, "Mode-II fracture behaviour of aerospace-grade carbon fibre/epoxy composites interleaved with thermoplastic veils," *Composites Science and Technology*, (2020); 191: 108065.
- [99] H. Saghafi, A. Zucchelli, R. Palazzetti and G. Minak, "The effect of interleaved composite nanofibrous mats on delamination behavior of polymeric composite materials," *Composite Structures*, 2014; 109: 41–47.
- [100] Y. C. Shin, W. I. Lee and H. S. Kim, "Mode II interlaminar fracture toughness of carbon nanotubes/epoxy film-interleaved carbon fiber composites," *Composite Structures*, 2020; 236: 111808.
- [101] V. Mirjalili, R. Ramachandramoorthy and P. Hubert, "Enhancement of fracture toughness of carbon fiber laminated composites using multi-wall carbon nanotubes," *Carbon*, 2014; 79: 413-423.
- [102] K. Katagiri, S. Honda, S. Minami, S. Yamaguchi, S. Kawakita, H. Sonomura, T. Ozaki, S. Uchida, M. Nedu, Y. Yoshioka and K. Sasaki, "Enhancement of the mechanical properties of the CFRP by cellulose nanofiber sheets using the electro-activated deposition resin molding method," *Composites Part A*, 2019; 123: 320–326.
- [103] B. E. B. Uribe, A. C. Soares-Pozzi and J. R. Tarpani, "Nanocellulose-coated carbon fibers towards developing hierarchical polymer matrix composites," *Materials Today: Proceedings*, 8 (2019) 820-831.
- [104] Japanese Industrial Standards JIS K7086; Testing methods for interlaminar fracture toughness of carbon fibre reinforced plastics, 1993.
- [105] Z. Zhang, K. Fu and Y. Li, "Improved interlaminar fracture toughness of carbon fiber/epoxy composites with a multiscale cellulose fiber interlayer," *Composites Communications*, 2021; 27: 100898.
- [106] I. DeBaere, S. Jacques, W. V. Paepegem and J. Degrieck, "Study of the Mode I and Mode II interlaminar behaviour of a carbon fabric reinforced thermoplastic," *Polymer Testing*, 31 (2012): 322–332.
- [107] L. Berger and W. J. Cantwell, "Temperature and loading rate effects in the mode II interlaminar fracture behavior of carbon fiber reinforced PEEK," *Polymer Composites*, 22 (2001): 271-281.
- [108] M. R. Hosseini, F. Taheri-Behrooz and M. Salamat-talab, "Mode II interlaminar fracture toughness of woven E-glass/epoxy composites in the presence of mat interleaves," *International Journal of Adhesion & Adhesives*, 98 (2020) 102523.

- [109] N. H. Nash, T. M. Young and W. F. Stanley, "The reversibility of Mode-I and -II interlaminar fracture toughness after hydrothermal aging of Carbon/Benzoxazine composites with a thermoplastic toughening interlayer," *Composite Structures*, 2016; 152: 558–567.